Molar Refractivity and Oxygen Solubility

by

Adriana Andreina Rivolta

A thesis submitted in partial fulfillment of the requirements for the degree of

Master of Science

In

Chemical Engineering

Department of Chemical and Materials Engineering

University of Alberta

Abstract

This study dealt with two experimental topics. One topic evaluated the relationship between molar refractivity and the experimentally measurable parameters refractive index, density and molar mass. The other topic dealt with an experimental method to determine oxygen solubility in hydrocarbons.

The objective of the molar refractivity study was to determine which of the different equations that correlate molar refractivity, refractive index, density, and molar mass better express the empirical data. Molar refractivity is a temperature invariant property, therefore, the best correlation would be the one in which the calculated molar refractivity is least temperature-dependent. To evaluate these correlations, high precision, and accurate temperature-dependent data for refractive index (0.000001 readability), and density (0.000001 g/cm^3 readability) of pure components were measured. The data were collected for different groups of reagents, namely: alkanes, alkenes, alkynes, cyclic compounds, alkyl aromatics, 1-alcohols, carboxylic acids and sulfur compounds of different compound classes. For each model compound, the measurements were performed nine times for each temperature condition. Measurements were obtained at five different temperatures when possible, depending on the boiling and melting point of the sample.

Once the data were collected, it was found that the molar refractivity calculated with the correlation by Eykman $\left(R_M = \left(\frac{n^2-1}{n+0.4} \right) \cdot \frac{M}{\rho} \right)$ was the least temperature-dependent. The Eykman correlation performed best for all of the model compounds, except propionic acid and butyric acid.

The average first derivative $(dn/d\rho)$ of refractive index with respect to density of alkanes (0.598 ± 0.003), alkenes, (0.604 ± 0.002), and alkynes (0.587 ± 0.005) were roughly the same as the value of 0.6 reported in literature for hydrocarbons. For the selected 1-alcohols and carboxylic acids, the $dn/d\rho$ increases with the increase of the carbon chain length and the decrease of the polarity, due to the presence of oxygen, which suggested that the $dn/d\rho$ could be used to track changes in chemical composition. In sulfur-containing compounds $dn/d\rho$ appeared to depend more on the hydrocarbon nature than in the position of the sulfur.

On the other hand, for the study of dissolved oxygen in hydrocarbons, the goal was to find or develop an experimental method to determine oxygen solubility in hydrocarbons, and to use the experimental measurement to calculate Henry's constant. The first method involved oxygen determination by titration, but could not be successfully adapted for use with hydrocarbons. The second method determined oxygen concentration from the pressure difference resulting from oxygen dissolving in the liquid hydrocarbon. Results from this method compared favorably with measurements reported in the literature.

Preface
(Mandatory due to collaborative work)

The molar refractivity study (Chapters IV to VIII) was done in collaboration with Dr. Natalia Montoya and Dr. Arno De Klerk. I was responsible for design of experiments, data collection and interpretation, and manuscript composition. Dr. Natalia Montoya was involved in the design of experiments, and reviewing the manuscript.

The dissolved oxygen study was done in collaboration with Dr. Muhammad Siddiquee and Dr. Arno De Klerk. I was responsible for design of methodology, data collection and interpretation, and manuscript composition. Dr Muhammad Siddiquee collaborated with design of methodology, data collection, and reviewing the manuscript.

The whole project was done with the supervision of Dr Arno De Klerk, he was involved in concept formulation, data interpretation and reviewing the manuscript.

To my parents and my sisters for their never ending support.

To Raunil for making me laugh even when I wanted to cry

Acknowledgements

I want to express my gratitude to my supervisor Arno De Klerk for all his support and guidance through this project. Thanks for your advice, and for the fun conversations. I feel fortunate to have had you as my supervisor.

Thanks to Natalia and Muhammad for all their help and guidance with this project. Thanks to you guys this project was completed on time.

I want to thanks my research group colleagues for their feedback and care. I want to specially thank Shruthi and Priscila for their advices and a little push when I needed it, moreover thanks for all the laughs and the coloring. Thanks to Garima for her contagious cheerfulness. Thanks to Cloribel for her unconditional support and friendship.

I would also like to thank Mariangel for her advice, and Astrid for her help. And thanks to Raunil for his company.

Thanks ☺!

Table of Contents

List of Tables

xvii

List of Figures

CHAPTER I – INTRODUCTION TO A FUNDAMENTAL STUDY OF MOLAR REFRACTIVITY AND OXYGEN SOLUBILITY

This chapter introduces the research topic. The current and desired situations around the topic are presented, as well as the objectives, and scope of the project.

1. Background

Two topics were investigated in this study, namely, (i) the relationship between molar refractivity, refractive index, density and molar mass, and (ii) the experimental determination of oxygen solubility in hydrocarbons. These two topics are related only by their fundamental nature.

Fundamental research means experimental or theoretical work carried out to create knowledge or deepen the understanding of foundations or basic principles of a given topic, without an immediate or direct application on view.[1,2] An example of fundamental research is the atom discovery when in 1808 Dalton discovered the atom and called the smallest unit in nature.[3] Then, Rutherford found out that inside of the atom there is a nucleus, changing the atom pre-existing definition, which continued to change until the one that is known today.[3]

As previously described, knowledge evolves, and fundamental studies are the means for that evolution to happen. Inspired by this, the present fundamental research analyzes and deepen the knowledge of refractive index use, and devised an experimental method to measure oxygen solubility for the determination of Henry's constant for hydrocarbons.

1.1   Refractive Index and Molar Refractivity

Asphalt, fuels, and newspaper ink are a few of the everyday products derived from bitumen and heavy oils. To obtain such products, these heavy feedstocks have to undergo transportation, upgrading, and refining processes. Bitumen and heavy oils are difficult to analyze during these processes due to their complex composition, high viscosity, high average molecular weight, and

low volatility. Bitumen or heavy oil, are characterized by techniques, however, most techniques cannot be used to record or track small changes during bitumen conversion.

To make the point, an example taken from literature[4] is given. Figure 1, which presents the change in viscosity of a visbroken product as a function of the temperature, illustrates the difficulty in the detection of change often experienced during characterization of products from bitumen conversion.
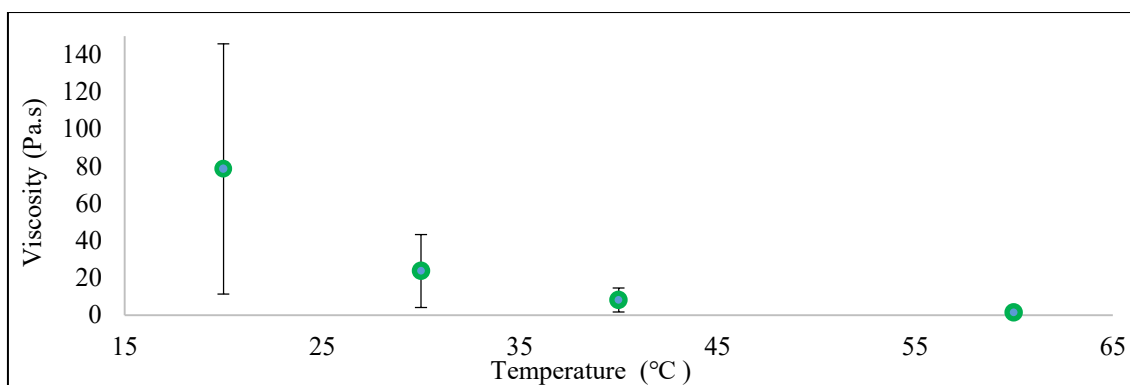
Figure 1.1. Viscosity change of a product from bitumen visbreaking after reaction at 250 °C.[4]

Figure 1 shows that the viscosity values at 20, 30, and 40 °C, could be considered the same, due to the high standard deviation shown by the error bars. Although it appears as if the error becomes less at lower viscosity values, the relative standard deviation remained of the same order.

However, figure 2 shows that the standard deviation is quite smaller for refractive index vs temperature data of the same visbreaking product. The low variability (small standard deviation) of refractive index measurements makes this technique an attractive one for bulk analysis. The present research aims to deepen the fundamental knowledge and understanding of refractive index so that in the future, it can be used by industry to analyze complex mixtures such as bitumen or bitumen derived products to infer composition related information.
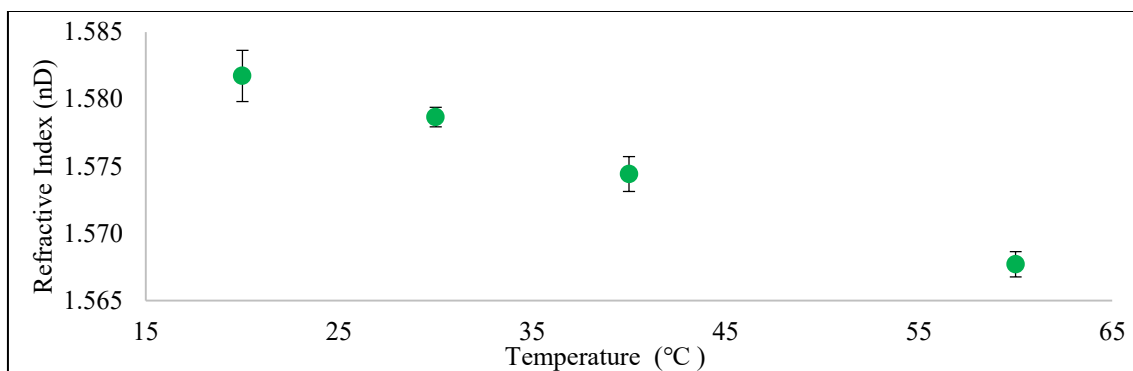
Figure 1.2. Refractive Index change of a product from bitumen visbreaking after reaction at 250 °C.[4]

Nowadays, refractive index has been used as an indirect measure of the onset of asphaltenes precipitation.[5–7] It has also assisted in the detection of small changes of composition during conversion,[8] and has been used as a convenient measure to approximate physical,[9–11] and chemical properties of heavy petroleum, including wax content,[12] paraffin/naphthenes/ aromatic composition,[13] and elemental analysis.[14]

Significant progress to establish relationships between composition and refractive index was made. However, no much progress on the study of refractive index measurement as a tool to indirectly determine the composition of complex mixtures has been made since the 1960s. Some fundamental aspects, which can unlock practical applications, remain not fully resolved. Therefore, the objective of this research is to revisit and resolve some of the fundamental aspects related to refractive index, specifically about molar refractivity.

Molar refractivity is a temperature invariant and intrinsic property, which can be related to chemical composition. However, in the literature[15], there are different equations that correlate molar refractivity to refractive index, density, and molar mass. Which of these correlations better express the empirical data is not clear from the literature[15].

To resolve this uncertainty, refractive index and density data sets at 5 different temperatures were experimentally measured for seventy two model compounds. The data was collected at atmospheric pressure. Afterward, the data was analyzed and compared with the data available

in the literature[16,17] and employed to evaluate equations to correlate molar refractivity to refractive index, molar mass, and density.

1.2   Oxygen solubility for hydrocarbons

Oxygen (O_2) transport from gas-phase to organic liquids plays an important role in different oxidation processes such as liquid-phase oxidation to produce petrochemicals and oxidative degradation of organic effluents by aerobic microorganism.[18–21] To calculate the solubility of O_2 in a liquid, Henry's constant of that specific gas on the desired liquid must be known. The majority of the methods used to calculate this constant involved an aqueous liquid phase.

Therefore, for many hydrocarbons, Henry's constant is not available in the literature. This is commonly solved by approximating the desired constant to one of a similar molecule, creating uncertainty in further calculations. The main objective of this research is to find an experimental method to determine oxygen solubility in organic liquids to calculate Henry's constant for hydrocarbons.

In the present research, two methods to measure oxygen solubility in organic liquids were explored. The first one, a modification of the method of Anderson and Hibbard[22], which corresponds to an iodine titration, was done at room temperature and atmospheric pressure. While the second method developed as part of this thesis was done at a pressure slightly higher than atmospheric, approximately 8 psi, and room temperature.

2. Problem formulation

2.1   Current Situation

2.1.1 Refractive index and molar refractivity

There are different relationships in the literature that correlates refractive index, and density with molar refractivity. In addition, the data used to formulate these relationships were collected a long time ago, when the equipment available to measure these properties

were not as precise as those available now, making it difficult to discriminate between the correlations. Nowadays, these correlations are used indiscriminately.

2.1.2 Oxygen solubility in hydrocarbons

Oxygen solubility has not been measured and Henry's constant has not been calculated for many hydrocarbons, and methods to experimentally determine oxygen solubility are mostly available when the liquid phase is aqueous and not organic.

2.2   Desired Situation

2.2.1 Refractive index and molar refractivity

Knowing which correlation best expresses the relationship between refractive index, density, and molar refractivity. This will enable the correlation of refractive index to chemical composition in the future, as well as the derivation of appropriate mixing rules for refractive index.

2.2.2 Oxygen solubility in hydrocarbons

Having a method to experimentally measure oxygen concentration in organic liquids, and to calculate the Henry's constant for hydrocarbons, which will improve the calculations of gas-liquid mass transfer and diffusivity in hydrocarbons.

3. Objective

Generate accurate engineering data. Improve the fundamental knowledge of refractive index, by finding the correlation between refractive index, density, molar mass, and molar refractivity that best expresses the empirical data; and Henry's constant for hydrocarbons, by finding an experimental method to measure oxygen solubility in organic liquids at room temperature.

4. Scope of work

4.1   Refractive index and molar refractivity

- Select 8 compound groups and 9 model compounds per group, to analyze the correlations between refractive index, density, and molar refractivity.
- Create data sets of refractive and density vs temperature with the selected model compounds, to find the best correlation
- Observe the difference between the refractive index and density of the different functional groups, to understand the effect of chemical nature in these properties and to analyze the relationship between refractive index and density.
- Calculate for the best correlation the group contribution, and elemental refractivity, to gain more knowledge about this correlation.

4.2   Oxygen solubility in hydrocarbons

- Develop a new experimental method or modify an existing one to measure the dissolved O_2 in a liquid hydrocarbon.
- Choose a hydrocarbon, which oxygen solubility is reported in the literature, as a model compound to test the selected methods.
- Measure oxygen solubility and calculate Henry's constant and compare it to the literature values to validate the experimental method.

4.3   Organization of the thesis

The present work will be divided into 11 chapters. The present chapter contains the introduction of the research topic, objectives, and scope of the project. Chapter II comprises the literature review. Chapters III to VIII deal with molar refractivity, while chapter IX and X with oxygen solubility. Lastly, chapter XI contains conclusions and recommendations.

The work presented in Chapters IV-VIII evaluates the performance of different correlations, available in literature, to calculate molar refractivity. Although, each chapter deals with different compound groups, the evaluation of such correlations is done in a similar way. As a result, the reader will encounter some similarities in the introduction to each chapter

5. References

(1)   Collins   English   Dictionary.   Definition   of   "fundamental   research" https://www.collinsdictionary.com/dictionary/english/fundamental-research (accessed Nov 12, 2019).

(2)   European Commission. Community Framework for State Aid for Research and Development and Innovation. *Off. J. Eur. Union* **2007**, *92* (5), 1286–1298.

(3)   The   Editors   of   Encyclopaedia   Britannica.   Atomic   Theory https://www.britannica.com/science/atomic-theory (accessed Nov 12, 2019).

(4)   Yañez Jaramillo, L. M.; De Klerk, A. Partial Upgrading of Bitumen by Thermal Conversion at   150-300   °C.   *Energy   and   Fuels*   **2018**,   *32*   (3),   3299–3311. https://doi.org/10.1021/acs.energyfuels.7b04145.

(5)   Buckley, J. S.; Hirasaki, G. J.; Liu, Y.; Von Drasek, S.; Wang, J. X.; Gill, B. S. Asphaltene Precipitation and Solvent Properties of Crude Oils. *Pet. Sci. Technol.* **1998**, *16* (3–4), 251–285. https://doi.org/10.1080/10916469808949783.

(6)   Castillo, J.; Gutierrez, H.; Ranaudo, M.; Villarroel, O. Measurement of the Refractive Index of Crude Oil and Asphaltene Solutions: Onset Flocculation Determination. *Energy and Fuels* **2010**, *24* (1), 492–495. https://doi.org/10.1021/ef900861d.

(7)   Bayat, M.; Sattarin, M.; Teymouri, M. Prediction of Asphaltene Self-Precipitation in Dead Crude Oil. *Energy and Fuels* **2008**, *22* (1), 583–586. https://doi.org/10.1021/ef700536z.

(8)   Zachariah, A.; De Klerk, A. Thermal Conversion Regimes for Oilsands Bitumen. *Energy and Fuels* **2016**, *30* (1), 239–248. https://doi.org/10.1021/acs.energyfuels.5b02383.

(9)   Wang, F.; Evangelista, R. F.; Threatt, T. J.; Tavakkoli, M.; Vargas, F. M. Determination of Volumetric Properties Using Refractive Index Measurements for Nonpolar Hydrocarbons and Crude   Oils.   *Ind.   Eng.   Chem.   Res.*   **2017**,   *56*   (11),   3107–3115. https://doi.org/10.1021/acs.iecr.6b04773.

(10)   Yarranton, H. W.; Okafor, J. C.; Ortiz, D. P.; Van Den Berg, F. G. A. Density and Refractive Index of Petroleum, Cuts, and Mixtures. *Energy and Fuels* **2015**, *29* (9), 5723–5736. https://doi.org/10.1021/acs.energyfuels.5b01376.

(11)   Hosseinifar, P.; Jamshidi, S. Development of a New Generalized Correlation to Characterize Physical Properties of Pure Components and Petroleum Fractions. *Fluid Phase Equilib.* **2014**, *363*,

189–198. https://doi.org/10.1016/j.fluid.2013.11.043.

(12) Eghbali, M. H.; Nazar, A. R. S.; Tavakoli, T. A Simple Method for Oil Content Determination of Petroleum Waxes by Refractive Index Measurement. *Pet. Sci. Technol.* **2014**, *32* (7), 856–861. https://doi.org/10.1080/10916466.2011.601504.

(13) Modarress, H.; Vakili-Nezhaad, G. R. A New Characterization Factor for Hydrocarbons and Petroleum Fluids Fractions. *Oil Gas Sci. Technol.* **2002**, *57* (2), 149–154. https://doi.org/10.2516/ogst:2002011.

(14) Goossens, A. G. Prediction of the Hydrogen Content of Petroleum Fractions. *Ind. Eng. Chem. Res.* **1997**, *36* (6), 2500–2504. https://doi.org/10.1021/ie960772x.

(15) Kurtz, S. S. Physical Properties and Hydrocarbon Structure. In *The chemistry of petroleum hydrocarbons. Vol 1*; Reinhold Publishing Corporation: New York, 1954; pp 275–331.

(16) Devi, R.; Gahlyan, S.; Rani, M.; Maken, S. Thermodynamic and Acoustic Properties of Binary Mixtures of Diisopropyl Ether, Benzene and Alkanes at 298.15, 308.15 and 318.15 K: Prigogine-Flory-Patterson Theory and Graph Theory. *J. Mol. Liq.* **2019**, *275*, 364–377. https://doi.org/10.1016/j.molliq.2018.11.045.

(17) Kashyap, P.; Rani, M.; Gahlyan, S.; Tiwari, D. P.; Maken, S. Volumetric, Acoustic and Optical Properties of Binary Mixtures of 2-Propanol with n-Alkanes (C6-C10) from 293.15 K to 303.15 K. *J. Mol. Liq.* **2018**, *268*, 303–314. https://doi.org/10.1016/j.molliq.2018.07.043.

(18) Chen, K. C.; Wu, J. Y.; Liou, D. J.; Hwang, S. C. J. Decolorization of the Textile Dyes by Newly Isolated Bacterial Strains. *J. Biotechnol.* **2003**, *101* (1), 57–68. https://doi.org/10.1016/S0168-1656(02)00303-6.

(19) Nigam, P.; Banat, I. M.; Singh, D.; Marchant, R. Microbial Process for the Decolorization of Textile Effluent Containing Azo, Diazo and Reactive Dyes. *Process Biochem.* **1996**, *31* (5), 435–442. https://doi.org/10.1016/0032-9592(95)00085-2.

(20) Siddiquee, M. N.; De Klerk, A.; Nazemifard, N. Application of Microfluidics to Control Product Selectivity during Non-Catalytic Oxidation of Naphthenic-Aromatic Hydrocarbons. *React. Chem. Eng.* **2016**, *1* (4), 418–435. https://doi.org/10.1039/c6re00010j.

(21) Siddiquee, M. N.; De Klerk, A. In Situ Measurement of Liquid Phase Oxygen during Oxidation. *Ind. Eng. Chem. Res.* **2016**, *55* (23), 6607–6618. https://doi.org/10.1021/acs.iecr.6b00949.

(22) Mckeown, A. B.; Hibbard, R. R. Determination of Dissolved Oxygen in Hydrocarbons. *Anal.*

Chem. **1956**, *28* (9), 1490–1492. https://doi.org/10.1021/ac60117a044.

CHAPTER II – LITERATURE REVIEW OF A FUNDAMENTAL STUDY OF MOLAR REFRACTIVITY AND OXYGEN SOLUBILITY

In this chapter, the relevant information about refractive index, oxygen solubility in hydrocarbons and Henry's law are introduced; in addition, points of interest for the current investigation will be explained.

1. Introduction

The present literature review is divided into two major sections dealing with: first section: refractive index, and second section: oxygen solubility in hydrocarbons and Henry's law. The first section of the review, which corresponds to refractive index, explores the scientific background of this property, with emphasis on its relationship with density and molar refractivity. Moreover, previous studies are analyzed, highlighting their similarities and differences with the present research.

The second section reviews the definition and formulation of the determination of dissolved oxygen content in hydrocarbons and Henry's law. This section also presents some of the previous research done to determine dissolved oxygen content and calculate Henry's constant.

At the end of this chapter, it is expected that the reader will have the general knowledge and understanding of the scientific background of this study.

2. Refractive index scientific background

2.1 Definition

Refractive index measures the change in angle (θ) when light passes from one medium to another due to the relative change in the speed of light (See Figure 2.1).[1,2] From a fundamental point of view, the speed of light changes due to the density, and the interaction with the species

present in the medium. In fact, the interaction of the light with the species in the medium is the origin of the composition dependence of refractive index.
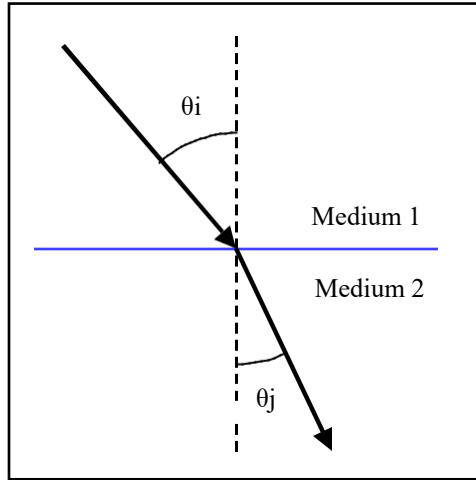
Figure 2.1. Refraction of a light beam passing from medium 1 to medium 2.[3]

The relationship between the refractive index (n_j), the angle (θ_j), and speed of light (u_j) in each medium (j) is given by the Snell's Law.[3]

$$\frac{n_2}{n_1} = \frac{u_1}{u_2} = \frac{\sin\theta_1}{\sin\theta_2}$$ (2.I)

Snell's Law

In addition, the refractive index of a substance can be calculated by the speed of light in vacuum (c) divided by the speed of light through the medium j (See equation 2.II).[2,3]

$$n = \frac{c}{u_j}$$ (2.II)

The refractive index of light in vacuum is 1 because $u_{vacuum} = c$.[2] However, for practical reasons, refractive index is not commonly measured using vacuum. It is more convenient to measure refractive index of light of a specific wavelength (λ) relative to air. The most commonly used wavelength is the sodium D-lines, $\lambda = 589$ nm.[1,2,4] It is not clearly stated in the

literature why is this wavelength commonly used, however, it is interesting that its wavelength its almost at the middle of the wavelengths of visible light range (400 nm to 700 nm)[5]. Also, the sodium D-lines have a bright wavelength doublet at 589 nm and 589.6 nm.[1,2] Some studies in the literature compare the refractive index measured for sodium D-lines (yellow light), and compare it to the refractive index measured for red ($\lambda = 652.3$nm), green ($\lambda = 486.1$nm) and violet ($\lambda = 434.0$nm) hydrogen lines.[6] The refractive index using the sodium D-lines in air (n_D) is related to the refractive index in vacuum (n_{vacuum}) through equation 2.III.[3]

$$n_{vacuum} = 1.00027 \, n_D \qquad\qquad (2.III)$$

Some variables that affect the refractive index of a compound are temperature, pressure, and wavelength of light used for the measurement.[1,2] Wavelength and temperature are usually controlled variables during measurement. These are often indicated as part of the symbol used to denote refractive index, e.g. n_D^T, where D refers to the sodium D-line and T to the temperature. Pressure is usually not controlled and although the assumption is often made that atmospheric pressure is invariant, it is not, and for careful experimental work, the atmospheric pressure at the time of measurement must be recorded.

2.1.1 Refractometer operation principles[1]

Figure 2.2 presents a schematic of the refractometer used in the present study. It uses reflected light to measure the refractive index. For this, the sample on top of the prism is irradiated by a light-emitting diode (LED). When the beam of light interacts with the sample, the beam is refracted into the sample or reflected back into the prism. The reflected beam is detected by a series of sensors. With this, the instrument calculates the angle of reflection, which is used to determine the refractive index of the sample. The instrument measures the refractive index relative to air at 1013 mbar and 50% relative humidity.
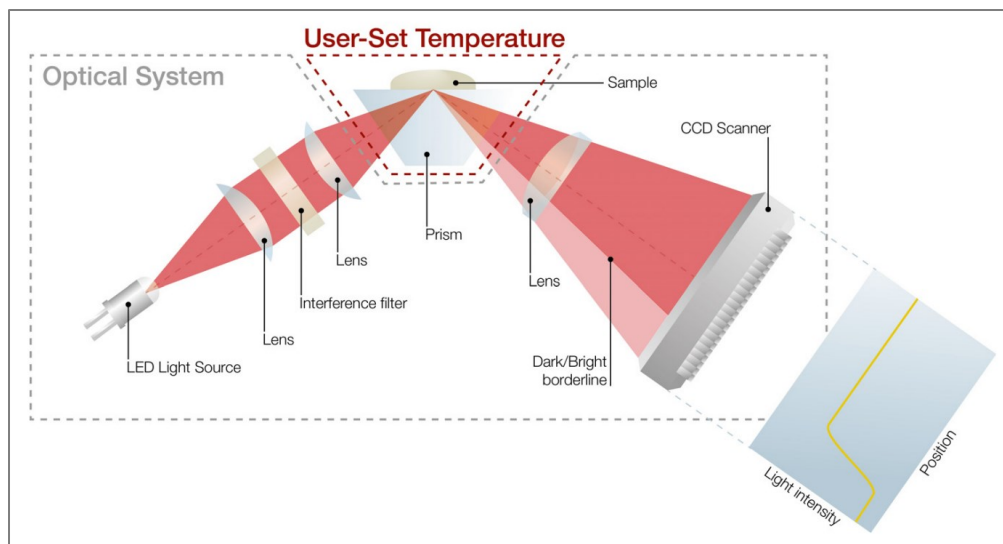
Figure 2.2. Refractometer Abbemat 500 functional scheme.[1]

2.2 Relationship between refractive index and polarizability [2,4]

Refractive index as a property, although simple to measure, is more complex in its origin. As stated before, the refraction of light caused by a medium is due to the interaction of the light with the medium. This interaction is related to the polarizability of the medium and the electromagnetic properties of the light interacting with the medium. To understand how polarizability and refractive index are related, it is useful to look at the polarization of a substance in an electric field.

A substance can be affected in three different ways when placed in a constant electric field:

(a) Orientation polarization (P_O), the electric field causes a force that acts on any permanent dipoles present in the molecule causing orientation of the molecule with respect to the field.

(b) Distortion polarization (P_D), the molecular skeleton may be deformed by the electric field.

14

(c) Electronic polarization (P_E), the electric field may cause displacement of the average position of electrons relative to the nuclei in the substance to cause additional polarization.

The polarizability of a substance reflects all three types of polarization. It is a property that can be measured under the influence of a constant electric field.[2,4] The polarizability of a substance j is expressed as the dielectric constant (ε_j) of the substance, which is the ratio of the capacitance of the substance (C_j) divided by the capacitance of vacuum (C_{vacuum}) given by equation 2.IV. Capacitance is the ability of a substance to store an electrical charge.[7]

$$\varepsilon = \frac{C_j}{C_{vacuum}} \qquad\qquad (2.\text{IV})$$

The amount of time that is required for each of these polarization processes to occur is different. The slowest process is the orientation polarization because it requires movement of molecules within the medium and must also compete with random movements that are affected by temperature. Distortion polarization is faster because it requires only the relative movement of nuclei within the molecule. The fastest process is electronic polarization, which acts only on electrons within the molecule.

Refractive index as measured by light in the visible spectrum, such as the sodium D-line, is an indirect measure of only electronic polarization. Light, which is electromagnetic radiation, is oscillatory in nature, and the frequency at which the electric field changes depends on the wavelength of the radiation. The frequency of light in the visible region of the spectrum is so high, 10^{14}–10^{15} Hz, that only electrons can respond fast enough to the change in the electric field.[2,4] The interaction of visible light with the medium which is passing through will cause only a change in the electronic polarization.

Maxwell showed that the refractive index and the dielectric constant (ε) of a substance measured with a capacitor at the same frequency are related when measured at a visible light frequency (See equation 2.V).

$$\varepsilon = n^2 \tag{2.V}$$

Maxwell

Another useful observation that was made, was related to the molar polarization of nonpolar compounds. It was found that for nonpolar compounds the molar polarization was temperature invariant when the molar polarization (P_M) was expressed in terms of the dielectric constant (ε), molar mass (M), and density (ρ) through equation 2.VI.[8]

$$P_M = P_O + P_D + P_E = \frac{\varepsilon-1}{\varepsilon+1} \cdot \frac{M}{\rho} \tag{2.VI}$$

Mosotti–Clausius[8]

For polar substances, molar polarization (P_M) was not constant, but a linear relationship related to reciprocal temperature (1/T).[8] The temperature dependence was due to the presence of permanent dipoles.[8] A theoretical treatment of the temperature dependence was given by Debye.[8] The orientation polarization (P_O) was expressed as a function of the temperature (T), dipole moment (μ), Avogadro number ($N_A = 6.022 \times 10^{23}$ mol^{-1}) and Boltzmann constant ($k = 1.381 \times$ J·K^{-1}) (See equation 2.VII).[8]

$$P_O = \frac{4\pi}{9} \cdot \frac{N_A}{k} \cdot \frac{\mu^2}{T} \tag{2.VII}$$

Debye[8]

The Mosotti–Clausius equation, although clothed on a theoretical basis, is *not* fundamental. The original relationship was derived from fitting empirical data and there are various assumptions even in the subsequent theoretical development.

2.3 Molar refraction

Molar refractivity is an intrinsic property, which does not depend on temperature (T) nor pressure (P), i.e., it is a constant number for a specific substance.[8] Molar refractivity can also be expressed as the relationship between molar volume ($V_m = M/\rho$) and a refractive index function, $f(n)$, as shown by equation 2.VIII.[8]

$$R_M = P_E = \left(\frac{n^2-1}{n^2+2}\right) \cdot \frac{M}{\rho} \qquad (2.\text{VIII})$$

This expression for molar refraction (R_M) can be derived in analogous terms to molar polarization (P_M) by using the Maxwell relationship (Equation 2.V) to express the Mosotti–Clausius equation (Equation 2.VI) in terms of refractive index instead of the dielectric constant.[8]

Since refractive index is measured using visible light, only the electronic polarization component of molar polarization is measured and it should be temperature invariant.[8] However, this expression of molar refraction builds on the assumptions made in relation to polarization.

Several expressions for calculating molar refraction in terms of refractive index, density, and molecular mass were proposed in the literature.[9] For example, expressions were proposed by Berthelot, Gladstone & Dale, Lorentz and Lorenz, and Eykman.[9]

$$R_M = (n^2 - 1) \cdot \frac{M}{\rho} \qquad (2.\text{IX})$$
$$\text{Berthelot}[9]$$

$$R_M = (n - 1) \cdot \frac{M}{\rho} \qquad (2.\text{X})$$
$$\text{Gladstone \& Dale}[9]$$

$$R_M = \left(\frac{n^2-1}{n^2+2}\right) \cdot \frac{M}{\rho} \qquad (2.\text{XI})$$
$$\text{Lorentz – Lorenz}[9]$$

$$R_M = \left(\frac{n^2-1}{n+0.4}\right) \cdot \frac{M}{\rho} \tag{2.XII}$$

Eykman[9]

Despite attempts to provide theoretical meaning to these relationships that were proposed for molar refraction, the correlations of the refractive index relationship to molar refraction are empirical. In addition, Table 2.1 shows that the numerical value of molar refractivity varies depending on the equation used to calculate it.

Table 2.1. Molar refractivity calculated with different correlations.[9]

Substance	Temperature (°C)	Correlation		
		Gladstone & Dale	Lorentz-Lorenz	Eykman
Hexane	14	48.78	29.76	65.24
	44.95	48.67	29.83	65.26

2.3.1 Atomic refraction and group contribution.[9]

In principle, all the contributions due to the electronic polarization effects of all the bonds for a species are captured by the molar refractivity of the species.[2] Knowing the structure and relating it to the molar refractivity is valuable because there is a theoretical basis for relating the bonds in the species to molar refractivity. Literature[9] reports the atomic refraction of some elements and uses it to calculate the molar refractivity.

Table 2.2. Atomic refraction constants for Lorentz-Lorenz equation.

Developed by	Carbon	Hydrogen	Double Bond	Triple Bond
Bruhl	2.501	1.051	+1.707	+2.10
Eisenlohr	2.418	1.100	+1.733	+2.398
Vander Hulst	2.590	1.025		
Van Nes & Van Westen	2.400	1.114		

The atomic refraction assumes that all bonds are single and then correct only for cases where it is not. Table 2.2 shows the atomic refractions for carbon (C), hydrogen (H), and double and triple bonds for Lorentz–Lorenz correlation.[6] The equation to calculate molar refractivity using the atomic refraction is the following:[9]

18

$$R_M = b_B \cdot A_D + b_T \cdot A_T + \sum_{i=1}^{N}(A_i \cdot k_i) \qquad \text{(2.XIII)}$$

Where,

N: quantity of elements present in the reagent structure

k_i: number of times that the element i is in the reagent structure

A: atomic refraction (cm^3/mol)

b: number of j bonds present in the structure

$_D$: double bond

$_T$: triple bond

To evaluate if the assumption done for the atomic refraction is valid, molar refractivity can also be calculated with group contribution. To calculate molar refractivity using group contribution the equation is the following:[9]

$$R_M = \sum_{i=1}^{y}(G_i \cdot x_i) \qquad \text{(2.XIV)}$$

Where,

y: quantity of groups present in the reagent structure

x_i: number of times that the group i is in the reagent structure

G_i: group contribution of the group i (cm^3/mol)

2.4 Density

Physical property defined as mass per unit of volume of a substance at a specific temperature.

2.4.1 Density and refractive index relationship

For hydrocarbons, Kurtz[9] reports a relationship between refractive index and density (equation 2.XIII). This relationship can be used to predict refractive index at a small temperature change of 10 °C or less.[9]

$$\Delta n = 0.6\Delta\rho \qquad \text{(2.XIII)}^{9}$$

However, Kurtz[9] does not report this relationship for non-hydrocarbons. Also, the questions arise if equation 2.XIII is valid for any hydrocarbon, because it then implies that

19

the density is linearly correlated with refractive index. This is not consistent with Equations 2.IX-XII.

2.4.2 Density meter operation principles[10]

The density meter used in this study is a digital one (See schematic in Figure 2.3). It has a U shaped glass tube which oscillates at a certain frequency depending on the sample filled in it. By determining the frequency, the density of the sample is calculated.
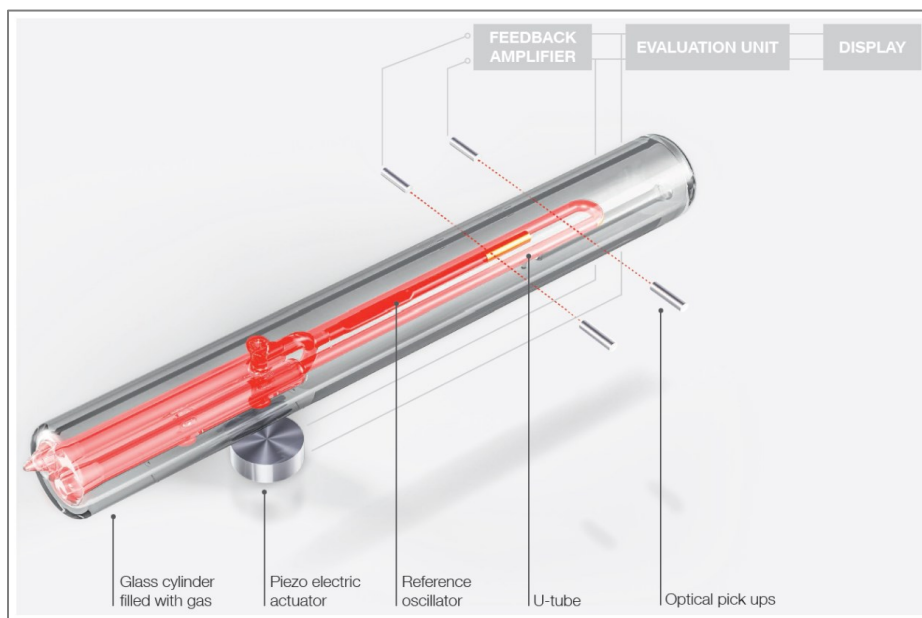
Figure 2.3. Density meter, DMA™ 5000 M, U-tube measuring cell.[10]

2.5 Study of asphaltenes precipitation using refractive index measurement

For example, asphaltenes must remain in solution when bitumen is transported by pipelines because they could deposit and block the pipes.[11] To reduce the risk of pipeline fouling, the asphaltenes can be separated from the bitumen by onset precipitation, using *n*-heptane or *n*-pentane as solvents.[12]

Taylor, et al.[13] studied the difference between the refractive index of bitumen, maltenes, and asphaltenes, and used this difference to estimate the bitumen volume fraction at which the

asphaltenes precipitation occurs. Wattana, et al.[14] also made a similar research, they studied if the binary mixing rule followed the expected linear tendency for the bitumen and paraffin solvent (*n*-heptane or *n*-pentane) binary mixture. This research concluded that the refractive index of the mixture was equal to the linear combination of the refractive indexes of each of the compounds of the mixture.[14] However, once the asphaltenes started to precipitate the refractive index of the mixture no longer followed the linear tendency, suggesting that refractive index could be used to predict the onset of asphaltenes precipitation.[14]

Even though this topic of application does not form part of the current study, it opens the door to questioning for what other applications could the refractive index be used.

3. Oxygen solubility and Henry's law

3.1 Definition

Henry's law, equation 2.XIV, states that the concentration of a gas dissolved in a liquid is proportional to the partial pressure of the gas upon the liquid when the system has reached equilibrium, see Figure 2.4.[2,16,17] If there is only 1 gas present in the system, the partial pressure of the gas is equal to total pressure of the system.[2,16,17]

$$s_g = H \cdot p_g \qquad (2.XIV)$$

Henry's law[16,18]

Where,

H: Henry's constant (mol / kPa·m^3)

s_g: solubility of the gas in the liquid (mol / m^3)

p_g: partial pressure of the gas (kPa)

Equation XIV is a way to quantify the solubility of a gas in a liquid at a certain temperature, however, the Henry's constant must be known.[16,18] Moreover, Henry's law can only be used for systems with gas concentration in the liquid below 1 mol % and partial pressure under 200 kPa.[18,19] Figure 2.4 shows that if more molecules of the gas (higher partial pressure) are present

the concentration of the gas in the liquid will increase proportionally, illustrating the foundation of Henry's law.[16]
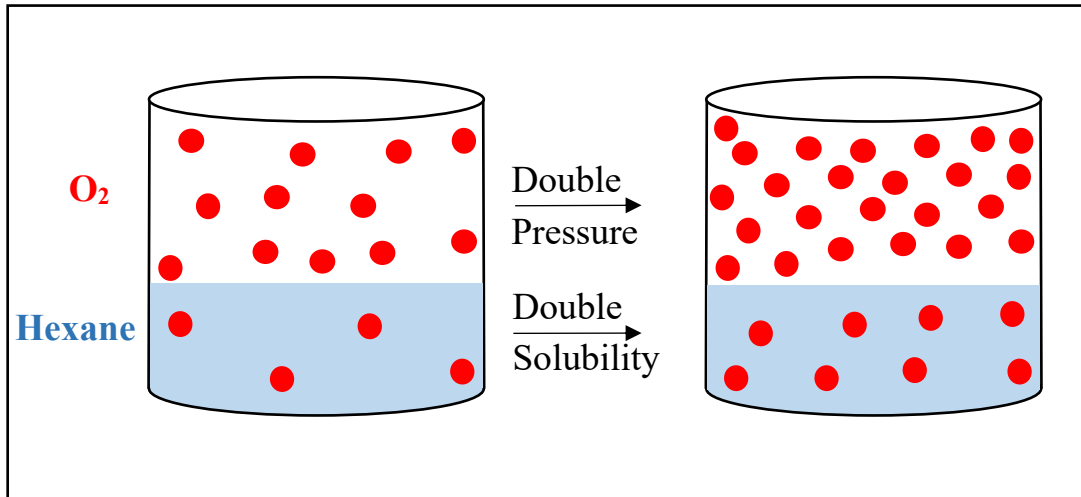
Figure 2.4. Henry's law representation.[16]

3.1.1 Henry's law derivation[20]

As mentioned before, Henry's law can only be used for systems at infinite dilution, this can be explained using Figure 2.5. This figure shows that Henry's law only overlaps with the behavior of a system at low concentration of the gas in the liquid.
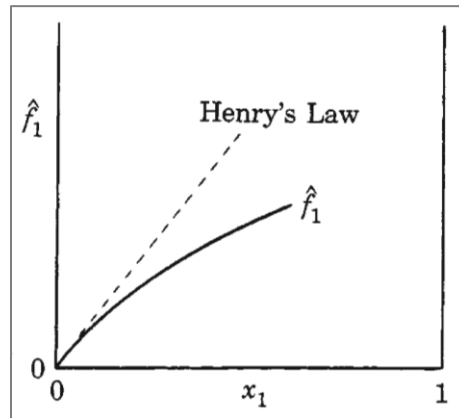
Figure 2.5. Solute fugacity ($\hat{f}_1$) vs. solute mole fraction (x_1).[20]

For a better understanding, the derivation of Henry's constant is shown in the following. Henry's constant is defined as the slope of Henry's law linear representation in Figure 2.5:

$$H \equiv \lim_{x_1 \to 0} \frac{\hat{f}_1}{x_1} \qquad (2.\text{XV})$$

Where,

x_1: solute mole fraction in the liquid-phase

$\hat{f}_1$: fugacity of the solute in solution

This definition applies for a temperature T, and pressure equal to the vapor pressure of the pure solvent (P_2^{sat}).

The activity coefficient of the solute (γ_1) at infinite dilution is defined as

$$\lim_{x_1 \to 0} \gamma_1 = \lim_{x_1 \to 0} \frac{\hat{f}_1}{x_1 f_1} = \frac{1}{f_1} \lim_{x_1 \to 0} \frac{\hat{f}_1}{x_1} \qquad (2.\text{XVI})$$

Where,

γ_1: activity coefficient of the solute

f_1: fugacity of pure solute

Combining equations 2.XV and 2.XVI

$$f_1 = \frac{H}{\gamma_1^\infty} \qquad (2.\text{XVII})$$

Where,

∞: infinite-dilution.

Because of H and γ_1^∞ are evaluated at P_2^{sat}, the same pressure applies to f_1. However, pressure does not have a significant effect on liquids fugacity, therefore it might be neglected. The γ_1 can be expressed by the following equation,

23

$$\gamma_1 \equiv \frac{\hat{f}_1}{x_1 f_1} = \frac{y_1 P \hat{\emptyset}_1}{x_1 f_1} \qquad \text{(2.XVIII)}$$

Where,

$^{\infty}$: infinite-dilution.

$\hat{\emptyset}_1$: fugacity coefficient of solute in solution

y_1: solute mole fraction in the vapour-phase

P: absolute pressure (kPa)

Combining 2.XVII and 2.XVIII,

$$\gamma_1 = \frac{y_1 P \hat{\emptyset}_1 \gamma_1^{\infty}}{x_1 H} \qquad \text{(2.XIX)}$$

Rewriting the previous equation,

$$y_1 = \frac{x_1 (\gamma_1 / \gamma_1^{\infty}) H}{P \hat{\emptyset}_1} \qquad \text{(2.XX)}$$

For the solvent,

$$y_2 = \frac{x_2 \gamma_2 P_2^{sat}}{P \emptyset_2} \qquad \text{(2.XXI)}$$

Knowing that,

$$y_1 + y_2 = 1 \qquad \text{(2.XXII)}$$

Combining equations 2.XX, 2.XXI, and 2.XXII

$$P = \frac{x_1 (\gamma_1 / \gamma_1^{\infty}) H}{\hat{\emptyset}_1} + \frac{x_2 \gamma_2 P_2^{sat}}{\emptyset_2} \qquad \text{(2.XXIII)}$$

The treatment applied to γ_1, it is also applied to γ_1^{∞}. For vapor-liquid equilibrium:

$$\hat{f}_1 = \hat{f}_1^{\,l} = \hat{f}_1^{\,v} = y_1 P \hat{\emptyset}_1 \qquad \text{(2.XXIV)}$$

24

Dividing by x_1

$$\frac{\hat{f}_1}{x_1} = P\widehat{\emptyset}_1 \frac{y_1}{x_1} \tag{2.XXV}$$

Combining 2.XV and 2.XXV

$$H = P_2^{sat}\widehat{\emptyset}_1^{\infty} \lim_{x_1 \to 0} \frac{y_1}{x_1} \tag{2.XVI}$$

Finally,

$$H \equiv \frac{y_1}{x_1} \tag{2.XXVII}$$

3.1.2 Henry's constant temperature-dependence

This constant is temperature-dependent and it is different for each gas-liquid system.[16,19] Literature[16,19] reports that at higher temperature the solubility of the gas in the liquid decreases. However, Carroll[21] states that this is not always the case and that the effect of the temperature on the gas solubility depends on the nature of liquid and the gas.[21,22]

3.2 Vapor-liquid equilibrium

As mentioned before, Henry's constant is applicable when the system that is being studied has reached vapor-liquid equilibrium.[16,19] Therefore, it is important to define when a system reaches equilibrium. This occurs when no more changes occurred between the phases (in the case of study: gas and liquid phases) that comprise the system.[19] Some of the characteristics of a system in equilibrium are:

- The temperature of the phases are equal.[19]
- The concentration of the gas in the liquid is no longer changing.[19]
- The pressure of the system is constant.[19]

In addition, when a liquid-vapor system reaches equilibrium, then the liquid is saturated with the gas.[18]

3.3 Dissolved oxygen determination - Previous works

As shown in equation 2.XIV, to calculate Henry's law the partial pressure upon the liquid and the concentration of the gas in the liquid phase must be known.[2,16] Measuring the first one can be done with an absolute pressure gauge. Measuring the second one requires a method to quantify the amount of gas in the liquid.

Most of the methods to determine Henry's constant reported in the literature are for gases dissolved in water or aqueous phases.[22–28] For example, Mohebbi, et al. performed measurements and calculated Henry's constant for light hydrocarbons gases, such as methane and propane, in water.[22] The literature also reports methods to measure dissolved gas and then calculate Henry's constant for gases dissolved in hydrocarbons.[29–32] Most of these methods are not explained in detail, making it difficult to use them to measure dissolved gas to determine Henry's constant for other hydrocarbons or gases. McKeown and Hibbard have a somewhat detailed methodology which the present research will study, modify, and apply to the determination of dissolved oxygen in hydrocarbons (See chapter IX).[32]

4. References

(1) AntonPaar. *Service Manual Abbemat 3200 Abbemat 3100 Abbemat 3000*; 2017.

(2) Atkins, P. W. *Physical Chemistry*, 3rd ed.; Oxford University Press: Oxford, 1986.

(3) Bueche, F. J.; Hecht, E. *General Physics*, 10th ed.; Mc Graw Hill, 1997.

(4) Alberty, R. A.; Daniels, F. *Physical Chemistry*, 3ed ed.; Wiley: New York, 1966.

(5) Arnon, S. *Visible Light Communication*; Cambridge University Press, 2015. https://doi.org/10.1017/CBO9781107447981.001.

(6) Gouw, T. H.; Vlugter, J. C. Physical Properties of Fatty Acid Methyl Esters. III Dispersion. *J. Am. Oil Chem. Soc.* **1964**, *41* (7), 514–515. https://doi.org/10.1007/BF02670037.

(7) Li, J.; Heath, J. An Introduction to Capacitance Spectroscopy in Semiconductors. In *Capacitance spectroscopy of semiconductors*; Tainan, 2018; pp 1–22.

(8) Glasstone, S.; Lewis, D. *Elements of Physical Chemistry*, 2nd ed.; Macmillan: London, 1960.

(9) Kurtz, S. S. Physical Properties and Hydrocarbon Structure. In *The chemistry of petroleum hydrocarbons. Vol 1*; Reinhold Publishing Corporation: New York, 1954; pp 275–331.

(10) AntonPaar. *Service Manual: DMA^{TM} 4100/4500/5000 M SCU, DSA^{TM} 5000 / SDA^{TM} M SCU*; 2018.

(11) Ting, P. D.; Gonzales, D. L.; Hirasaki, G. J.; Chapman, W. G. Application of the PC-SAFT Equation of State to Asphaltene Phase Behavior. In *Asphaltenes, heavy oils and petroleomics*; Springer: Texas, 2007; Vol. 53, pp 1689–1699. https://doi.org/10.1017/CBO9781107415324.004.

(12) Nahar, S. N. Phase - Separation Characteristics of Bitumen and Their Relation to Damage - Healing, Wöhrmann Print Service, Zutphen, 2016.

(13) Taylor, S. D.; Czarnecki, J.; Masliyah, J. Refractive Index Measurements of Diluted Bitumen Solutions. *Fuel* **2001**, *80* (14), 2013–2018. https://doi.org/10.1016/S0016-2361(01)00087-4.

(14) Wattana, P.; Wojciechowski, D. J.; Bolaños, G.; Fogler, H. S. Study of Asphaltene Precipitation Using Refractive Index Measurement. *Pet. Sci. Technol.* **2003**, *21* (3–4), 591–613. https://doi.org/10.1081/LFT-120018541.

(15) Angle, C. W.; Long, Y.; Hamza, H.; Lue, L. Precipitation of Asphaltenes from Solvent-Diluted Heavy Oil and Thermodynamic Properties of Solvent-Diluted Heavy Oil Solutions. *Fuel* **2006**, *85* (4), 492–506. https://doi.org/10.1016/j.fuel.2005.08.009.

(16) Cengel, Y. A.; Boles, M. A. *Termodinámica*, 7th ed.; Mc Graw Hill: Mexico D.F, 2012.

(17) Poling, B.; Prausnitz, J.; O'Connell, J. *The Properties of Gases and Liquids*, 5th ed.; Mc Graw Hill, 2001.

(18) Smith, J. M.; Van Ness, H. C.; Abbott, M. M. *Introduction to Chemical Engineering Thermodynamics*, 7th ed.; Mc Graw Hill, 2005.

(19) Carroll, J. J. What Is Henry's Law? *Chem. Eng. Prog.* **1991**, *9*, 48–52.

(20) Perry, R.; Green, D. *Perry's Chemical Engineer's Handbook*; Mc Graw Hill, 1999.

(21) Carroll, J. J. Henry's Law Revisited. *Chem. Eng. Prog.* **1999**, *1*, 49–56.

(22) Mohebbi, V.; Naderifar, A.; Behbahani, R. M.; Moshfeghian, M. Determination of Henry's Law Constant of Light Hydrocarbons Gases at Low Temperature. *J. Chem. Thermodyn.* **2012**, *51*, 8–11. https://doi.org/10.1016/j.jct.2012.02.014.

(23) Nirmalakhandan, N.; Brennan, R. A.; Speece, R. E. Predicting Hernry's Law Constant and the Effect of Temperature on Henry's Law Constant. **1997**, *31* (6), 1471–1481.

(24) Costa Gomes, M. F.; Grolier, J.-P. Determination of Henry's Law Constants for Aqueous Solutions of Tetradeuteriomethane between 285 and 325 K and Calculation of the H/D Isotope Effect. *Phys. Chem. Chem. Phys.* **2001**, *3*, 1047–1052. https://doi.org/10.1039/b008755f.

(25) Kutsuna, S. Experimental Determination of Henry's Law Constants of Difluoromethane (HFC-32) and the Salting-out Effects in Aqueous Salt Solutions Relevant to Seawater. *Atmos. Chem. Phys.* **2017**, *17* (12), 7495–7507. https://doi.org/10.5194/acp-17-7495-2017.

(26) Levy, J. B.; Hornack, F. M.; Levy, M. A. Simple Determination of Henry's Law Constant for Carbon Dioxide. *J. Chem. Educ.* **1987**, *64* (3), 260–261. https://doi.org/10.1021/ed064p260.

(27) Hiatt, M. H. Determination of Henry's Law Constants Using Internal Standards with Benchmark Values. *J. Chem. Eng. Data* **2013**, *58* (4), 902–908. https://doi.org/10.1021/je3010535.

(28) Vendruscolo, F.; Rossi, M. J.; Schmidell, W.; Ninow, J. L. Determination of Oxygen Solubility in Liquid Media. *ISRN Chem. Eng.* **2012**, *2012*, 1–5. https://doi.org/10.5402/2012/601458.

(29) Fischer, K.; Noll, O.; Gmehling, J. Experimental Determination of the Oxygen Solubility in Benzene. *J. Chem. Eng. Data* **2001**, *46* (6), 1504–1505. https://doi.org/10.1021/je010163i.

(30) Yaffe, D.; Cohen, Y.; Espinosa, G.; Arenas, A.; Giralt, F. A Fuzzy ARTMAP-Based Quantitative Structure-Property Relationship (QSPR) for the Henry's Law Constant of Organic Compounds. *J. Chem. Inf. Comput. Sci.* **2003**, *43* (1), 85–112. https://doi.org/10.1021/ci025561j.

(31) Dias, A. M. A.; Bonifácio, R. P.; Marrucho, I. M.; Pádua, A. A. H.; Costa Gomes, M. F. Solubility of Oxygen in N-Hexane and in n-Perfluorohexane. Experimental Determination and Prediction by Molecular Simulation. *Phys. Chem. Chem. Phys.* **2003**, *5* (3), 543–549. https://doi.org/10.1039/b207512c.

(32) Mckeown, A. B.; Hibbard, R. R. Determination of Dissolved Oxygen in Hydrocarbons. *Anal. Chem.* **1956**, *28* (9), 1490–1492. https://doi.org/10.1021/ac60117a044.

CHAPTER III – PLANNING OF EXPERIMENTAL WORK FOR A FUNDAMENTAL STUDY OF MOLAR REFRACTIVITY AND OXYGEN SOLUBILITY

In this chapter, the criteria to select the model compounds used in the present investigation are explained. In addition, the specifications of the instruments used for the refractive index and density studies are shown, highlighting the reasons to use these particular instruments.

1. Introduction

"Every minute you spend in planning saves 10 minutes in execution…"[1]. Before starting the experimental work, the selection of reagents, and instruments was done, and the experimental procedure was developed.

The criteria used to select the instruments and reagents are explained in this chapter, as well as the experimental methodologies, which are common to more than one chapter. The current section is not part of the experimental work, but it presents all the work done in preparation for the experimental work.

The planning for the molar refractivity study, as well as the dissolved oxygen determination research, will be explained.

2. Refractive index and molar refractivity

2.1   Compound groups selection

As mentioned in chapter I, the objective of this study is to work with 8 different compound groups. To select these compound groups, the following parameters were considered:

- **Presence in the bitumen:** using compound classes generally found in bitumen as the first screening criterion.[2]
- **Relevance to the petrochemical industry:** if a compound class that is not present in the bitumen is of interest for the petrochemical industry, it was also considered.
- **Safety:** if a compound class fulfills any or both of the previous criteria but is highly toxic, it was excluded from the study.

The compound groups considered at first instance were: alkanes, alkenes, alkyl aromatics, sulfur compounds, nitrogen compounds, cyclic compounds, and carboxylic acids because they can be found in bitumen.[2,3] Alkynes were chosen to study the effect of single, double, and triple bonds on the density and refractive index.

However, some nitrogen compounds, such as pyridine, can be harmful to human life if not properly handled, therefore, this compound class was excluded from the final list of compound groups.[4] Instead, alcohols were chosen because of their relevance to organic chemistry, and their chemical flexibility: they can be formed from different compounds and also transform into many others.[5]

Finally, the selected groups were: alkanes, alkenes, alkynes, alkyl aromatics, cyclic compounds, carboxylic acids, sulfur compounds, and alcohols.

2.2   Criteria to model compound selection

The criteria used to choose specific reagents, in order of selection, were the number of carbons, purity, physical properties, price, safety, and availability. The method of selection was sequential, for example, does the number of carbons fall in the range six to sixteen carbons? If the answer was positive, the next criterion was tested.

- **Number of carbon** was chosen to be in the range of six to sixteen carbons when possible.

- **Purity,** reagents should have an assay of 95% or above.

- **Melting and boiling point**, model compounds in liquid state in the temperature range of study were preferred.

- **Price**, the reagents must have an affordable price.

- **Safety,** a highly important criterion, carcinogenic reagents were avoided when possible.

- **Availability**, due to time constraint and the long lead times that take for ordered reagents to reach the laboratory, reagents available in the laboratory were given preference

9 model compounds were selected per compound group. They are listed in their corresponding chapters.

2.3 Equipment selection

To accomplish the objective of this project, the data collected for refractive index and density must be highly precise, therefore the criterion used to select the instruments to measure these properties was the lowest readability available in the market for the instruments. Table 3.1 shows the instruments selected and their readability.

Table 3.1. Instruments used in the refractive index research

Equipment	Description	Temperature (℃)
Density meter	Brand: Anton Paar Model: DMA™ 5000 M. Readability: ($\pm$ 0.001) kg/m^3	Range: -25.000 – 100.000 Readability: $\pm$0.001
Refractometer	Brand: Anton Paar Model: Abbemat 500 Readability: ($\pm$ 0.000001)	Range: 4.00 – 85.00 Readability: $\pm$0.01
Sonicator	Brand: Branson Model: 2800 Frequency: 40 kHz	-

In addition, the density meter and the refractometer shown in table 3.1 were used exclusively for the present research.

2.4 Procedure to collect refractive index data

The aim was to collect refractive index highly precise data at 5 different temperatures for each model compound. The data for the model compounds were collected at the same temperatures so that it can be compared. The selected temperatures were 10, 25, 45, 65 and 85 °C. The main constraints to select these temperatures were the temperature range of the refractometer $(4.00 \pm 0.01$ to $85.00 \pm 0.01)$ °C, and the water condensation that was observed in the measuring cell at approximately 5 °C.

On the other hand, time was also a constraint, it was preferred to start and finish the measurements of one model component on the same day to ensure that room conditions, such as pressure, temperature, and humidity were as constant as possible throughout the whole experiment. Room conditions were recorded using a digital barometer, Fisherbrand Traceable®. Because the density meter takes a long time to stabilize when a new temperature is set, it was considered that 5 temperatures were the maximum practical number of measurements that could be done in one day. This will be explained in more detail in Section 2.6.

It is important to mention that, it was not possible to measure the properties at all the desired temperatures for all the model compounds, due to their boiling and freezing point. To measure density with the instrument indicated in Table 3.1, a liquid sample is required. In addition, all the measurements were done with a wavelength of 589 nm.

2.5 Methodology to collect refractive index data

The refractometer measurement cell and lid were cleaned with approximately 0.5 mL of ethanol and dried with clean and dry soft tissue paper. After, the cell and lid were cleaned with 0.5 mL of the model compound that was going to be measured and dried with clean and dry soft tissue paper. Then, the desired lowest temperature of analysis, (10.00 ± 0.01) °C, was set. When the equipment reached the desired temperature, 1 mL of the model compound was placed on the measurement cell and covered with the lid. The refractive index is not volume sensitive,

33

however, to keep the measurements as comparable as possible a 1 mL volume was set as a fixed value. The volume of the sample was measured using a micropipette of 1 µL of capacity, Cat No: S902432H from Fisher Scientific, and the same tip was used until all the refractive index measurements were finished for the model compound being analyzed.

The analysis was started and the first value measured by the instrument was discarded, to allow the equipment to stabilize. The next three values measured by the instrument were recorded. Three values were recorded to account for the equipment error. After these three measurements, the cell was dried using a clean and dry soft tissue paper. Then, a new 1 mL aliquot of the model compound was placed on the measuring cell. Three measurements were recorded for the second aliquot, and the cell was dried again. This methodology was repeated a third time, to account for researcher variability.

In the end, three aliquots were used and nine values of refractive index were recorded for one model compound at (10.00 ± 0.01) °C. Once all the measurements at (10.00 ± 0.01) °C were completed, the equipment was set at (25.00 ± 0.01) °C, and the methodology was repeated. Consecutively, the same was done at (45.00 ± 0.01), (65.00 ± 0.01) and (85.00 ± 0.01) °C. The temperature was changed from lower to higher to optimize the stabilization time of the instrument.

2.5.1 Water check

To check that the numerical values of this instrument were not just precise but accurate, a water check was done to ensure that the equipment was calibrated. For this check, ultra-pure water, provided by Anton Paar, was used. The measuring cell was cleaned first with ethanol and then with ultra-pure water, following the steps explained before. Then, ultra-pure water was placed on the cell and the first measuring was done. The refractive indices of three aliquots were measured.

In Table 3.2, the average result per check is shown for all the checks done for the present research. A first check was done before starting the measurements, afterward, checks were done periodically after every 18 reagents were analyzed.

Table 3.2. Refractometer ultra-pure water check at (20.00 ± 0.01) °C.

Check Number	Average refractive index measured (n ± 0.000002) nD	Average measured deviation[a] (Δn ± 0.000003) nD	Barometric pressure (Patm±2) (mb)
1	1.333001	0.000014	924
2	1.333000	0.000013	943
3	1.332999	0.000012	933
4	1.333002	0.000015	945
5	1.333005	0.000018	934

[a] Refractive index reference value for ultra-pure water: (1.332987± 0.000001) nD at (20.00 ± 0.01) °C.

In Table 3.2, it is shown that the deviation is smaller than 0.000100 nD, which is the maximum deviation defined by the equipment, and smaller than 0.000050 nD, which is the maximum acceptable deviation defined by the researcher. Therefore, the calibration of the instrument was not required.

2.5.2 Data accuracy verification

To verify the accuracy of the data, the measured refractive index of water at (20.00 ± 0.01) °C was compared to the data available in the literature[6]. Figure 3.1 shows the average value of each set of data, plotted with their standard deviation.
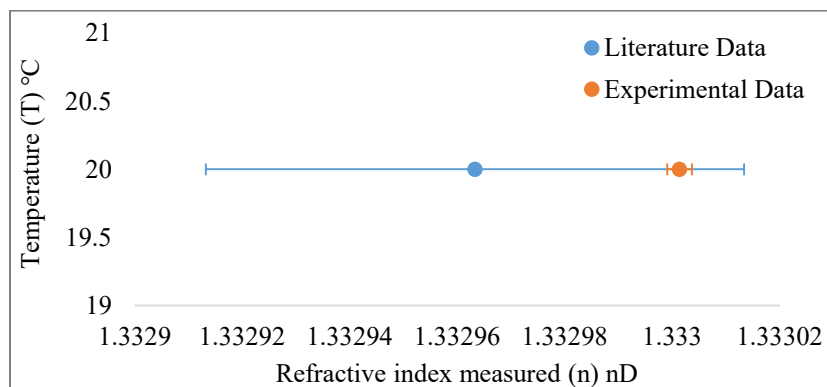
Figure 3.1. Comparison between experimental and literature[6] refractive index of water at 20 °C and 589 nm.

As can be seen in the previous figure, the experimental value has low standard deviation and it overlaps with the literature[6] data. It is important to mention that only the

literature[6] data measured at experimental conditions, 20 °C and 589 nm, was considered. Also, the literature[6] does not specify which water was used, distilled, ultra-pure, or some other type, which could explain the relatively large standard deviation of the literature[6] data.

2.6   Procedure to collect density data

Similar to the refractive index procedure, the objective was to collect very accurate density data at 5 different temperatures for each model compound. The temperatures used were the same as the refractive index, to enable the data correlation. The selected temperatures were 10, 25, 45, 65 and 85 °C, which are within the temperature range of the density meter (-25.000 ± 0.001 – 100.000 ± 0.001) °C.

As mentioned before, time was also a constraint, the density meter takes between 1 h to stabilize at (10.000 ± 0.001) °C, to approximately 2 h to stabilize at (85.000 ± 0.001) °C. The methodology was developed from low to high temperatures to minimize its stabilization time, but due to the high accuracy data no measurement was taken until the instrument indicate that the desired temperature was reached (i.e. (10.000 ± 0.001) °C). Therefore, it was considered that density measurements at 5 temperatures were the maximum that could be done in one day.

It was not possible to measure the density of all the model compounds at all the desired temperatures, due to the reagents approaching their freezing or boiling point.

2.7   Methodology to collect density data

The sample tube was cleaned with approximately 2mL of ethanol by injecting the sample to equipment and moving the plunger of the syringe in and out several times to create air bubbles, which improved the cleaning action after the sample tube was dried with air. Once the sample tube was dried, a new syringe was used to clean the sample tube the sample following the same procedure as with the ethanol.

A third new syringe was used to inject 2mL of the sample, avoiding to inject air bubbles to the tube sample. The sample was injected, leaving approximately 1 cm of the sample in the waste tube, and 0.5 to 1 mL of sample in the syringe (See figure 3.2). The column of liquid before and after the sample tube helps to ensure that there is no air in the sample tube.
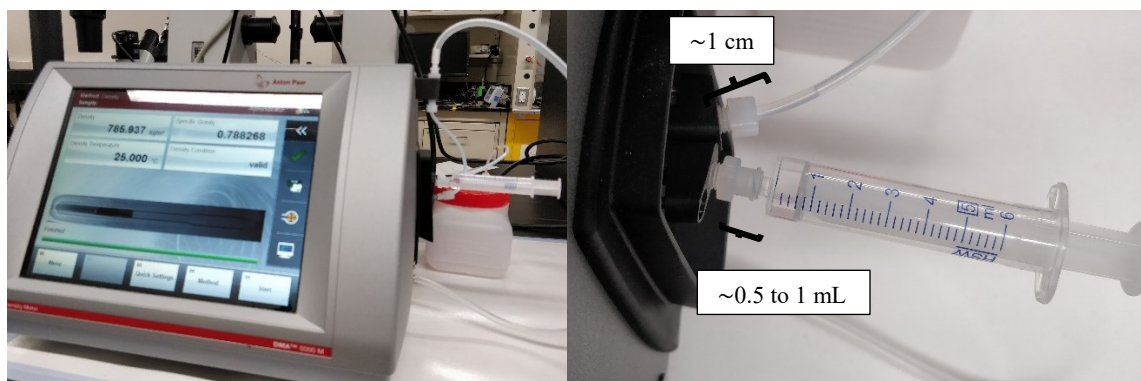
Figure 3.2. Density meter, sample injection specifications.

Then, it was checked that air bubbles were not present in the sample tube. If bubbles were located in the sample tube, a new 2 mL aliquot was injected after drying the sample tube. If bubbles were still present, the sample was put on a close jar on a sonicator for 5 min. to remove the air of the sample. After, using the third syringe, a new 2 mL aliquot of the sample was injected. The sonicator was often used for the alcohols and carboxylic acids compound classes, while for the other groups it was rarely used.

When the instrument reached exactly (10.000 ± 0.001) °C, the first measurement was discarded, to allow the equipment to stabilize. The following three measurements were collected, to account for the instrument error. After the next temperature, (25.000 ± 0.001) °C was set, and when the equipment reached the desired temperature, the measurements were taken following the previous steps. This was repeated with (45.000 ± 0.001), (65.000 ± 0.001) and (85.000 ± 0.001) °C. When all the measurements were done, the remaining sample in the syringe was injected, the syringe was removed and the sample tube was dried with air.

Using the third syringe, a second aliquot was injected in the sample tube, and the measurements were done. A third aliquot was placed in the sample tube, and the methodology

37

was repeated to account for researcher variability. In the end, three aliquots were injected, and nine values of density were recorded for one model compound at each one of the temperatures.

2.7.1 Air and water checks

To check that the numerical values of the density meter were not just precise but accurate, water checks were done to ensure that the equipment was calibrated. In addition, air checks were done to verify if the tube sample was clean and in good conditions.

Water check

Ultra-pure water, provided by Anton Paar, was used to do the water check following the method explained in section 2.7. First, the sample tube was cleaned with 2 mL of ethanol and, dried with air. Then the sample tube was cleaned with 2 mL of ultra-pure water and dried. After, 2 mL of ultra-pure water was injected into the sample tube. At last, the check was done recording three measurements per aliquot, three aliquots were analyzed.

In Table 3.3, the average result per check is shown for all the checks done for the present research. As done for the refractive index, a first check was done before starting the data collection, afterward, the check was done periodically after every 18 reagents were analyzed.

Table 3.3. Density meter ultra-pure water check at (20.000 ± 0.001) °C

Check number	Average density measured $(\rho \pm 0.000002)$ (g/cm^3)	Measured deviation $(\Delta\rho \pm 0.000003)$ (g/cm^3)[a]
1	0.998207	0.000004
2	0.998205	0.000002
3	0.998204	0.000001
4	0.998203	0.000000
5	0.998199	0.000004

[a] Density reference value for ultra-pure water: 0.998203 g/cm^3 at (20.000 ± 0.001) °C.

In table 3.3, it can be seen that the deviations are less than 0.000005 g/cm^3, and smaller than the maximum deviation defined by the equipment 0.000050 g/cm^3. Therefore, the calibration of the instrument was not required.

Air check

For the air check, the sample tube was cleaned with ethanol and dried with air for approximately 5 min, ensuring that the sample tube was completely dry. Then the check was done. After air was blown through the sample tube, and a second measurement was done. This was repeated a third time. An average density and deviation were calculated per check. The results are shown in table 3.4. As done for the previous check, a first check was done before starting the measurements, afterward, checks were done periodically after the analysis of every 18 reagents.

Table 3.4. Density meter air check at (20.000 ± 0.001) °C

Measurement number	Density measured (ρ± 0.000002) (g/cm³)	Reference density (ρ_R± 0.000002) (g/cm³)	Measured deviation ($\Delta\rho$± 0.000003) (g/cm³)	Barometric pressure (Patm±2) (mb)
1	0.001106	0.001105	0.000001	924
2	0.001108	0.001105	0.000003	943
3	0.001109	0.001105	0.000004	933
4	0.001105	0.001105	0.000000	945
5	0.001106	0.001106	0.000000	934

As it can be seen in table 3.4, the deviation between the measured and reference air density values are lower than 0.000005 g/cm^3, while the maximum deviation accepted by the equipment is 0.000050 g/cm^3. Therefore, the calibration of the equipment was not required.

2.7.2 Data accuracy verification

To verify the accuracy of the data, the measured density of water at (20.00 ± 0.001) °C was compared to the data available in the literature[6]. Figure 3.3 shows the average value of each set of data, plotted with their standard deviation.
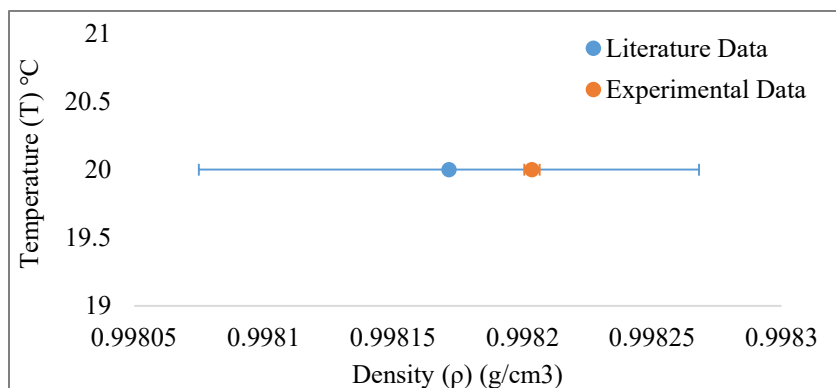
Figure 3.3. Comparison between experimental and literature[6] density of water at 20 °C.

As can be seen in the previous figure, the experimental value has low standard deviation and it overlaps with the literature[6] data.

2.8   Calculations

In this section, the calculations done to process the data are shown.

2.8.1 Molar refractivity

The molar refractivity is an intrinsic and temperature invariant property. However, there is not one but four correlations in the literature[7] used to calculate the molar refractivity. These equations are formulated as a function of refractive index, density, and molar mass. The aim of this research is to use the high precision data collected to verify which correlation better expresses the empirical data. The molar refractivity calculated with the best equation would be constant or the least temperature invariant.

The correlations to be analyzed are equations 2.IX, 2.X, 2.XI, and 2.XII from chapter II, for ease of reference they are repeated in this chapter.

$$R_M = (n^2 - 1) \cdot \frac{M}{\rho} \qquad\qquad\qquad (2.IX)$$

Berthelot [7]

Where,

R_M: molar refractivity (cm^3/mol)

n: refractive index (nD)

M: molar weight (g/mol)

ρ: density (g/ cm^3)

$$R_M = (n - 1) \cdot \frac{M}{\rho} \qquad\qquad\qquad (2.X)$$

Gladstone & Dale[7,8]

$$R_M = \left(\frac{n^2 - 1}{n^2 + 2}\right) \cdot \frac{M}{\rho} \qquad\qquad\qquad (2.XI)$$

Lorentz – Lorenz [7]

$$R_M = \left(\frac{n^2 - 1}{n + 0.4}\right) \cdot \frac{M}{\rho} \qquad\qquad\qquad (2.XII)$$

Eykman [7]

2.8.2 Atomic refraction, and group contribution

The molar refractivity of a sample can also be calculated as a weighted sum of refractivities of the elements or groups present in it. The refractivity of an element (i.e. C) is called atomic refraction, while that of a group (i.e. C-H) is known as group contribution.

Atomic refraction and group contribution were calculated only for the least bias correlation for molar refractivity found after processing of all the experimental data. The atomic refraction equation is the following,

$$R_M = b_B \cdot A_D + b_T \cdot A_T + \sum_{i=1}^{N}(A_i \cdot k_i) \qquad\qquad (2.XIII)[7]$$

Where,

N: quantity of elements present in the reagent structure

k_i: number of times that the element i is in the reagent structure

A: atomic refraction (cm^3/mol)

b: number of j bonds present in the structure

$_D$: double bond

$_T$: triple bond

For group contribution the equation is the following:

$$R_M = \sum_{i=1}^{y}(G_i \cdot x_i) \qquad (2.XIV)^7$$

Where,

y: quantity of groups present in the reagent structure

x_i: number of times that the group i is in the reagent structure

G_i: group contribution of the group i (cm^3/mol)

These equations were solved using a system of two equations and two unknown variables, by using the molar refractivity of *n*-hexane and *n*-heptane the atomic refraction for C, and H was calculated; similarly the group contribution for C-H and C-C. The calculated refractivities were validated using the molar refractivity of the other model compounds.

3. Measurement of oxygen solubility in hydrocarbons

The oxygen solubility study was done to advance the research beyond the assumptions made in another study to calculate diffusion and mass transfer coefficients.[9] Contrary to the refractive index and density study where a common materials and methodology were used throughout the research, the determination of oxygen solubility was done with two different approaches. Each approach will be explained separately in chapters IX and X.

4. References

(1)   Tracy, B. Quotable Quote https://www.goodreads.com/quotes (accessed Nov 23, 2019).

(2)   Strausz, O.; Lown, E. *The Chemistry of Alberta Oil Sands, Bitumen and Heavy Oil*; Alberta Energy Research Institute: Calgary, 2003.

(3)   Montoya Sánchez, N.; de Klerk, A. Autoxidation of Aromatics. *Appl. Petrochemical Res.* **2018**, *8* (2), 55–78. https://doi.org/10.1007/s13203-018-0199-4.

(4)   Magee, P. E. Nitrogen as Health Hazard. *R. Swedish Acad. Sci.* **2019**, *6* (2), 123–125.

(5)   Simmonds, C. *Alcohol. Its Production, Properties, Chemistry and Industrial Applications*; London, 1919.

(6)   RELXGroup. Reaxys database https://www.reaxys.com/#/login (accessed Sep 20, 2005).

(7)   Kurtz, S. S. Physical Properties and Hydrocarbon Structure. In *The chemistry of petroleum hydrocarbons. Vol 1*; Reinhold Publishing Corporation: New York, 1954; pp 275–331.

(8)   Gladstone, J. H.; Dale, T. P. Researches on the Refraction, Dispersion and Sensitiveness of Liquids. *Philos. Trans. R. Soc. A* **1863**, *153*, 317–343.

(9)   Siddiquee, M. N.; De Klerk, A. In Situ Measurement of Liquid Phase Oxygen during Oxidation. *Ind. Eng. Chem. Res.* **2016**, *55* (23), 6607–6618. https://doi.org/10.1021/acs.iecr.6b00949.

CHAPTER IV - FUNDAMENTAL STUDY OF MOLAR REFRACTIVITY WITH LINEAR ALKANES AS MODEL COMPOUNDS

In this chapter, the accuracy of the refractive index and density data collected for linear alkanes is established. Furthermore, the best molar refractivity correlation for the selected model compounds is found.

Abstract

The present chapter seeks to revisit and evaluate some of the unsolved fundamental issues about refractive index and molar refractivity. Literature reports different correlations to calculate the molar refractivity; hence, the main objective of this chapter is to evaluate such correlations using linear alkanes as model compounds.

To accomplish this, the first step was to compare the refractive index and density data to literature as an indirect indication of accuracy using *n*-hexane, as this compound has been widely studied before and there is data available in the literature. Once the experimental data was collected and a good agreement with the literature was established, the correlations to calculate molar refractivity were evaluated. Concluding that the best correlation is that by Eykman $\left(R_M = \left(\frac{n^2-1}{n+0.4} \right) \cdot \frac{M}{\rho} \right)$.

Lastly, the atomic refraction and group contribution were calculated for the molar refractivity calculated by Eykman correlation, concluding that both of them can be used to calculate the molar refractivity of linear alkanes resulting in comparable values.

Keywords: *Alkanes, n-hexane, density, refractive index, molar refractivity, Eykman.*

1. Introduction

The fundamental aspect that the present research aims to revisit and resolve is related to molar refractivity. Molar refractivity is a temperature invariant and intrinsic property.

However, literature[1] reports different equations to correlate molar refractivity, refractive index, molar mass, and density. To assess these correlations, high precision and accurate refractive index and density data are required. The data should be collected at different temperatures so that the temperature invariability of the molar refractivity can be used as criteria to determine which correlation better expresses the empirical data.

As mentioned in Chapter III, data sets from different compound classes would be collected to analyze the molar refractivity correlations. Linear alkanes were selected as the first compound class to study. Alkanes comprise compounds exhibiting single bonds connecting carbon to carbon (C-C) and carbon to hydrogen (C-H) atoms.[2] In addition, literature[3–5] about the refractive index and density of linear alkanes is widely available.

To sum up, the objective of this section is to assess the accuracy of the collected data by comparing it to literature[3–5] data and to evaluate the available molar refractivity correlations to determine which one better expresses the empirical data.

2. Experimental

2.1   Materials

The selected alkanes are listed in Table 4.1. As can be seen, the selected alkanes are linear, branched alkanes were excluded with the aim of studying the effect of the length of the linear carbon chain.

Table 4.1. Linear alkanes used in the present research

| Reagent | CASRN[a] | Structure | Purity (wt %) | | Supplier |
			Supplier[b]	FID[c]	
n-Hexane	110-54-3	$CH_3(CH_2)_4CH_3$	>99	99.2	Acros Organic
n-Heptane	142-82-5	$CH_3(CH_2)_5CH_3$	99.8	99.5	Fisher
n-Octane	111-65-9	$CH_3(CH_2)_6CH_3$	>99	99.7	Sigma-Aldrich
n-Nonane	111-84-2	$CH_3(CH_2)_7CH_3$	>99	99.6	Acros Organic
n-Decane	124-18-5	$CH_3(CH_2)_8CH_3$	>99	99.9	Sigma-Aldrich
n-Dodecane	112-40-3	$CH_3(CH_2)_{10}CH_3$	99	99.9	Sigma-Aldrich
n-Tetradecane	629-59-4	$CH_3(CH_2)_{12}CH_3$	>99	99.6	Sigma-Aldrich
n-Pentadecane	629-62-9	$CH_3(CH_2)_{13}CH_3$	>99	99.8	Aldrich
n-Hexadecane	544-76-3	$CH_3(CH_2)_{14}CH_3$	99	99.3	Sigma-Aldrich

[a] CASRN: Chemical Abstracts Services Registry Number

[b] Purity of the material guaranteed by the supplier; the material was not further purified.

[c] Purity calculated based on peak area obtained by GC-FID analysis

In Table 4.1, it can be observed that the only component that has a lower purity than the one indicated by the supplier was *n*-heptane.

2.2   Equipment, procedures, methodologies, and calculations

For details about any of the equipment, procedures, methodologies, and calculations refer to Chapter III, where these topics have been extensively explained.

3. Results

Table 4.2 presents the average densities per temperature for each of the alkane model compounds listed in Table 4.1. Each density value is an average of nine measurements, the average values are reported alongside with their corresponding standard deviation. It is worth to note that the calculated standard deviation is not higher than 0.000023 (g/cm^3), and in some cases are as low as 0.000000 (g/cm^3), which means that all repeat measurements were numerically the same at the readability of the instrument.

Table 4.2. Density of selected linear alkanes at different temperatures

Model Compound	Temperature (T ± 0.001) °C	Average density (ρ ± 0.000003) g/cm³	Standard deviation (g/cm³)
n-Hexane	10.000	0.668620	0.000001
	25.000	0.655135	0.000002
	45.000	0.636622	0.000000
n-Heptane	10.000	0.692354	0.000001
	25.000	0.679622	0.000001
	45.000	0.662391	0.000000
	65.000	0.644616	0.000002
n-Octane	10.000	0.710804	0.000003
	25.000	0.698756	0.000001
	45.000	0.682421	0.000001
	65.000	0.665688	0.000000
	85.000	0.648450	0.000001
n-Nonane	10.000	0.725728	0.000002
	25.000	0.714101	0.000003
	45.000	0.697052	0.000020
	65.000	0.682394	0.000001
	85.000	0.666008	0.000001
n-Decane	10.000	0.737626	0.000000
	25.000	0.726311	0.000001
	45.000	0.711081	0.000007
	65.000	0.695626	0.000001
	85.000	0.679873	0.000001
n-Dodecane	10.000	0.756203	0.000002
	25.000	0.745322	0.000001
	45.000	0.730760	0.000000
	65.000	0.716066	0.000001
	85.000	0.701185	0.000001
n-Tetradecene	10.000	0.770037	0.000003
	25.000	0.759419	0.000001
	45.000	0.745289	0.000001
	65.000	0.731100	0.000001
	85.000	0.716799	0.000001

Table 4.2. Density of selected linear alkanes at different temperatures. Continuation

Model Compound	Temperature (T ± 0.001) °C	Average density (ρ ± 0.000003) g/cm³	Standard deviation (g/cm³)
n-Pentadecane	10.000	0.775354	0.000005
	25.000	0.764818	0.000023
	45.000	0.750852	0.000013
	65.000	0.736866	0.000001
	85.000	0.722787	0.000002
n-Hexadecane	25.000	0.769943	0.000001
	45.000	0.756102	0.000000
	65.000	0.742267	0.000000
	85.000	0.728375	0.000000

Table 4.3 shows the average refractive indices per temperature for each alkane model compound. The average is reported with their respective standard deviation. The highest standard deviation is 0.000075 nD, while the lowest 0.000001 nD. Same as the density, the average refractive indices are an average of nine measurements.

Table 4.3. Refractive index at different temperatures of the selected linear alkanes

Model Compound	Temperature (T ± 0.01) °C	Average Refractive Index (n ± 0.000003) nD	Standard deviation (nD)	Barometric pressure (Patm±0.2) (kPa)
n-Hexane	10.00	1.380536	0.000005	
	25.00	1.361271	0.000002	95.2
	45.00	1.372317	0.000001	
n-Heptane	10.00	1.392841	0.000001	
	25.00	1.385041	0.000006	95.7
	45.00	1.375270	0.000003	
	65.00	1.364311	0.000012	
n-Octane	10.00	1.402493	0.000001	
	25.00	1.395201	0.000002	
	45.00	1.385375	0.000004	96.1
	65.00	1.375553	0.000003	
	85.00	1.365352	0.000006	

Table 4.3. Refractive index at different temperatures of the selected linear alkanes. Continuation

Model Compound	Temperature (T ± 0.01) °C	Average Refractive Index (n ± 0.000003) nD	Standard deviation (nD)	Barometric pressure (Patm±0.2) (kPa)
n-Nonane	10.00	1.410283	0.000001	
	25.00	1.403253	0.000021	
	45.00	1.393727	0.000001	94.0
	65.00	1.384256	0.000001	
	85.00	1.374672	0.000002	
n-Decane	10.00	1.416656	0.000021	
	25.00	1.409837	0.000002	
	45.00	1.400410	0.000075	95.2
	65.00	1.391297	0.000021	
	85.00	1.381981	0.000021	
n-Dodecane	10.00	1.426358	0.000025	
	25.00	1.419700	0.000002	
	45.00	1.410898	0.000004	94.1
	65.00	1.402206	0.000013	
	85.00	1.393345	0.000007	
n-Tetradecane	10.00	1.433538	0.000004	
	25.00	1.427010	0.000003	
	45.00	1.418497	0.000002	94.3
	65.00	1.410279	0.000004	
	85.00	1.401579	0.000001	
n-Pentadecane	10.00	1.436345	0.000014	
	25.00	1.429954	0.000000	
	45.00	1.421409	0.000008	95.2
	65.00	1.413277	0.000008	
	85.00	1.404806	0.000006	
n-Hexadecane	25.00	1.432521	0.000003	
	45.00	1.424192	0.000018	96.0
	65.00	1.416126	0.000007	
	85.00	1.407763	0.000002	

From Tables 4.2 and 4.3, it can be noticed that some reagents have values reported just at three or four temperatures due to their boiling point, for the hexane (68 °C)[3] and heptane (98.4 °C)[3], or their freezing point, hexadecane (18 °C)[3].

4. Discussion

4.1   Assessment of data accuracy

The first step was to assess if the collected data is accurate. For this, the measured refractive index and density of *n*-hexane were compared to the data available in the literature[3]. Figure 4.1 shows that the measured density data (circular marker) overlaps with most of the data available in the literature[3] (star marker), proving that the experimental density data has a good agreement with the literature.
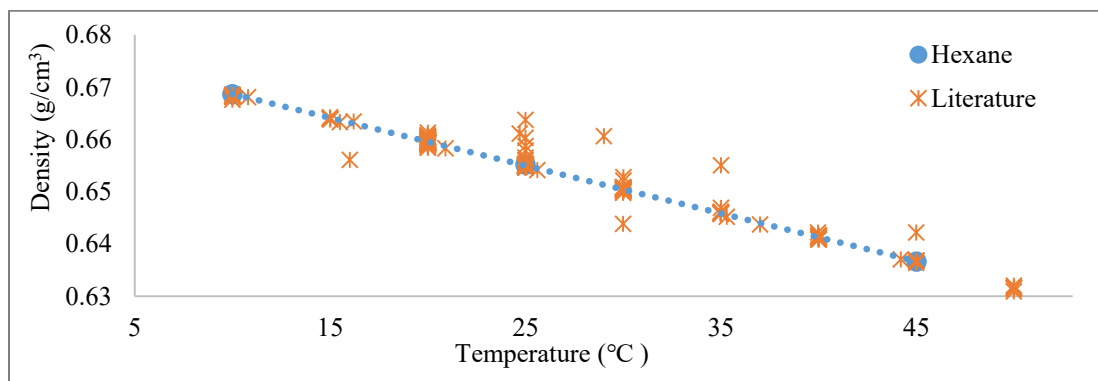
Figure 4.1. Density of hexane at different temperatures, experimental and literature data.[3]

Similarly, figure 4.2 shows the experimentally measured refractive index of *n*-hexane plotted alongside with the refractive index data available in the literature[3] for the same compound. Literature[3] data seems to be more scattered in this figure than in figure 4.1. However, the literature[3] data is concentrated around the experimental values and the two data sets overlap. This shows that both the refractive index and density data have good agreement with the literature[3] data. Moreover, it validates the experimental method used to collect the data.
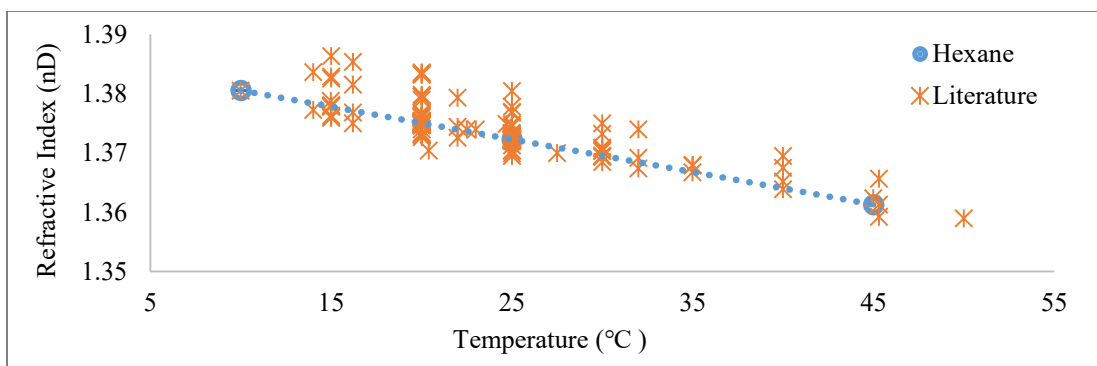
Figure 4.2. Refractive index of hexane at different temperatures, experimental and literature[3] data.

To further confirm the accuracy of the data, figure 4.3 shows three plots of refractive index vs. density for *n*-hexane, *n*-heptane, and *n*-octane respectively. In each of these plots three series are shown, experimental, Devi et al.[4], and Kashyap et al[5]. data.
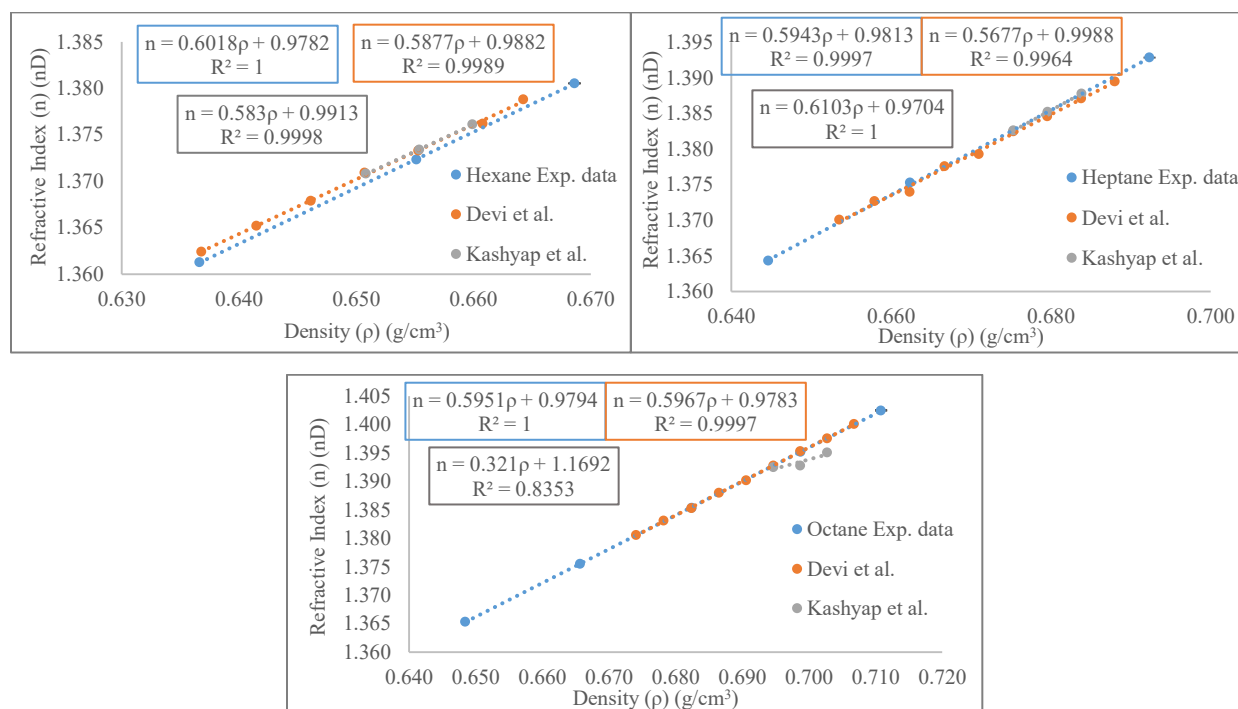
Figure 4.3. Density vs refractive index of *n*-hexane, *n*-heptane, and *n*-octane of literature[4,5] and experimental data.

The *n*-hexane plot shows that both of the literature[4,5] series overlaps, while the experimental data has a similar slope, it does not overlap. For the *n*-heptane Kashyap et al. [5]

and the experimental data seem to overlap, meanwhile, the Devi et al.[4] data intercept the other series around 0.670g/cm^3, the difference in the slopes explains why Devi et al.[4] series do not overlap with the other series. At least, for *n*-octane, Devi et al.[4] data overlap with the experimental data, while Kashyap et al.[5] do not exhibit a linear trend. A linear trend is expected in refractive index vs. density plots for hydrocarbons,[1] the fact that Kashyap et al.[5] data for *n*-octane does not follow the expected trend suggests an experimental problem with their data set.

4.2 First derivative of refractive index vs. density.

Literature[1] reports that refractive index vs. density for hydrocarbons follows linear tendency with a slope of 0.6, to verify if this applies to the studied alkanes, figure 4.4 shows a plot of refractive index vs. density and Table 4.4 lists the slope of each model.
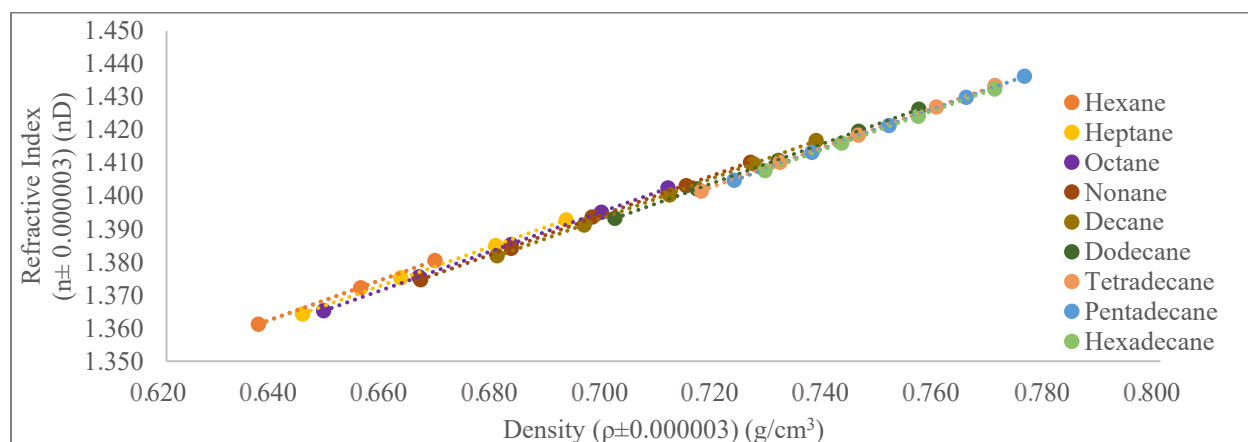
Figure 4.4. Refractive index vs. density of the selected linear alkanes.

Figure 4.4 shows that the data of the studied linear alkanes follows a linear trend and that density and refractive index increase as the carbon chain length increased. As expected, the highest density and refractive index per each model compound were found at (10.00 ± 0.01) °C.

Table 4.4 shows that there is not a direct correlation between the slope and the carbon length of the selected alkanes.

Table 4.4. Slope of the linear function of refractive index vs density
for the selected linear alkanes

Model Compound	First derivative $(dn/d\rho \pm 0.0005)$
n-Hexane	0.6018
n-Heptane	0.5943
n-Octane	0.5951
n-Nonane	0.5968
n-Decane	0.6043
n-Dodecane	0.5994
n-Tetradecane	0.5981
n-Pentadecane	0.5991
n-Hexadecane	0.5943
Average Slope	*0.598*
Standard deviation	*0.003*

Table 4.4 also shows that the average slope (0.598± 0.001) is nearly the same as reported by literature[1] (0.6). In addition, the low standard deviation (0.003) shows the low variation of the slope of refractive index with respect to density for alkanes from C_6 to C_{16}.

4.3   Molar refractivity

Table 4.5 shows the molar refractivity (Rm) at different temperatures for the alkane model compounds calculated with equations 2.IX, 2.X, 2.XI, and 2.XII from Chapter II, with the aim of evaluating the different correlations.

Table 4.5. Molar refractivity of selected linear alkanes calculated with equations 2.IX-2.XII

Model Compound	Temperature $(T \pm 0.01)$ °C	Molar Refractivity (Rm) (cm³/mol)			
		Berthelot (Eq. 2.IX) (Rm ± 0.002)	Gladstone & Dale (Eq. 2.X) (Rm ± 0.0006)	Lorentz-Lorenz (Eq. 2.XI) (Rm ± 0.0003)	Eykman (Eq. 2.XII) (Rm ± 0.0007)
	10.00	116.761	49.0482	29.8936	65.5763
n-Hexane	25.00	116.188	48.9766	29.9203	65.5572
	45.00	115.479	48.9055	29.9708	65.5658

Table 4.5. Molar refractivity of selected linear alkanes
calculated with equations 2.IX-2.XII. Continuation

Model Compound	Temperature (T ± 0.01) °C	Molar Refractivity (cm^3/mol)			
		Berthelot (Eq. 2.IX) (Rm ± 0.002)	Gladstone & Dale (Eq. 2.X) (Rm ± 0.0006)	Lorentz-Lorenz (Eq. 2.XI) (Rm ± 0.0003)	Eykman (Eq. 2.XII) (Rm ± 0.0007)
n-Heptane	10.00	136.055	56.8591	34.5316	75.8878
	25.00	135.409	56.7742	34.5577	75.8576
	45.00	134.851	56.7729	34.6538	75.9608
	65.00	133.902	56.6346	34.6775	75.8947
n-Octane	10.00	155.399	64.6827	39.1732	86.2138
	25.00	154.745	64.6061	39.2097	86.1990
	45.00	153.875	64.5077	39.2612	86.1864
	65.00	153.089	64.4438	39.3330	86.2209
	85.00	152.234	64.3599	39.3961	86.2343
n-Nonane	10.00	174.689	72.4766	43.7938	96.4982
	25.00	173.983	72.3947	43.8341	96.4827
	45.00	173.338	72.4132	43.9667	96.6354
	65.00	172.118	72.1895	43.9507	96.4649
	85.00	171.263	72.1208	44.0297	96.5041
n-Decane	10.00	194.237	80.3741	48.4753	106.9198
	25.00	193.486	80.2902	48.5215	106.9082
	45.00	192.329	80.1235	48.5539	106.8253
	65.00	191.399	80.0396	48.6313	106.8491
	85.00	190.426	79.9445	48.7040	106.8621
n-Dodecane	10.00	233.014	96.0345	57.7554	127.5841
	25.00	232.085	95.9149	57.7967	127.5404
	45.00	230.903	95.7747	57.8612	127.5075
	65.00	229.825	95.6723	57.9461	127.5241
	85.00	228.685	95.5502	58.0210	127.5184
n-Tetradecane	10.00	271.816	111.6956	67.0316	148.2464
	25.00	270.737	111.5518	67.0747	148.1860
	45.00	269.422	111.4006	67.1518	148.1564
	65.00	268.343	111.3326	67.2726	148.2328
	85.00	266.926	111.1459	67.3303	148.1621

Table 4.5. Molar refractivity of selected linear alkanes
calculated with equations 2.IX-2.XII. Continuation

Model Compound	Temperature (T ± 0.01) °C	Molar Refractivity (cm³/mol)			
		Berthelot (Eq. 2.IX) (Rm ± 0.002)	Gladstone & Dale (Eq. 2.X) (Rm ± 0.0006)	Lorentz-Lorenz (Eq. 2.XI) (Rm ± 0.0003)	Eykman (Eq. 2.XII) (Rm ± 0.0007)
n-Pentadecane	10.00	291.249	119.5432	71.6816	158.6023
	25.00	290.174	119.4153	71.7405	158.5688
	45.00	288.678	119.2190	71.8032	158.4915
	65.00	287.511	119.1373	71.9254	158.5589
	85.00	286.096	118.9684	72.0013	158.5189
n-Hexadecane	25.00	309.386	127.1873	76.3516	168.8306
	45.00	307.925	127.0216	76.4400	168.8007
	65.00	306.676	126.9289	76.5654	168.8628
	85.00	305.184	126.7501	76.6449	168.8187

To check if the calculations were performed correctly, the *n*-hexane molar refractivity at 45.00 ± 0.01 °C was compared with the data available in the literature[1] (See Table 4.6).

Table 4.6. Hexane molar refractivity reported in the literature.[1]

Data source	Temperature (T) °C	Molar Refractivity (cm³/mol)			Delta Molar Refractivity (cm³/mol)		
		Gladstone & Dale (Eq. 2.X)	Lorentz-Lorenz (Eq. 2.XI)	Eykman (Eq. 2.XII)	Gladstone & Dale	Lorentz-Lorenz	Eykman
Literature	14	48.78	29.76	65.24	0.11	0.07	0.02
	44.95	48.67	29.83	65.26			
Experimental	45.00	48.9055	29.9708	65.5658	0.2355	0.1408	0.3058

Comparing the data for *n*-hexane at 45.00 ± 0.01 °C from Table 4.5 and at 44.95 °C, from Table 4.6, it can be seen that the differences are not bigger than 0.5 cm³/mol for the molar refractivity regardless of the correlation used to calculate it. It can also be seen that only three of the four equations could be compared since Rm calculated with the correlation by Berthelot was not reported in the literature[1] that was consulted.

The next step was to find which correlation better expresses the empirical data for the selected linear alkanes. To accomplish this, the average molar refractivity was calculated per each correlation for each model compound, having a total of four average molar refractivities per compound (See Table 4.7).

This average was calculated using the Rm calculated at each of the different temperatures (See Table 4.6). However, as mentioned in Chapter II, Rm is an intrinsic property that does not depend on temperature. Therefore, the best correlation would be the one in which the calculated Rm varies the least with the change of temperature or in mathematical terms the one with the lowest standard deviation. The results of this analysis can be found in Table 4.7.

Table 4.7. Average molar refractivity and its standard deviation for the selected linear alkanes

Model Compound		Molar Refractivity (cm^3/mol)				Best Correlation
		Berthelot (Eq. 2.IX) (Rm ± 0.002)	Gladstone & Dale (Eq. 2.X) (Rm ± 0.0006)	Lorentz-Lorenz (Eq. 2.XI) (Rm ± 0.0003)	Eykman (Eq. 2.XII) (Rm ± 0.0007)	
n-Hexane	Av. Rm	116.143	48.9768	29.9282	65.5664	Eykman
	s	0.642	0.0714	0.0392	0.0096	
n-Heptane	Av. Rm	135.054	56.7602	34.6052	75.9002	Eykman
	s	0.912	0.0929	0.0713	0.0435	
n-Octane	Av. Rm	153.869	64.5200	39.2747	86.21086	Eykman
	s	1.264	0.1279	0.0906	0.0187	
n-Nonane	Av. Rm	173.078	72.3189	43.9150	96.51706	Eykman
	s	1.387	0.1545	0.0979	0.0679	
n-Decane	Av. Rm	192.403	80.1642	48.5824	106.8852	Eykman
	s	1.580	0.1925	0.0841	0.0616	
n-Dodecane	Av. Rm	230.902	95.7893	57.8761	127.5349	Eykman
	s	1.728	0.1917	0.1084	0.0300	
n-Tetradecane	Av. Rm	269.449	111.4253	67.1722	148.1967	Eykman
	s	1.927	0.2099	0.1272	0.0410	
n-Pentadecane	Av. Rm	288.741	119.2566	71.8304	158.5481	Eykman
	s	2.053	0.2270	0.1315	0.0434	
n-Hexadecane	Av. Rm	307.293	126.9720	76.5005	168.8282	Eykman
	s	1.789	0.1825	0.1302	0.0261	

Av. Rm: Average molar refractivity.   s: standard deviation.

Table 4.7 shows that even though the correlations are somewhat similar, the Rm calculated with each one of them is quite different, because of this the Rm calculated with one correlation cannot be compared to an Rm calculated with another correlation.

In addition, Table 4.7 also shows that for all of the alkanes model compounds the correlation by Eykman had the lowest standard deviation, lower by almost an order of magnitude compared to that one by Lorentz-Lorenz. The Lorentz-Lorenz correlation had the second-lowest deviation, followed by Gladstone & Dale correlation and at last, Berthelot had the biggest standard deviation.

The comparison presented in Table 4.6 indicated that the least difference in Rm calculated using literature[1] data at different temperatures, was the Rm calculated using the Eykman correlation (Eq. 2.XII). The results in Table 4.7 based on calculations using the data collected in this study, also found that the Eykman correlation resulted in the least difference in Rm values.

4.4   Atomic refraction & group contribution

In this section, the aim was to calculate the atomic refraction and group contribution for the correlation by Eykman, since in the consulted literature[1] the atomic refraction was calculated only for Lorentz-Lorenz correlation. With the Rm of *n*-hexane and *n*-heptane, the values of interest were calculated and are listed in Table 4.8.

Table 4.8. Atomic refraction and group contribution for Eykman

Atomic refraction (cm³/mol)		Group contribution (cm³/mol)	
Carbon	Hydrogen	C-H Bond	C-C Bond
6.770	1.782	3.474	3.38608

Table 4.8 shows that the C atomic refraction almost doubles the group contribution of the C-H bond, which suggested that if the Rm was calculated with either of these methods, the values will be similar. To check this, the Rm was calculated for each model compound with the atomic refraction (AR) and the group contribution (GC) equations (See equation 2.XIII and

2.XIV from Chapter II), and then these Rm were compared with the Rm calculated using the correlation by Eykman, and the results are shown in Table 4.9.

Table 4.9. Comparison between Rm calculated with the experimental data and Rm calculated with atomic refraction and group contribution for the correlation by Eykman

Model Compound	Molar Refractivity (cm^3/mol)		Average calculated value with exp. data (Rm ± 0.0007)	Delta between average exp. Rm and Rm calculated with AR or GC (cm^3/mol)
	Calculated with atomic refraction and group contribution			
n-Hexane	AR	65.5655	65.5664	0.0009
	GC	65.5664		0.0000
n-Heptane	AR	75.8992	75.9002	0.0010
	GC	75.9005		0.0003
n-Octane	AR	86.2328	86.2109	0.0219
	GC	86.2346		0.0237
n-Nonane	AR	96.5665	96.5171	0.0494
	GC	96.5686		0.0516
n-Decane	AR	106.9001	106.8852	0.0149
	GC	106.9027		0.0176
n-Dodecane	AR	127.5674	127.5349	0.0325
	GC	127.5709		0.0360
n-Tetradecane	AR	148.2347	148.1967	0.0380
	GC	148.2390		0.0423
n-Pentadecane	AR	158.5684	158.5481	0.0203
	GC	158.5704		0.0224
n-Hexadecane	AR	168.9020	168.8282	0.0738
	GC	168.9020		0.0738

AR: atomic refraction

GC: group contribution

The difference between $\left|\text{Rm}_{exp} - \text{Rm}_{AR}\right|$ and $\left|\text{Rm}_{exp} - \text{Rm}_{GC}\right|$ does not differ by more than 0.0050 cm^3/mol, therefore it appears that both, atomic refraction and group contribution, can be used to predict the molar refractivity of a linear alkane. It should further be pointed out that the numbers in Table 4.8 were calculated using the data from only two compounds, instead of by regression using the complete dataset. In the next chapter, it will be studied if double bonds, triple bonds, or heteroatoms make one method better than the other.

5. Conclusions

- The refractive index and density experimental data have a good agreement with the literature[3–5] data, providing external validation of the experimental method used to collect the data.

- The average first derivate of refractive index vs. density for the selected linear alkanes was 0.598 ± 0.001, showing that the collected data follows the same behavior as the literature[1].

- Eykman was the correlation with the least temperature-dependent variation of the Rm of linear alkanes.

- Both, atomic refraction and group contribution, resulted in comparable prediction of the molar refractivity of linear alkanes compared to the correlation by Eykman.

6. References

(1)   Kurtz, S. S. Physical Properties and Hydrocarbon Structure. In *The chemistry of petroleum hydrocarbons. Vol 1*; Reinhold Publishing Corporation: New York, 1954; pp 275–331.

(2)   Strausz, O.; Lown, E. *The Chemistry of Alberta Oil Sands, Bitumen and Heavy Oil*; Alberta Energy Research Institute: Calgary, 2003.

(3)   RELXGroup. Reaxys database https://www.reaxys.com/#/login (accessed Sep 20, 2019).

(4)   Devi, R.; Gahlyan, S.; Rani, M.; Maken, S. Thermodynamic and Acoustic Properties of Binary Mixtures of Diisopropyl Ether, Benzene and Alkanes at 298.15, 308.15 and 318.15 K: Prigogine-Flory-Patterson Theory and Graph Theory. *J. Mol. Liq.* **2019**, *275*, 364–377. https://doi.org/10.1016/j.molliq.2018.11.045.

(5)   Kashyap, P.; Rani, M.; Gahlyan, S.; Tiwari, D. P.; Maken, S. Volumetric, Acoustic and Optical Properties of Binary Mixtures of 2-Propanol with n-Alkanes (C6-C10) from 293.15 K to 303.15 K. *J. Mol. Liq.* **2018**, *268*, 303–314. https://doi.org/10.1016/j.molliq.2018.07.043.

CHAPTER V - FUNDAMENTAL STUDY OF MOLAR REFRACTIVITY WITH LINEAR ALKENES & ALKYNES AS MODEL COMPOUNDS

In the present chapter, the correlation to calculate the molar refractivity with least temperature-dependent variation for linear alkenes & alkynes model compounds is determined.

Abstract

The present chapter evaluated different correlations to calculate the molar refractivity reported in the literature using linear alkenes and alkynes as model compounds. To accomplish this refractive index and density high precision data were collected at different temperatures.

The collected data sets were used to evaluate the correlations to calculate molar refractivity. The correlation by Eykman $\left(R_M = \left(\frac{n^2-1}{n+0.4} \right) \cdot \frac{M}{\rho} \right)$ was the least biased for both of the compound classes. Then the atomic refraction and group contribution were calculated to estimate the molar refractivity calculated by Eykman correlation. It was found that both, atomic refraction and group contribution, can be used to predict the molar refractivity of linear alkenes and alkynes.

Keywords: *Alkenes, alkynes, density, refractive index, molar refractivity, Eykman.*

1. Introduction

The objective of the present chapter is to revisit and resolve fundamental aspects related to molar refractivity and refractive index. Molar refractivity is a temperature invariant and intrinsic property, but it is not clear in the literature[1] which correlation should be used to calculate it.

As mention in Chapter IV, literature[1] reports different equations to correlate molar refractivity, refractive index, molar mass, and density. High precision and accurate refractive index and density data at different temperatures are required to evaluate these correlations and discriminate between them. The data would be used to calculate molar refractivity with different correlations. The correlation in which molar refractivity is least temperature-dependent would better express the empirical data.

Data sets from different compound classes would be collected to analyze the molar refractivity correlations. Linear alkanes were studied in Chapter IV. The present chapter will study linear alkenes and alkynes. Alkenes are hydrocarbons with carbon to carbon single or double bonds (C-C or C=C), and carbon to hydrogen bonds (C-H).[2] The selected linear alkenes have only one double bond (C=C) in the first carbon.

Alkynes are also hydrocarbons with carbon to carbon single or triple bonds (C-C or C≡C), and hydrogen to carbon bonds (C-H).[2] Following the same analyzes as alkenes, the selected linear alkynes have only one triple bond (C≡C) in the first carbon. Making it possible to compare one compound class to the other.

To conclude, the collected data would be used to evaluate which molar refractivity correlation better expresses the alkenes and alkynes empirical data.

2. Experimental

2.1 Materials

The selected linear alkenes and alkynes are listed in Table 5.1. The selected model compounds are linear with the double (C=C) or triple (C≡C) bond in the first carbon. Branched, cyclic, or compounds with multiple double or triple bonds were excluded.

Table 5.1. Model compounds used in the present chapter

Compound Class	Reagent	CASRN[a]	Structure	Purity (wt %) Supplier[b]	FID[c]	Supplier
Alkene	1-Hexene	592-41-6	$CH_2 = (CH_2)_4CH_3$	97	99.3	Aldrich
	1-Heptene	592-76-7	$CH_2 = (CH_2)_5CH_3$	97	98.6	Sigma-Aldrich
	1-Octene	111-66-0	$CH_2 = (CH_2)_6CH_3$	98	99.5	Sigma-Aldrich
	1-Nonene	124-11-8	$CH_2 = (CH_2)_7CH_3$	>95	95.8	TCI
	1-Decene	872-05-9	$CH_2 = (CH_2)_8CH_3$	95	96.2	Sigma-Aldrich
	1-Undecene	821-95-4	$CH_2 = (CH_2)_9CH_3$	97	99.7	Sigma-Aldrich
	1-Dodecene	112-41-4	$CH_2 = (CH_2)_{10}CH_3$	95	96.7	Aldrich
	1-Tetradecene	1120-36-1	$CH_2 = (CH_2)_{12}CH_3$	>99.8	99.9	Sigma-Aldrich
	1-Hexadecene	629-73-2	$CH_2 = (CH_2)_{14}CH_3$	>98.5	99.9	Aldrich
Alkyne	1-Hexyne	693-02-7	$CH_2 \equiv (CH_2)_4CH_3$	97	98.9	Sigma-Aldrich
	1-heptyne	628-71-7	$CH_2 \equiv (CH_2)_5CH_3$	98	99.2	Alfa Aesar
	1-octyne	629-05-0	$CH_2 \equiv (CH_2)_6CH_3$	97	99.2	Alfa Aesar
	1-nonyne	3452-09-3	$CH_2 \equiv (CH_2)_7CH_3$	99	98.5	Sigma-Aldrich
	1-decyne	764-93-2	$CH_2 \equiv (CH_2)_8CH_3$	99	98.6	Sigma-Aldrich
	1-undecyne	2243-98-3	$CH_2 \equiv (CH_2)_9CH_3$	97	99.2	Alfa Aesar
	1-dodecyne	765-03-7	$CH_2 \equiv (CH_2)_{10}CH_3$	98	99.6	Sigma-Aldrich
	1-tetradecyne	765-10-6	$CH_2 \equiv (CH_2)_{12}CH_3$	97	99.4	Sigma-Aldrich
	1-Hexadecyne	629-74-3	$CH_2 \equiv (CH_2)_{14}CH_3$	90	95.2	Alfa Aesar

[a] CASRN: Chemical Abstracts Services Registry Number

[b] Purity of the material guaranteed by the supplier; the material was not further purified.

[c] Purity calculated based on peak area obtained by GC-FID analysis

Table 5.1 shows that the only components with lower purity than the one indicated by the supplier were 1-nonyne and 1-decyne.

2.2   Equipment, procedures, methodologies, and calculations

The details of the equipment, procedures, methodologies, and calculations are explained in Chapter III.

3. Results

Table 5.2 shows the density at different temperatures for the selected linear alkenes and alkynes. Each density value is an average of nine measurements. The density is reported with its standard deviation which is not bigger than $\pm$ 0.000025 g/cm^3 and as low as $\pm$ 0.000000 g/cm^3 showing the high repeatability of the measurement.

Table 5.2. Density at different temperatures of selected alkenes and alkynes

Compound Class	Model Compound	Temperature (T $\pm$ 0.001) °C	Average density ($\rho \pm$ 0.000003) g/cm^3	Standard deviation (g/cm^3)
Alkene	1-Hexene	10.000	0.682513	0.000003
		25.000	0.668495	0.000003
		45.000	0.649241	0.000003
	1-Heptene	10.000	0.706362	0.000011
		25.000	0.693297	0.000012
		45.000	0.675493	0.000013
		65.000	0.657140	0.000021
	1-Octene	10.000	0.723386	0.000001
		25.000	0.710994	0.000004
		45.000	0.694198	0.000004
		65.000	0.677005	0.000002
		85.000	0.659296	0.000001
	1-Nonene	10.000	0.739363	0.000021
		25.000	0.727474	0.000021
		45.000	0.711420	0.000021
		65.000	0.695066	0.000023
		85.000	0.678319	0.000024

Table 5.2. Density at different temperatures of selected alkenes and alkynes. Continuation

Compound Class	Model Compound	Temperature (T ± 0.001) °C	Average density (ρ ± 0.000003) g/cm3	Standard deviation (g/cm3)
Alkene	1-Decene	10.000	0.748622	0.000002
		25.000	0.737107	0.000004
		45.000	0.721599	0.000002
		65.000	0.705855	0.000003
		85.000	0.689808	0.000003
	1-Undecene	10.000	0.759035	0.000007
		25.000	0.747774	0.000010
		45.000	0.732662	0.000010
		65.000	0.717374	0.000012
		85.000	0.701858	0.000012
	1-Dodecene	10.000	0.765957	0.000002
		25.000	0.754952	0.000001
		45.000	0.740205	0.000000
		65.000	0.725323	0.000001
		85.000	0.710245	0.000001
	1-Tetradecene	10.000	0.778312	0.000005
		25.000	0.767630	0.000007
		45.000	0.753381	0.000007
		65.000	0.739061	0.000009
		85.000	0.724619	0.000008
	1-Hexadecene	10.000	0.777593	0.000002
		25.000	0.763678	0.000002
		45.000	0.788075	0.000001
		65.000	0.735755	0.000001
		85.000	0.749750	0.000001
Alkyne	1-Hexyne	10.000	0.726055	0.000004
		25.000	0.711477	0.000004
		45.000	0.691540	0.000004
		65.000	0.670881	0.000014

Table 5.2. Density at different temperatures of selected alkenes and alkynes. Continuation

Compound Class	Model Compound	Temperature (T ± 0.001) °C	Average density (ρ ± 0.000003) g/cm3	Standard deviation (g/cm3)
Alkyne	1-Heptyne	10.000	0.745628	0.000001
		25.000	0.732021	0.000001
		45.000	0.713539	0.000001
		65.000	0.694580	0.000001
		85.000	0.674949	0.000011
	1-Octyne	10.000	0.757708	0.000003
		25.000	0.744834	0.000005
		45.000	0.727433	0.000005
		65.000	0.709681	0.000006
		85.000	0.691453	0.000019
	1-Nonyne	10.000	0.768194	0.000011
		25.000	0.755880	0.000011
		45.000	0.739283	0.000013
		65.000	0.722433	0.000002
		85.000	0.705217	0.000010
	1-Decyne	10.000	0.774387	0.000006
		25.000	0.762488	0.000006
		45.000	0.746496	0.000006
		65.000	0.730293	0.000007
		85.000	0.713846	0.000005
	1-Undecyne	10.000	0.781888	0.000003
		25.000	0.770314	0.000002
		45.000	0.754795	0.000003
		65.000	0.739122	0.000007
		85.000	0.723236	0.000016
	1-Dodecyne	10.000	0.786579	0.000003
		25.000	0.775269	0.000003
		45.000	0.760137	0.000003
		65.000	0.744885	0.000002
		85.000	0.729456	0.000001

Table 5.2. Density at different temperatures of selected alkenes and alkynes. Continuation

Compound Class	Model Compound	Temperature (T ± 0.001) °C	Average density (ρ ± 0.000003) g/cm³	Standard deviation (g/cm³)
Alkyne	1-Tetradecyne	10.000	0.797443	0.000003
		25.000	0.786486	0.000002
		45.000	0.771890	0.000002
		65.000	0.757236	0.000002
		85.000	0.742480	0.000003
	1-Hexadecyne	25.000	0.794233	0.000001
		45.000	0.780027	0.000005
		65.000	0.765828	0.000006
		85.000	0.751573	0.000004

Table 5.3 reports the refractive indices at different temperatures for the selected model compounds. Similar to the density (see Table 5.2), the refractive indices are also an average of nine measurements and the values are reported with their standard deviation. The standard deviation of the density was not higher than ± 0.000051 nD and as low as ± 0.000000 nD.

Table 5.3. Refractive index at different temperatures of the selected alkenes and alkynes

Compound Class	Model Compound	Temperature (T ± 0.01) °C	Average Refractive Index (n ± 0.000003) nD	Standard deviation (nD)	Barometric pressure (Patm±0.2) (kPa)
Alkene	1-Hexene	10.00	1.393625	0.000007	
		25.00	1.385079	0.000001	93.5
		45.00	1.373404	0.000012	
	1-Heptene	10.00	1.405279	0.000004	
		25.00	1.397483	0.000051	
		45.00	1.386677	0.000050	93.3
		65.00	1.375699	0.000014	
	1-Octene	10.00	1.413997	0.000003	
		25.00	1.406189	0.000001	
		45.00	1.395983	0.000002	93.4
		65.00	1.385780	0.000005	
		85.00	1.375296	0.000001	

Table 5.3. Refractive index at different temperatures of the selected alkenes and alkynes. Continuation

Compound Class	Model Compound	Temperature (T ± 0.01) °C	Average Refractive Index (n ± 0.000003) nD	Standard deviation (nD)	Barometric pressure (Patm±0.2) (kPa)
Alkene	1-Nonene	10.00	1.421656	0.000000	
		25.00	1.414415	0.000002	
		45.00	1.404585	0.000003	93.2
		65.00	1.394787	0.000003	
		85.00	1.384911	0.000007	
	1-Decene	10.00	1.426333	0.000003	
		25.00	1.419417	0.000003	
		45.00	1.409782	0.000004	93.8
		65.00	1.400328	0.000003	
		85.00	1.390840	0.000001	
	1-Undecene	10.00	1.431013	0.000014	
		25.00	1.423956	0.000025	
		45.00	1.414719	0.000017	93.9
		65.00	1.405617	0.000002	
		85.00	1.396401	0.000004	
	1-Dodecene	10.00	1.434701	0.000005	
		25.00	1.427991	0.000005	
		45.00	1.419208	0.000001	93.7
		65.00	1.410195	0.000002	
		85.00	1.401188	0.000007	
	1-Tetradecene	10.00	1.440842	0.000006	
		25.00	1.434257	0.000005	
		45.00	1.425547	0.000003	93.2
		65.00	1.417082	0.000004	
		85.00	1.408428	0.000010	
	1-Hexadecene	10.00	1.445434	0.000002	
		25.00	1.439326	0.000005	
		45.00	1.430720	0.000006	93.4
		65.00	1.422370	0.000014	
		85.00	1.413958	0.000010	

Table 5.3. Refractive index at different temperatures of the selected alkenes and alkynes. Continuation

Compound Class	Model Compound	Temperature (T ± 0.01) °C	Average Refractive Index (n ± 0.000003) nD	Standard deviation (nD)	Barometric pressure (Patm±0.2) (kPa)
Alkyne	1-Hexyne	10.00	1.404446	0.000002	92.8
		25.00	1.395847	0.000004	
		45.00	1.384280	0.000016	
		65.00	1.372375	0.000014	
	1-Heptyne	10.00	1.414497	0.000005	92.9
		25.00	1.406490	0.000002	
		45.00	1.395600	0.000003	
		65.00	1.384771	0.000013	
		85.00	1.373494	0.000009	
	1-Octyne	10.00	1.421719	0.000001	93.4
		25.00	1.413982	0.000003	
		45.00	1.403757	0.000009	
		65.00	1.393461	0.000021	
		85.00	1.383009	0.000011	
	1-Nonyne	10.00	1.427420	0.000002	93.7
		25.00	1.420377	0.000002	
		45.00	1.410390	0.000003	
		65.00	1.400588	0.000013	
		85.00	1.390680	0.000014	
	1-Decyne	10.00	1.431828	0.000000	93.6
		25.00	1.424690	0.000001	
		45.00	1.415198	0.000004	
		65.00	1.405739	0.000022	
		85.00	1.396128	0.000004	
	1-Undecyne	10.00	1.435857	0.000003	93.3
		25.00	1.428964	0.000003	
		45.00	1.419964	0.000009	
		65.00	1.410556	0.000018	
		85.00	1.401318	0.000009	

Table 5.3. Refractive index at different temperatures of the selected alkenes and alkynes. Continuation

Compound Class	Model Compound	Temperature (T ± 0.01) °C	Average Refractive Index (n ± 0.000003) nD	Standard deviation (nD)	Barometric pressure (Patm±0.2) (kPa)
Alkyne	1-Dodecyne	10.00	1.439263	0.000002	93.5
		25.00	1.432362	0.000001	
		45.00	1.423318	0.000002	
		65.00	1.414245	0.000002	
		85.00	1.405329	0.000005	
	1-Tetradecyne	10.00	1.444485	0.000006	93.6
		25.00	1.438179	0.000001	
		45.00	1.429283	0.000004	
		65.00	1.420825	0.000012	
		85.00	1.412062	0.000007	
	1-Hexadecyne	25.00	1.442279	0.000004	93.9
		45.00	1.433862	0.000005	
		65.00	1.425459	0.000006	
		85.00	1.417185	0.000008	

The aim was to measure the properties at 5 different temperatures (10, 25, 45, 65, and 85 °C). However this was not possible for all the reagents due to their boiling point, 1-hexene (62 °C)[3], 1-heptene (93 °C)[3], and 1-hexyne (71 °C)[3], or their freezing point 1-hexadecyne (16 °C)[3].

4. Discussion

4.1 Precision and accuracy of the data

The precision and accuracy of the experimental protocol were evaluated in Chapter IV.

4.2 First derivative of refractive index vs. density.

As mentioned in Chapter IV, literature[1] reports that refractive index vs. density for hydrocarbons follows a linear tendency with a slope of 0.6. In Chapter IV, it was shown that linear alkanes follow this tendency with a slope of 0.598 ± 0.001. The aim of this section is to verify if linear alkenes and alkynes follow the same trend.

4.2.1 Alkenes

Figure 5.1 shows a plot of refractive index vs. density for linear alkenes, and Table 5.4 lists the slope of each one of the selected alkenes.
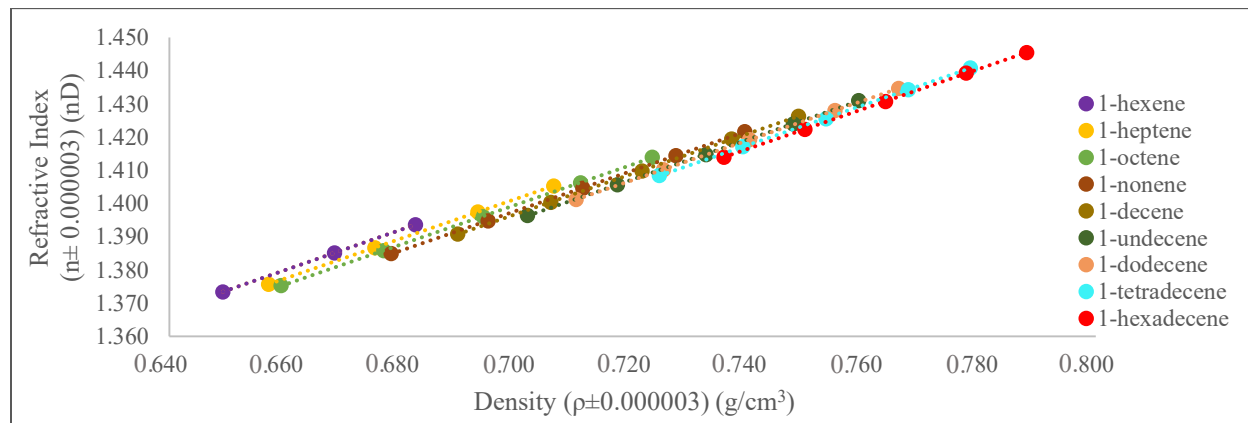
Figure 5.1. Refractive index vs. density of the selected linear alkenes.

Figure 5.1 shows that the data of the selected linear alkenes follow a linear trend. It also shows that density and refractive index increased as the carbon chain length increased.

Table 5.4. Slope (dn/dρ) of the linear tendency of refractive index vs density for the selected linear alkenes

Model Compound	First derivative $(dn/d\rho \pm 0.0005)$
1-Hexene	0.6077
1-Heptene	0.6016
1-Octene	0.6027
1-Nonene	0.6021

Table 5.4. Slope (dn/dρ) of the linear tendency of refractive index vs density for the selected linear alkenes. Continuation

Model Compound	First derivative $(dn/d\rho \pm 0.0005)$
1-Decene	0.6058
1-Undecene	0.6046
1-Dodecene	0.6013
1-Tetradecene	0.6030
1-Hexadecene	0.6033
Average	*0.604*
Standard deviation	*0.002*

As can be seen in Table 5.4, the average slope (0.604± 0.002) for the first derivative of refractive index with respect to density of the selected alkenes is nearly the same as reported by literature (0.6).[1]

4.2.2 Alkynes

Figure 5.2 shows a plot of refractive index vs. density for the selected linear alkynes. Table 5.5 lists the slope of each linear alkynes.
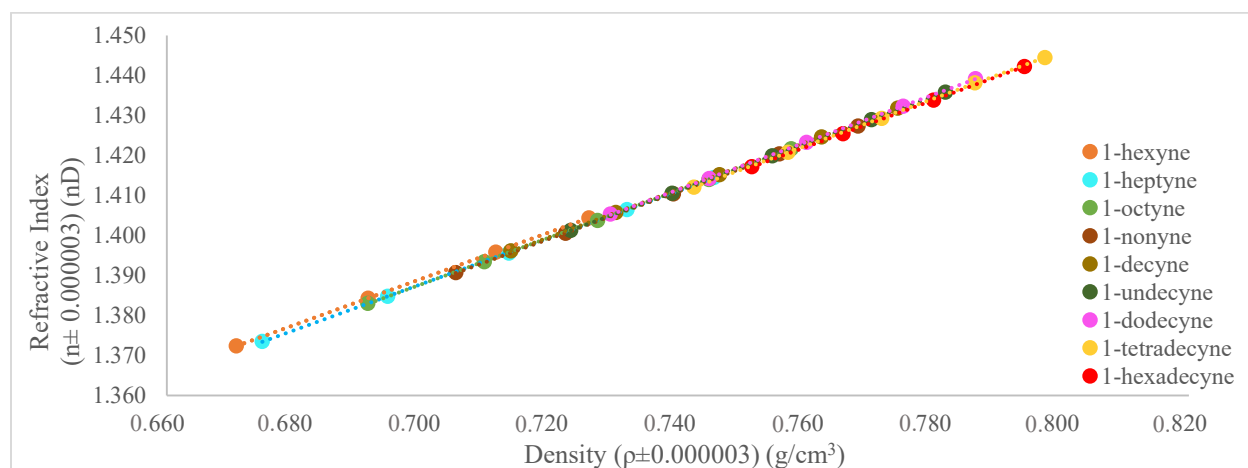
Figure 5.2. Refractive index vs. density of the selected linear alkynes.

72

Figure 5.2 shows that the density vs refractive index of the selected linear alkynes follows a linear trend, which slope is reported in Table 5.5. As expected the density and refractive index increased as the carbon chain length increased.

Table 5.5. Slope ($dn/d\rho$) of the linear function of refractive index vs density for the selected alkynes.

Model Compound	First derivative ($dn/d\rho \pm 0.0005$)
1-Hexyne	0.5808
1-Heptyne	0.5799
1-Octyne	0.5839
1-Nonyne	0.5851
1-Decyne	0.5893
1-Undecyne	0.5891
1-Dodecyne	0.5943
1-Tetradecyne	0.5907
1-Hexadecyne	0.5886
Average $\delta n/\delta\rho$	*0.587*
Standard deviation	*0.005*

Table 5.5 shows that the average slope (0.587± 0.005) is practically the same as reported by literature (0.6).[1]

4.2.3 Comparing alkanes, alkenes, and alkynes

The average first derivative of refractive index with respect to density for the selected alkanes, alkenes and alkynes model compounds are listed in Table 5.6.

Table 5.6. Average slope ($dn/d\rho$) of the linear function of refractive index vs density for alkanes, alkenes, and alkynes compound classes.

Table 5.6 and Figure 5.3 show that the slopes of the studied compound classes are nearly the same. Implying that a double or triple bond in a linear hydrocarbon does not change the trend of the first derivative of refractive index with respect to density.
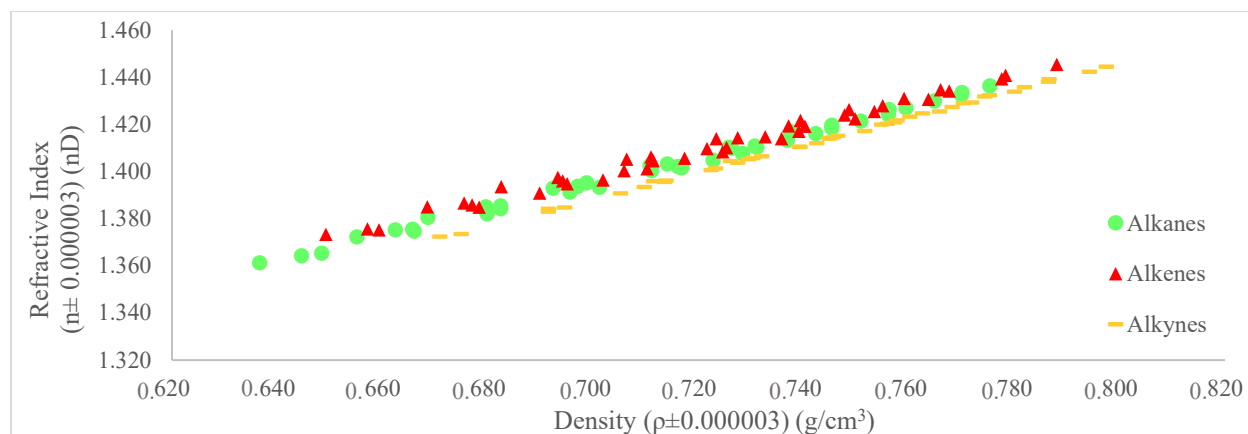
Figure 5.3. Refractive index vs. density of different compound classes.

4.3　Molar refractivity

4.3.1 Alkene

Table 5.7 shows the molar refractivity (Rm) of selected linear alkenes at different temperatures calculated with equations 2.IX, 2.X, 2.XI, and 2.XII from Chapter II. The uncertainty reported in the table next to each of the correlations was calculated by error propagation using the partial derivative method.

Table 5.7. Molar refractivity of selected linear alkenes calculated with equations 2.IX-2.XII

| Model Compound | Temperature (T ± 0.01) °C | Molar Refractivity (Rm) (cm³/mol) | | | |
		Berthelot (Eq. 2.IX) (Rm ± 0.002)	Gladstone & Dale (Eq. 2.X) (Rm ± 0.0006)	Lorentz-Lorenz (Eq. 2.XI) (Rm ± 0.0003)	Eykman (Eq. 2.XII) (Rm ±0.0007)
	10.00	118.969	49.7025	30.1784	66.3289
1-Hexene	25.00	118.402	49.6430	30.2167	66.3290
	45.00	117.639	49.5655	30.2706	66.3351

74

Table 5.7. Molar refractivity of selected linear alkenes calculated with equations 2.IX-2.XII. Continuation

Model Compound	Temperature (T ± 0.01) °C	Molar Refractivity (cm³/mol)			
		Berthelot (Eq. 2.IX) (Rm ± 0.002)	Gladstone & Dale (Eq. 2.X) (Rm ± 0.0006)	Lorentz-Lorenz (Eq. 2.XI) (Rm ± 0.0003)	Eykman (Eq. 2.XII) (Rm ±0.0007)
1-Heptene	10.00	135.506	56.3370	34.0912	75.0611
	25.00	134.966	56.2947	34.1429	75.0858
	45.00	134.149	56.2076	34.1967	75.0831
	65.00	133.365	56.1371	34.2616	75.1055
1-Octene	10.00	155.064	64.2354	38.7720	85.4820
	25.00	154.291	64.1224	38.7921	85.4233
	45.00	153.399	64.0236	38.8474	85.4126
	65.00	152.590	63.9581	38.9222	85.4472
	85.00	150.202	63.3238	38.6890	84.7657
1-Nonene	10.00	174.345	71.9943	43.3576	95.7071
	25.00	173.607	71.9045	43.3956	95.6822
	45.00	172.632	71.7927	43.4527	95.6628
	65.00	171.712	71.7025	43.5218	95.6727
	85.00	170.842	71.6346	43.6047	95.7146
1-Decene	10.00	193.851	79.8926	48.0470	106.1385
	25.00	193.099	79.8120	48.0973	106.1321
	45.00	191.950	79.6544	48.1380	106.0623
	65.00	190.952	79.5523	48.2089	106.0650
	85.00	190.009	79.4736	48.2937	106.1003
1-Undecene	10.00	212.997	87.6166	52.6205	116.3274
	25.00	212.048	87.4799	52.6479	116.2569
	45.00	210.899	87.3389	52.7059	116.2157
	65.00	209.872	87.2425	52.7879	116.2328
	85.00	208.835	87.1452	52.8704	116.2518
1-Dodecene	10.00	232.576	95.5254	57.3077	126.7650
	25.00	231.684	95.4220	57.3594	126.7422
	45.00	230.613	95.3258	57.4500	126.7656
	65.00	229.427	95.1902	57.5199	126.7416
	85.00	228.297	95.0765	57.6022	126.7478

Table 5.7. Molar refractivity of selected linear alkenes calculated
with equations 2.IX-2.XII. Continuation

Model Compound	Temperature (T ± 0.01) °C	Molar Refractivity (cm³/mol)			
		Berthelot (Eq. 2.IX) (Rm ± 0.002)	Gladstone & Dale (Eq. 2.X) (Rm ± 0.0006)	Lorentz-Lorenz (Eq. 2.XI) (Rm ± 0.0003)	Eykman (Eq. 2.XII) (Rm ± 0.0007)
1-Tetradecene	10.00	271.495	111.2301	66.6078	147.4842
	25.00	270.430	111.0933	66.6560	147.4327
	45.00	269.051	110.9240	66.7260	147.3812
	65.00	267.871	110.8241	66.8320	147.4181
	85.00	266.583	110.6875	66.9189	147.4114
1-Hexadecene	10.00	310.210	126.8529	75.8594	168.0962
	25.00	309.307	126.8000	75.9657	168.1630
	45.00	307.684	126.5814	76.0284	168.0672
	65.00	306.268	126.4333	76.1267	168.0604
	85.00	304.816	126.2723	76.2178	168.0392

The objective was to find which correlation better expresses the empirical data for the selected linear alkenes. The best correlation would be the one in which the calculated molar refractivity varies the least with the change of temperature, in other terms the one with the lowest standard deviation.

To discriminate between the equations, the average molar refractivity and its standard deviation were calculated per each correlation using the data reported in Table 5.7. Table 5.8 shows four average molar refractivities per model compound.

Table 5.8. Average molar refractivity and its standard deviation for the selected linear alkenes

Model Compound		Molar Refractivity (cm³/mol)				Best Correlation
		Berthelot (Eq. 2.IX) (Rm ± 0.002)	Gladstone & Dale (Eq. 2.X) (Rm ± 0.0006)	Lorentz-Lorenz (Eq. 2.XI) (Rm ± 0.0003)	Eykman (Eq. 2.XII) (Rm ± 0.0007)	
1-Hexene	Av. Rm	118.337	49.6370	30.2219	66.3310	Eykman
	s	0.668	0.0687	0.0463	0.0036	
1-Heptene	Av. Rm	134.496	56.2441	34.1731	75.0839	Eykman
	s	0.938	0.0894	0.0730	0.0182	

Av. Rm: Average molar refractivity.

s: standard deviation.

Table 5.8. Average molar refractivity and its standard deviation for the selected linear alkenes. Continuation

Model Compound		Molar Refractivity (cm³/mol)				Best Correlation
		Berthelot (Eq. 2.IX) (Rm ± 0.002)	Gladstone & Dale (Eq. 2.X) (Rm ± 0.0006)	Lorentz-Lorenz (Eq. 2.XI) (Rm ± 0.0003)	Eykman (Eq. 2.XII) (Rm ± 0.0007)	
1-Octene	Av. Rm	153.109	63.9327	38.8045	85.3062	Eykman
	s	1.872	0.3561	0.0869	0.3033	
1-Nonene	Av. Rm	172.628	71.8057	43.4665	95.6879	Eykman
	s	1.409	0.1461	0.0990	0.0222	
1-Decene	Av. Rm	191.972	79.6770	48.1570	106.0996	Eykman
	s	1.557	0.1747	0.0967	0.0359	
1-Undecene	Av. Rm	210.930	87.3646	52.7265	116.2569	Eykman
	s	1.661	0.1874	0.1029	0.0426	
1-Dodecene	Av. Rm	230.519	95.3080	57.4479	126.7524	Eykman
	s	1.712	0.1789	0.1188	0.0120	
1-Tetradecene	Av. Rm	269.086	110.9518	66.7481	147.4255	Eykman
	s	1.959	0.2147	0.1274	0.0378	
1-Hexadecene	Av. Rm	307.657	126.5880	76.0396	168.0852	Eykman
	s	2.193	0.2443	0.1391	0.0480	

Av. Rm: Average molar refractivity.

s: standard deviation.

Table 5.8 shows that the Rm calculated with one correlation cannot be compared to a Rm calculated with another correlation. The table also shows that the correlation by Eykman (Equation 2.XII) had the lowest standard deviation for all of the selected alkenes. The correlation by Lorentz-Lorenz (Equation 2.XI) had the second-lowest deviation, followed by Gladstone & Dale correlation (Equation 2.X) and at last, Berthelot (Equation 2.IX) which had the biggest standard deviation.

4.3.2 Alkyne

The same analysis was applied to the selected alkynes. Table 5.9 shows the molar refractivity (Rm) at different temperatures calculated with equations 2.IX, 2.X, 2.XI, and 2.XII from Chapter II.

Table 5.9. Molar refractivity of alkyne model compounds calculated
with equations 2.IX-2.XII from Chapter II

| Model Compound | Temperature (T ± 0.01) °C | Molar Refractivity (Rm) (cm³/mol) | | | |
		Berthelot (Eq. 2.IX) (Rm ± 0.002)	Gladstone & Dale (Eq. 2.X) (Rm ± 0.0006)	Lorentz-Lorenz (Eq. 2.XI) (Rm ± 0.0003)	Eykman (Eq. 2.XII) (Rm ± 0.0007)
1-Hexyne	10.00	110.017	45.7558	27.6949	60.9701
	25.00	109.486	45.6983	27.7293	60.9663
	45.00	108.828	45.6441	27.7890	60.9928
	65.00	108.162	45.5921	27.8522	61.0263
1-Heptyne	10.00	129.082	53.4612	32.2640	71.1392
	25.00	128.514	53.4031	32.3044	71.1402
	45.00	127.730	53.3186	32.3555	71.1350
	65.00	127.168	53.3180	32.4536	71.2392
	85.00	126.311	53.2172	32.5000	71.2214
1-Octyne	10.00	148.730	61.4153	36.9858	81.6429
	25.00	147.856	61.2497	36.9699	81.5088
	45.00	147.028	61.1657	37.0297	81.5119
	65.00	146.233	61.0970	37.0987	81.5370
	85.00	145.464	61.0420	37.1771	81.5832
1-Nonyne	10.00	167.772	69.1154	41.5532	91.8082
	25.00	167.209	69.0839	41.6205	91.8541
	45.00	166.213	68.9569	41.6658	91.8106
	65.00	165.352	68.8798	41.7382	91.8322
	85.00	164.517	68.8161	41.8194	91.8741
1-Decyne	10.00	187.478	77.0936	46.2894	102.3449
	25.00	186.707	77.0023	46.3322	102.3225
	45.00	185.714	76.8940	46.3963	102.3108
	65.00	184.783	76.8094	46.4735	102.3311
	85.00	183.826	76.7178	46.5479	102.3455
1-Undecyne	10.00	206.774	84.8878	50.9085	112.6310
	25.00	205.978	84.8006	50.9601	112.6198
	45.00	205.040	84.7284	51.0519	112.6614
	65.00	203.901	84.5867	51.1073	112.6179
	85.00	202.910	84.4995	51.1922	112.6454

Table 5.9. Molar refractivity of alkyne model compounds calculated
with equations 2.IX-2.XII from Chapter II. Continuation

Model Compound	Temperature (T ± 0.01) °C	Molar Refractivity (cm³/mol)			
		Berthelot (Eq. 2.IX) (Rm ± 0.002)	Gladstone & Dale (Eq. 2.X) (Rm ± 0.0006)	Lorentz-Lorenz (Eq. 2.XI) (Rm ± 0.0003)	Eykman (Eq. 2.XII) (Rm ± 0.0007)
1-Dodecyne	10.00	226.522	92.8649	55.6363	123.1591
	25.00	225.587	92.7442	55.6778	123.1130
	45.00	224.428	92.6120	55.7471	123.0879
	65.00	223.276	92.4826	55.8177	123.0681
	85.00	222.267	92.4060	55.9169	123.1171
1-Tetradecyne	10.00	264.823	108.3351	64.8039	143.5758
	25.00	264.021	108.2859	64.8961	143.6315
	45.00	262.590	108.0936	64.9517	143.5480
	65.00	261.484	108.0144	65.0661	143.6074
	85.00	260.182	107.8672	65.1446	143.5835
1-Hexadecyne	25.00	302.467	123.8463	74.1311	164.1810
	45.00	301.074	123.7020	74.2299	164.1747
	65.00	299.678	123.5551	74.3261	164.1657
	85.00	298.402	123.4502	74.4439	164.2111

Once the Rm was calculated for the different temperatures with each of the correlations (see Table 5.9). The next step was to define which correlation better expressed the empirical data. For this, an average molar refractivity with its standard deviation was calculated for each correlation. A total of four average molar refractivities per model compound were calculated (See Table 5.10).

As mentioned in the previous section, Rm is an intrinsic property that does not depend on temperature. Therefore, the best correlation was the one with the least standard deviation (See Table 5.10).

Table 5.10. Average molar refractivity and standard deviation for the selected alkynes

| Model Compound | | Molar Refractivity (cm³/mol) | | | | Best Correlation |
		Berthelot (Eq. 2.IX) (Rm ± 0.002)	Gladstone & Dale (Eq. 2.X) (Rm ± 0.0006)	Lorentz-Lorenz (Eq. 2.XI) (Rm ± 0.0003)	Eykman (Eq. 2.XII) (Rm ± 0.0007)	
1-Hexyne	Av. Rm	109.123	45.6726	27.7664	60.9889	Eykman
	s	0.805	0.0704	0.0692	0.0276	
1-Heptyne	Av. Rm	127.761	53.3436	32.3755	71.1750	Eykman
	s	1.092	0.0930	0.0993	0.0509	
1-Octyne	Av. Rm	147.062	61.1939	37.0523	81.5568	Eykman
	s	1.290	0.1461	0.0858	0.0566	
1-Nonyne	Av. Rm	166.213	68.9704	41.6794	91.8359	Eykman
	s	1.327	0.1286	0.1032	0.0283	
1-Decyne	Av. Rm	185.702	76.9034	46.4078	102.3309	Eykman
	s	1.460	0.1494	0.1046	0.0149	
1-Undecyne	Av. Rm	204.921	84.7006	51.0440	112.6351	Eykman
	s	1.553	0.1575	0.1134	0.0183	
1-Dodecyne	Av. Rm	224.416	92.6220	55.7592	123.1090	Eykman
	s	1.712	0.1872	0.1120	0.0343	
1-Tetradecyne	Av. Rm	262.620	108.1192	64.9725	143.5893	Eykman
	s	1.874	0.1934	0.1352	0.0317	
1-Hexadecyne	Av. Rm	300.405	123.6384	74.2827	164.1831	Eykman
	s	1.755	0.1729	0.1337	0.0197	

Av. Rm: Average molar refractivity.

s: standard deviation.

As can be seen in Table 5.10, the results obtained for the alkynes are similar to those of the alkenes. Being the correlation by Eykman the one with the lowest standard deviation, followed by Lorentz-Lorenz correlation, then by Gladstone & Dale correlation and at last, Berthelot's correlation.

4.4   Atomic refraction & group contribution

In this section, the atomic refraction and group contribution for double and triple bonds for the correlation by Eykman were calculated. The atomic refraction (AR) of carbon (C) and hydrogen (H) and the group contribution (GC) of C-H and C-C bonds were calculated in Chapter IV. In the present chapter, AR and GC of double and triple bonds were calculated. The

data of 1-heptene were used to calculate the AR and GC of the double bond (C=C), while 1-hexyne data were used to calculate the AR and GC of the triple bond (C≡C) (See Table 5.11)

Table 5.11. Atomic refraction and group contribution for Eykman

Atomic refraction (cm³/mol)				Group contribution (cm³/mol)			
Carbon	Hydrogen	Double bond	Triple bond	C-H Bond	C-C Bond	C=C	C≡C
6.770	1.782	2.748	2.551	3.474	3.38608	9.517	12.705

Table 5.11 shows that the values calculated for the double and triple bond atomic refraction are very different than those calculated for their group contribution. To test which method (AR or GC) would estimate the Rm with higher accuracy, Tables 5.12 for alkenes and 5.13 for alkynes show the Rm calculated per each model compound by AR and GC. And compared the results with the Rm calculated using the correlation by Eykman.

4.4.1 Alkene

Table 5.12. Comparison between Rm calculated with the experimental data and Rm calculated with AR and GC for the selected alkenes for the correlation by Eykman

Model Compound	Molar Refractivity (cm³/mol)			Delta between average exp. Rm and Rm calculated with AR or GC (cm³/mol)
	Calculated with atomic refraction and group contribution		Average calculated value with exp. data (Rm ± 0.0007)	
1-Hexene	AR	64.7502	66.3310	1.5808
	GC	64.7498		1.5812
1-Heptene	AR	75.0839	75.0839	0.0000
	GC	75.0839		0.0000
1-Octene	AR	85.4175	85.3062	0.1114
	GC	85.4180		0.1118
1-Nonene	AR	95.7512	95.6879	0.0633
	GC	95.7520		0.0642
1-Decene	AR	106.0848	106.0996	0.0148
	GC	106.0861		0.0135
1-Undecene	AR	116.4185	116.2569	0.1615
	GC	116.4202		0.1633
1-Dodecene	AR	126.7521	126.7524	0.0003
	GC	126.7543		0.0018

AR: atomic refraction   GC: group contribution

Table 5.12. Comparison between Rm calculated with the experimental data and Rm calculated with AR and GC for the selected alkenes for the correlation by Eykman. Continuation

Model Compound	Molar Refractivity (cm³/mol)		Average calculated value with exp. data (Rm ± 0.0007)	|Delta between average exp. Rm and Rm calculated with AR or GC (cm³/mol)|
	Calculated with atomic refraction and group contribution			
1-Tetradecene	AR	147.4194	147.4255	0.0061
	GC	147.4224		0.0031
1-Hexadecene	AR	168.0867	168.0852	0.0015
	GC	168.0906		0.0054

AR: atomic refraction   GC: group contribution

The difference between $|Rm_{exp} - Rm_{AR}|$ and $|Rm_{exp} - Rm_{GC}|$ is not bigger than 0.0050 cm³/mol, implying that both, AR and GC, can be used to estimate the Rm.

4.4.2 Alkyne

Table 5.13. Comparison between Rm calculated with the experimental data and Rm calculated with AR and GC for the correlation by Eykman for alkyne model compounds

Model Compound	Molar Refractivity (cm³/mol)		Average calculated value with exp. data (Rm ± 0.0007)	|Delta between average exp. Rm and Rm calculated with AR or GC (cm³/mol)|
	Calculated with atomic refraction and group contribution			
1-Hexyne	AR	60.9889	60.9889	0.0000
	GC	60.9893		0.0004
1-Heptyne	AR	71.3225	71.1750	0.1476
	GC	71.3234		0.1484
1-Octyne	AR	81.6562	81.5568	0.0994
	GC	81.6575		0.1007
1-Nonyne	AR	91.9898	91.8359	0.1540
	GC	91.9916		0.1557
1-Decyne	AR	102.3235	102.3309	0.0074
	GC	102.3256		0.0053
1-Undecyne	AR	112.6571	112.6351	0.0220
	GC	112.6597		0.0246
1-Dodecyne	AR	122.9908	123.1090	0.1182
	GC	122.9938		0.1152
1-Tetradecyne	AR	143.6581	143.5893	0.0688
	GC	143.6620		0.0727

AR: atomic refraction   GC: group contribution

Table 5.13. Comparison between Rm calculated with the experimental data and Rm calculated with AR and GC for the correlation by Eykman for alkyne model compounds. Continuation

Model Compound	Molar Refractivity (cm³/mol)			|Delta between average exp. Rm and Rm calculated with AR or GC (cm³/mol)|
	Calculated with atomic refraction and group contribution		Average calculated value with exp. data (Rm ± 0.0007)	
1-Hexadecyne	AR	164.3254	164.1831	0.1423
	GC	164.3301		0.1470

AR: atomic refraction

GC: group contribution

Similar to alkenes, the difference between $|Rm_{exp} - Rm_{AR}|$ and $|Rm_{exp} - Rm_{GC}|$ does not differ by more than 0.0050 cm³/mol, therefore atomic refraction and group contribution, it seems that AR and GC can be used indistinctly to predict the Rm of linear alkynes. In the next chapter, the effect of cyclic compounds will be studied.

5. Conclusions

▪ The average first derivate of refractive index vs. density for the selected linear alkenes was 0.604 ± 0.002 and for the selected alkynes was 0.587 ± 0.002, showing that the collected data follows the same behavior as the literature (0.6).[1]

▪ The average first derivate of refractive index vs. density for alkenes and alkynes also showed similar behavior to the selected alkanes studied in Chapter IV.

▪ The correlation by Eykman resulted in the least temperature-dependent for both, linear alkenes and alkynes.

▪ Atomic refraction and group contribution predicted the molar refractivity of linear alkenes and alkynes for the correlation by Eykman with high accuracy.

6. References

(1)   Kurtz, S. S. Physical Properties and Hydrocarbon Structure. In *The chemistry of petroleum hydrocarbons. Vol 1*; Reinhold Publishing Corporation: New York, 1954; pp 275–331.

(2)   Yurkanis, P. *Organic Chemistry*; Pearson Education: California, 2006.

(3)   RELXGroup. Reaxys database https://www.reaxys.com/#/login (accessed Sep 20, 2019).

CHAPTER VI - FUNDAMENTAL STUDY OF MOLAR REFRACTIVITY WITH CYCLIC HYDROCARBONS MODEL COMPOUNDS

In this chapter, the molar refractivity correlations found in the consulted literature are evaluated using cyclic and aromatic hydrocarbon model compounds, with the aim to find the least temperature-dependent correlation.

Abstract

As Chapters IV and V, the present chapter aims to revisit and evaluate a fundamental unsolved aspect of the molar refractivity. Molar refractivity is a temperature invariant, and intrinsic property. Different equations are reported in the literature which correlates molar refractivity, refractive index, and density. However, it is not clear which correlation better expresses the empirical data.

In this section of the study, the correlations were evaluated using cyclic and alkyl aromatic model compounds. It was found that the least temperature-dependent for these compounds was that one by Eykman $\left(R_M = \left(\frac{n^2-1}{n+0.4} \right) \cdot \frac{M}{\rho} \right)$. Moreover, when refractive index vs density was plotted, the model compounds showed a linear tendency as expected. The average slope for cyclic hydrocarbon compounds was (0.61 ± 0.02) showing good agreement with the literature, which reported a slope of 0.6 for hydrocarbons.

At last, atomic refraction and group contribution were evaluated. The molar refractivity estimated with atomic refraction was comparable to the one estimated with group contribution. In addition, for most of the model compounds the results were nearly the same as the molar refractivity calculated with the correlation by Eykman, with the exception of 1-methylnaphthalene which had a difference of 5.2 cm^3/mol between the predicted and the experimentally determined molar refractivity.

Keywords: *Cyclic hydrocarbon compounds, molar refractivity, refractive index, density, Eykman.*

1. Introduction

The same methodology that was introduced and used in Chapters IV and V, was employed. In this chapter, the group of compounds investigated was cyclic hydrocarbons. Unlike the previous chapters, the analysis of the data was not based purely on compound class. It was of interest to see how increasing degrees of unsaturation in cyclic hydrocarbons affected refractive index and molar refractivity.
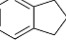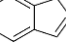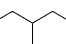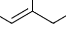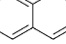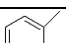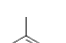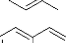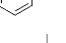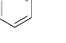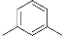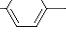
The selected hydrocarbons were separated into two groups, cyclic, and alkyl aromatic compounds. The selected cyclic compounds are alkanes or alkenes with a close structure call rings.[1] While the aromatics are cyclic compounds with double bonds that become stable due to the resonance of electrons π, for example, benzene ($\bigcirc$).[2] At last, the alkyl aromatics are aromatics molecules with alkyl substituents.

2. Experimental

2.1 Materials

Table 6.1 shows the selected cyclic and alkyl aromatic compounds. The cyclic compounds were selected to study the effect of double bonds and double rings in the refractive index and density of different cyclic carbon chains. Starting from cyclohexane, then cyclohexene and finally benzene. Indan to indene, and decahydronaphthalene to 1-methylnaphthalene. Notice that it was not possible to use naphthalene because its melting point is 80 °C.[3] In the other hand, the alkyl aromatics seeks to study the effect of the length and position of the alkyl group in the properties of interest.

Table 6.1. Selected model compounds

| Compound Group | Reagent | CASRN[a] | Structure | Purity (wt %) | | Supplier |
				Supplier[b]	FID[c]	
Cyclic	Cyclohexane	110-82-7		99.9	100.0	Sigma-Aldrich
	Cyclohexene	110-83-8		99	99.0	Acros Organic
	Benzene	71-42-2		99	100.0	Alfa Aesar
	Indan	496-11-7		95	96.3	Acros Organic
	Indene	95-13-6		98	98.3	Aldrich
	Decahydronaphthalene (Decalin)	91-17-8		98	99.7	Acros Organic
	1,2,3,4 Tetrahydronaphthalene (tetralin)	119-64-2		99	99.3	Sigma-Aldrich
	1,2 Dihydronaphthalene	447-53-0		98	97.4	Sigma-Aldrich
	1-Methylnaphthane	90-12-0		96	98.7	Alfa Aesar
Alkyl aromatics	Toluene	108-88-3		99.9	100.0	Fisher
	m-Xylene	108-38-3		>99	99.8	Sigma-Aldrich
	Styrene	100-42-5		>99	99.9	Sigma-Aldrich
	Cumene	98-82-8		98	99.9	Acros Organic
	α-methylstyrene	98-83-9		99	99.6	Aldrich
	Mesitylene	108-67-8		98	99.1	Sigma-Aldrich
	p-Cymene	99-87-6		99	99.7	Aldrich
	Hexylbenzene	1077-16-3	$CH_2(CH_2)_4CH_3$	97	99.0	Sigma-Aldrich
	1-Phenyldecane	104-72-3	$CH_2(CH_2)_7CH_3$	>98	100.0	TCI

[a] CASRN: Chemical Abstracts Services Registry Number
[b] Purity of the material guaranteed by the supplier; the material was not further purified.
[c] Purity calculated based on peak area obtained by GC-FID analysis

Table 6.1 shows that the only component for which the purity determined using GC-FID analysis was lower than the one indicated by the supplier was 1,2 dihydronaphthalene.

2.2 Equipment, procedures, methodologies, and calculations

The equipment, procedures, methodologies, and calculations used in this chapter have been explained in detail in Chapter III.

For safety, the density meter and refractometer were placed inside the fume hood.

3. Results

Table 6.2 shows the average density data at different temperatures of the selected alkyl aromatic and cyclic model compounds. The values are reported alongside with their standard deviation. The low standard deviation (not higher than $\pm$ 0.00005 g/cm^3) showed the high repeatability of the density measurements.

Table 6.2. Average density at different temperatures of selected model compounds

Compound Group	Model Compound	Temperature (T ± 0.001) °C	Average density (ρ ± 0.000003) g/cm³	Standard deviation (g/cm³)
Cyclic	Cyclohexane	10.000	0.787906	0.000003
		25.000	0.773876	0.000002
		45.000	0.754786	0.000002
		65.000	0.735204	0.000002
	Cyclohexene	10.000	0.820398	0.000009
		25.000	0.806268	0.000007
		45.000	0.787112	0.000004
		65.000	0.767511	0.000004
	Benzene	10.000	0.873663	0.000009
		25.000	0.889652	0.000007
		45.000	0.852159	0.000007
		65.000	0.830306	0.000006

Table 6.2. Average density at different temperatures of selected model compounds. Continuation

Compound Group	Model Compound	Temperature (T ± 0.001) °C	Average density (ρ ± 0.000003) g/cm3	Standard deviation (g/cm3)
Cyclic	Indan	10.000	0.967689	0.000003
		25.000	0.954929	0.000001
		45.000	0.937889	0.000001
		65.000	0.920767	0.000001
		85.000	0.903520	0.000004
	Inden	10.000	1.003628	0.000003
		25.000	0.990540	0.000003
		45.000	0.973139	0.000003
		65.000	0.955724	0.000003
		85.000	0.938252	0.000004
	Decahydronaphthalene (Decalin)	10.000	0.887844	0.000002
		25.000	0.876549	0.000002
		45.000	0.861493	0.000002
		65.000	0.846390	0.000003
		85.000	0.831192	0.000001
	1,2,3,4-Tetrahydronaphthalene (Tetralin)	10.000	0.976765	0.000009
		25.000	0.964870	0.000006
		45.000	0.949013	0.000006
		65.000	0.933112	0.000005
		85.000	0.917108	0.000004
	1,2 Dihydronaphthalene	10.000	1.012761	0.000033
		25.000	1.000558	0.000034
		45.000	0.984339	0.000036
		65.000	0.968127	0.000046
	1-Methylnaphthalene	10.000	1.030815	0.000006
		25.000	1.019601	0.000001
		45.000	1.004663	0.000001
		65.000	0.989695	0.000000
		85.000	0.974655	0.000001

Table 6.2. Average density at different temperatures of selected model compounds. Continuation

Compound Group	Model Compound	Temperature (T ± 0.001) °C	Average density (ρ ± 0.000003) g/cm3	Standard deviation (g/cm3)
Alkyl aromatic	Toluene	10.000	0.876178	0.000002
		25.000	0.862242	0.000002
		45.000	0.824420	0.000003
		65.000	0.804923	0.000004
		85.000	0.872675	0.000002
	m-Xylene	10.000	0.859824	0.000003
		25.000	0.843487	0.000002
		45.000	0.842537	0.000003
		65.000	0.824992	0.000003
		85.000	0.807089	0.000003
	Styrene	10.000	0.847770	0.000006
		25.000	0.866052	0.000004
		45.000	0.901862	0.000004
		65.000	0.884053	0.000004
		85.000	0.915139	0.000004
	Cumene	10.000	0.805609	0.000004
		25.000	0.823193	0.000003
		45.000	0.840501	0.000001
		65.000	0.857605	0.000001
		85.000	0.870346	0.000000
	α-methylstyrene	10.000	0.918467	0.000003
		25.000	0.870335	0.000002
		45.000	0.905446	0.000002
		65.000	0.887982	0.000001
		85.000	0.852438	0.000001
	Mesitylene	10.000	0.873357	0.000001
		25.000	0.861121	0.000001
		45.000	0.844682	0.000001
		65.000	0.828022	0.000000
		85.000	0.811061	0.000002

Table 6.2. Average density at different temperatures of selected model compounds. Continuation

Compound Group	Model Compound	Temperature (T ± 0.001) °C	Average density (ρ ± 0.000003) g/cm³	Standard deviation (g/cm³)
Alkyl aromatic	p-Cymene	10.000	0.864944	0.000001
		25.000	0.852920	0.000000
		45.000	0.836814	0.000000
		65.000	0.820549	0.000001
		85.000	0.804053	0.000000
	Hexylbenzene	10.000	0.867027	0.000005
		25.000	0.855635	0.000002
		45.000	0.840416	0.000001
		65.000	0.825120	0.000001
		85.000	0.809720	0.000002
	1-Phenyldecane	10.000	0.862564	0.000002
		25.000	0.851986	0.000011
		45.000	0.837914	0.000001
		65.000	0.823824	0.000001

Table 6.3 shows the average refractive index at different temperatures of the alkyl aromatic and cyclic model compounds. Each value is an average of nine measurements. The values are reported with their standard deviation and the barometric pressure at which the experiment was conducted. The refractive index measurement had high repeatability (the standard deviation was lower than ± 0.000037 nD)

Table 6.3. Average refractive index at different temperatures of the selected model compounds

Compound Group	Model Compound	Temperature (T ± 0.01) °C	Average Refractive Index (n ± 0.000003) nD	Standard deviation (nD)	Barometric pressure (Patm±0.2) (kPa)
Cyclic	Cyclohexane	10.00	1.432020	0.000000	93.4
		25.00	1.423629	0.000002	
		45.00	1.412311	0.000005	
		65.00	1.400993	0.000008	

Table 6.3. Average refractive index at different temperatures of the
selected model compounds. Continuation

Compound Group	Model Compound	Temperature (T ± 0.01) °C	Average Refractive Index (n ± 0.000003) nD	Standard deviation (nD)	Barometric pressure (Patm±0.2) (kPa)
Cyclic	Cyclohexene	10.00	1.452279	0.000002	93.3
		25.00	1.443920	0.000004	
		45.00	1.432715	0.000002	
		65.00	1.421318	0.000019	
	Benzene	10.00	1.507739	0.000002	92.6
		25.00	1.497947	0.000001	
		45.00	1.484775	0.000012	
		65.00	1.471600	0.000008	
	Indan	10.00	1.541583	0.000002	93.2
		25.00	1.533913	0.000004	
		45.00	1.523693	0.000002	
		65.00	1.513606	0.000003	
		85.00	1.503424	0.000006	
	Inden	10.00	1.580728	0.000001	92.7
		25.00	1.572492	0.000001	
		45.00	1.561607	0.000003	
		65.00	1.550799	0.000005	
		85.00	1.540050	0.000003	
	Decalin	10.00	1.478400	0.000002	93.4
		25.00	1.471821	0.000002	
		45.00	1.463049	0.000004	
		65.00	1.454328	0.000021	
		85.00	1.445763	0.000017	
	Tetralin	10.00	1.546098	0.000002	93.4
		25.00	1.538999	0.000001	
		45.00	1.529492	0.000003	
		65.00	1.520126	0.000003	
		85.00	1.510752	0.000007	

Table 6.3. Average refractive index at different temperatures of the selected model compounds. Continuation

Compound Group	Model Compound	Temperature (T ± 0.01) °C	Average Refractive Index (n ± 0.000003) nD	Standard deviation (nD)	Barometric pressure (Patm±0.2) (kPa)
Cyclic	1,2 Dihydronaphthalene	10.00	1.588869	0.000007	
		25.00	1.581205	0.000005	93.2
		45.00	1.571034	0.000003	
		65.00	1.560946	0.000006	
	1-Methylnaphthalene	10.00	1.621772	0.000003	
		25.00	1.614440	0.000002	
		45.00	1.604722	0.000007	93.1
		65.00	1.595071	0.000003	
		85.00	1.585378	0.000003	
Alkyl Aromatic	Toluene	10.00	1.502703	0.000001	
		25.00	1.494119	0.000005	
		45.00	1.482578	0.000001	94.0
		65.00	1.471036	0.000008	
		85.00	1.459255	0.000005	
	m-Xylene	10.00	1.502574	0.000002	
		25.00	1.494685	0.000002	
		45.00	1.484050	0.000003	93.0
		65.00	1.473421	0.000003	
		85.00	1.462641	0.000007	
	Styrene	10.00	1.509004	0.000034	
		25.00	1.532513	0.000006	
		45.00	1.520837	0.000006	93.1
		65.00	1.552854	0.000002	
		85.00	1.544129	0.000002	
	Cumene	10.00	1.496557	0.000002	
		25.00	1.488818	0.000001	
		45.00	1.478507	0.000006	94.8
		65.00	1.468129	0.000004	
		85.00	1.457554	0.000004	

Table 6.3. Average refractive index at different temperatures of the selected model compounds. Continuation

Compound Group	Model Compound	Temperature (T ± 0.01) °C	Average Refractive Index (n ± 0.000003) nD	Standard deviation (nD)	Barometric pressure (Patm±0.2) (kPa)
Alkyl Aromatic	α-Methylstyrene	10.00	1.544567	0.000003	94.3
		25.00	1.536155	0.000001	
		45.00	1.524894	0.000007	
		65.00	1.513624	0.000009	
		85.00	1.502322	0.000020	
	Mesitylene	10.00	1.504444	0.000002	93.1
		25.00	1.496972	0.000001	
		45.00	1.486896	0.000005	
		65.00	1.476817	0.000012	
		85.00	1.466629	0.000006	
	p-Cymene	10.00	1.495832	0.000009	94.3
		25.00	1.488535	0.000003	
		45.00	1.478748	0.000010	
		65.00	1.468933	0.000037	
		85.00	1.459159	0.000004	
	Hexylbenzene	10.00	1.491683	0.000001	94.1
		25.00	1.484804	0.000001	
		45.00	1.475585	0.000005	
		65.00	1.466459	0.000019	
		85.00	1.457259	0.000032	
	1-Phenyldecane	10.00	1.487501	0.000002	92.9
		25.00	1.481139	0.000003	
		45.00	1.472640	0.000004	
		65.00	1.464282	0.000004	
		85.00	1.455870	0.000006	

As mentioned in Chapter III, the aim was to measure the refractive index and density of each model compound at 5 different temperatures (10, 25, 45, 65, and 85 °C). However, it was not possible for some of the reagents due to their relative low boiling point, cyclohexane (80 °C)[3], cyclohexene (83 °C)[3], benzene (80 °C)[3], and 1,2-dihydronaphthalene (89 °C)[3].

4. Discussion

4.1 Precision and accuracy of the data

To evaluate the fundamental issues of molar refractivity, high precision, and accurate data were required. To ensure that the collected data complied with these requirements, they were evaluated in Chapter IV.

4.2 First derivative of refractive index vs. density.

Literature[4] reports that refractive index vs. density for hydrocarbons follows a linear trend with a slope of 0.6. In Chapter IV and V, it was shown that linear alkanes, alkenes, and alkynes follow this tendency with an average slope of 0.598 ± 0.003, 0.604 ± 0.002, and 0.587 ± 0.005 respectively. The following section evaluates if alkyl aromatics and other cyclic compounds follow the same tendency.

4.2.1 Cyclic compounds

A plot of refractive index vs. density of the selected cyclic compounds is shown in Figure 6.1. In Table 6.4 reports the slope of the cyclic model compounds.
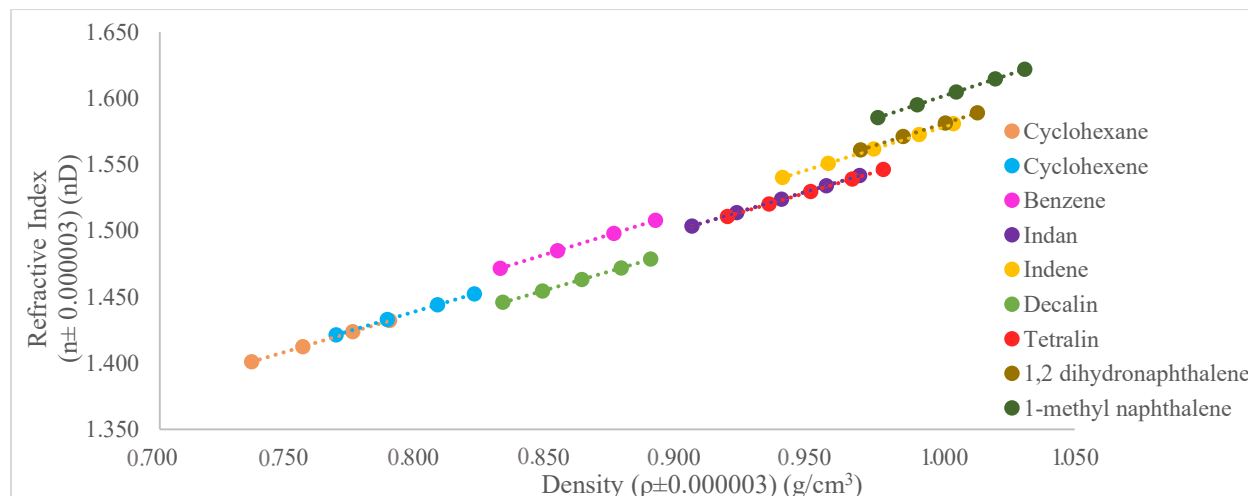
Figure 6.1. Refractive index vs. density of the selected cyclic compounds.

It can be seen in Figure 6.1 that all the cyclic model compounds follow a linear tendency and the slope appears to be similar.

Table 6.4. Slope of the linear trend of refractive index vs density
for the selected cyclic compounds

Model Compound	First derivative $(dn/d\rho \pm 0.0005)$
Cyclohexane	0.5889
Cyclohexene	0.5852
Benzene	0.6092
Indan	0.5945
Indene	0.6223
Decalin	0.5768
Tetralin	0.5928
1,2 Dihydronaphthalene	0.6257
1-Methylnaphthalene	0.6479
Average	0.61
Standard deviation	0.02

Table 6.4 shows that the average slope (0.61± 0.02) for refractive index vs density of the selected cyclic compounds is roughly comparable to the value reported by literature (0.6).[4] This table also shows that the slopes of the different components are not as closed as it was expected. In addition, for isostructural compounds, such as cyclohexane, cyclohexene, and benzene, there is a noticeable difference in slope between cyclohexane and cyclohexene on the one hand, and benzene on the other hand."

4.2.2 Alkyl aromatics

Figure 6.2 shows a plot of refractive index vs. density for the selected alkyl aromatics, most of the reagents have similar slopes, with the exception of styrene and α-methylstyrene. These two seem to have a higher slope (see Table 6.5) which can be due to the double bond present in the alkyl substituent.
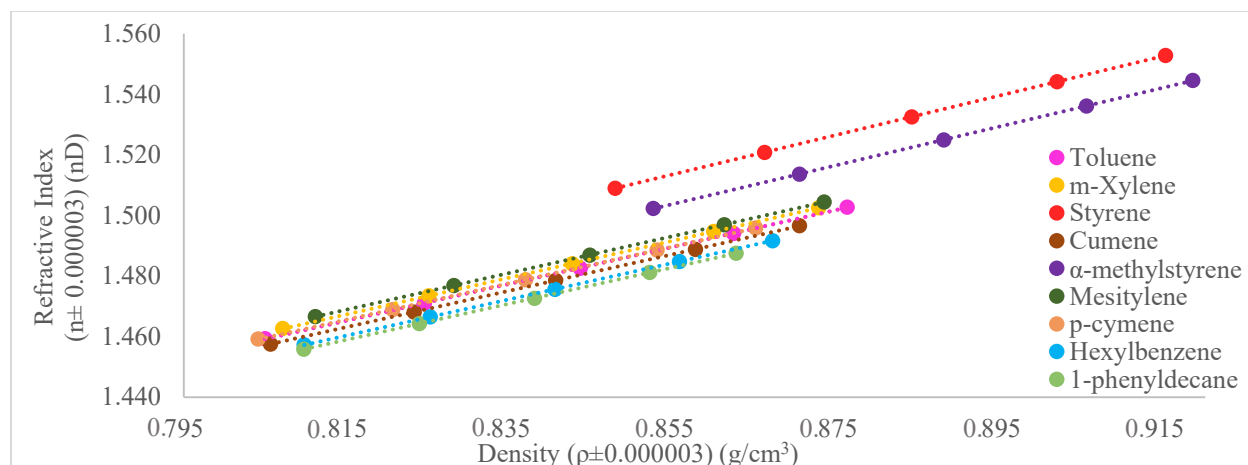
Figure 6.2. Refractive index vs. density of the selected alkyl aromatics.

Table 6.5 lists the slopes of the model alkyl aromatic model compounds. This table shows the same behavior as in Figure 6.2.

Table 6.5. Slope ($dn/d\rho$) of the linear function of refractive index vs density for the selected alkyl aromatics

Model Compound	First derivative ($dn/d\rho \pm 0.0005$)	Average first derivative (dn/dρ)	Standard deviation
Toluene	0.6097		
m-Xylene	0.6091		
Cumene	0.6021		
Mesitylene	0.6073	0.604	0.004
p-Cymene	0.6029		
Hexylbenzene	0.6007		
1-Phenyldecane	0.5982		
Styrene	0.6507	0.645	0.008
α-methylstyrene	0.6400		
Average	0.61		
Standard deviation	0.02		

Table 6.5 shows that average dn/dρ of the compounds with an olefinic group that can benefit from resonance with the aromatic (styrene and α-methylstyrene) is 0.645± 0.008, whereas, the aromatics compounds with an unsaturated alkyl group have an average

97

dn/dρ is 0.604± 0.004. This table also shows that the average slope for all the alkyl aromatic model compounds is 0.61± 0.02.

It can be seen, that the average dn/dρ of aromatics compounds with an unsaturated alkyl group is nearly the same as the slope reported by literature (0.6).[4]

4.2.3 Comparing alkanes, alkenes, alkynes, alkyl aromatic and cyclic compounds

Figure 6.3 is a plot of refractive index vs density of different compound groups. In this figure, cyclohexane and cyclohexene overlap with alkanes, alkenes, and alkynes, showing that regardless of the compound structure, cyclic or linear, it would be plotted in the same region. In addition, benzene overlaps with alkyl aromatics. Alkyl aromatics are benzenes with an alkyl substituent, therefore, it makes sense that benzene and these compound groups are plotted in the same region.
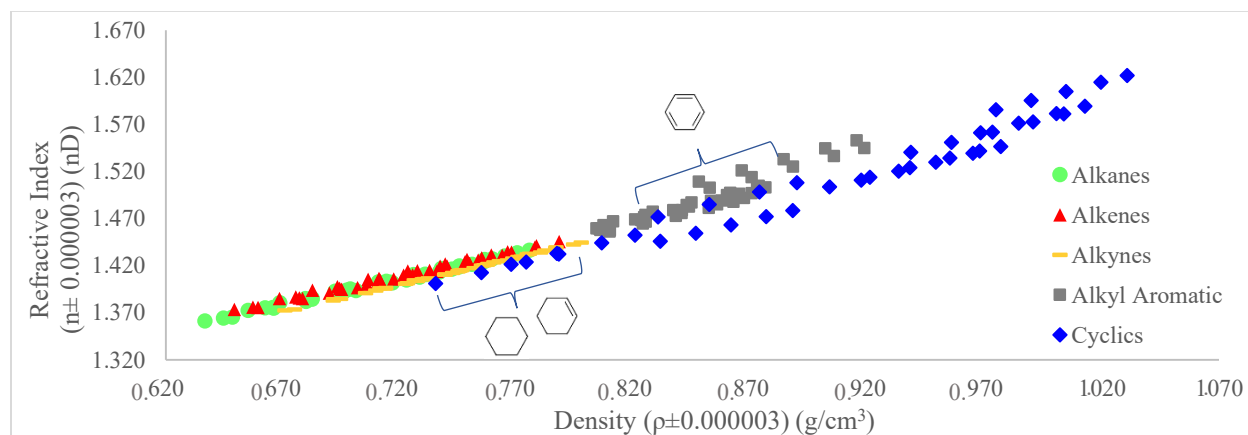
Figure 6.3. Refractive index vs density of different compound groups.

4.3 Molar refractivity

4.3.1 Cyclic

Table 6.6 shows the molar refractivity (Rm) of selected linear alkenes at different temperatures calculated with equations 2.IX, 2.X, 2.XI, and 2.XII from Chapter II.

Table 6.6. Molar refractivity of selected cyclic compounds calculated with equations 2.IX-2.XII

Model Compound	Temperature (T ± 0.01) °C	Molar Refractivity (Rm) (cm³/mol)			
		Berthelot (Eq. 2.IX) (Rm ± 0.002)	Gladstone & Dale (Eq. 2.X) (Rm ± 0.0006)	Lorentz-Lorenz (Eq. 2.XI) (Rm ± 0.0003)	Eykman (Eq. 2.XII) (Rm ± 0.0007)
Cyclohexane	10.00	112.228	46.1461	27.7060	61.2593
	25.00	111.657	46.0702	27.7290	61.2279
	45.00	110.902	45.9734	27.7629	61.1938
	65.00	110.211	45.9023	27.8116	61.1947
Cyclohexene	10.00	111.051	45.2848	27.0255	59.9537
	25.00	110.531	45.2268	27.0583	59.9433
	45.00	109.857	45.1581	27.1073	59.9422
	65.00	109.181	45.0916	27.1585	59.9462
Benzene	10.00	117.564	46.8803	27.5114	61.6246
	25.00	116.948	46.8177	27.5571	61.6182
	45.00	116.112	46.7294	27.6158	61.6053
	65.00	115.315	46.6559	27.6826	61.6129
Indan	10.00	168.098	66.1392	38.4095	86.5779
	25.00	167.425	66.0737	38.4630	86.5732
	45.00	166.529	65.9864	38.5339	86.5676
	65.00	165.694	65.9189	38.6143	86.5873
	85.00	164.839	65.8454	38.6920	86.6013
Inden	10.00	173.460	67.2135	38.5577	87.5737
	25.00	172.706	67.1358	38.6132	87.5574
	45.00	171.723	67.0370	38.6883	87.5417
	65.00	170.763	66.9449	38.7659	87.5348
	85.00	169.829	66.8607	38.8470	87.5387
Decalin	10.00	184.626	74.4938	44.1090	98.2887
	25.00	183.943	74.4160	44.1507	98.2695
	45.00	183.026	74.3088	44.2038	98.2401
	65.00	182.136	74.2102	44.2608	98.2223
	85.00	181.335	74.1427	44.3338	98.2441

Table 6.6. Molar refractivity of selected cyclic compounds
calculated with equations 2.IX-2.XII. Continuation

Model Compound	Temperature (T ± 0.01) °C	Molar Refractivity (Rm) (cm³/mol)			
		Berthelot (Eq. 2.IX) (Rm ± 0.002)	Gladstone & Dale (Eq. 2.X) (Rm ± 0.0006)	Lorentz-Lorenz (Eq. 2.XI) (Rm ± 0.0003)	Eykman (Eq. 2.XII) (Rm ± 0.0007)
Tetralin	10.00	188.186	73.9115	42.8629	96.6991
	25.00	187.505	73.8500	42.9219	96.7020
	45.00	186.574	73.7596	42.9960	96.6961
	65.00	185.707	73.6896	43.0797	96.7161
	85.00	184.852	73.6243	43.1659	96.7433
1,2 Dihydronaphthalene	10.00	195.974	75.6988	43.3140	98.5356
	25.00	195.203	75.6248	43.3765	98.5275
	45.00	194.179	75.5258	43.4586	98.5165
	65.00	193.182	75.4339	43.5433	98.5147
1-Methylnaphthalene	10.00	224.877	85.7728	48.5680	111.2275
	25.00	224.041	85.6937	48.6367	111.2175
	45.00	222.944	85.5924	48.7296	111.2096
	65.00	221.879	85.5002	48.8263	111.2137
	85.00	220.805	85.4054	48.9219	111.2157

Table 6.6 shows that the Rm obtained with one correlation is different from the Rm calculate with other equations. To determine which equation is the least biased, the average Rm and its standard deviation were calculated and shown in table 6.7. The least bias correlation would be the one in which the calculated Rm varies the least with the change of temperature, the one with the lowest standard deviation.

Table 6.7. Average molar refractivity for the selected cyclic compounds

Model Compound		Molar Refractivity (cm³/mol)				Best Correlation
		Berthelot (Eq. 2.IX) (Rm ± 0.002)	Gladstone & Dale (Eq. 2.X) (Rm ± 0.0006)	Lorentz-Lorenz (Eq. 2.XI) (Rm ± 0.0003)	Eykman (Eq. 2.XII) (Rm ± 0.0007)	
Cyclohexane	Av. Rm	111.250	46.0230	27.7524	61.2189	Eykman
	s	0.880	0.1071	0.0458	0.0313	
Cyclohexene	Av. Rm	110.155	45.1903	27.0874	59.9464	Eykman
	s	0.813	0.0837	0.0581	0.0052	
Benzene	Av. Rm	116.485	46.7708	27.5917	61.6152	Eykman
	s	0.981	0.0985	0.0741	0.0082	
Indan	Av. Rm	166.517	65.9927	38.5425	86.5815	Eykman
	s	1.306	0.1175	0.1136	0.0133	
Inden	Av. Rm	171.696	67.0384	38.6944	87.5493	Eykman
	s	1.457	0.1418	0.1159	0.0161	
Decalin	Av. Rm	183.013	74.3143	44.2116	98.2530	Eykman
	s	1.327	0.1439	0.0890	0.0262	
Tetralin	Av. Rm	186.565	73.7670	43.0053	96.7113	Eykman
	s	1.340	0.1164	0.1211	0.0194	
1,2 Dihydronaphthalene	Av. Rm	194.635	75.5708	43.4231	98.5236	Eykman
	s	1.216	0.1156	0.0996	0.0098	
1-Methylnaphthalene	Av. Rm	222.909	85.5929	48.7365	111.2168	Eykman
	s	1.631	0.1469	0.1422	0.0067	

Av. Rm: Average molar refractivity.

s: standard deviation.

Table 6.7 shows that for all the cyclic compound, the correlation by Eykman (Equation 2.XII) had the lowest standard deviation. Followed by the correlation by Lorentz-Lorenz (Equation 2.XI), then by Gladstone & Dale correlation (Equation 2.X) and at last, Berthelot (Equation 2.IX) with the biggest standard deviation.

4.3.2 Alkyl aromatics

Table 6.8 shows the Rm of the selected alkyl aromatic compounds at different temperatures. Rm was calculated with equations 2.IX, 2.X, 2.XI, and 2.XII from Chapter II.

Table 6.8. Molar refractivity of alkyl aromatic compounds, calculated with equations 2.IX-2.XII from Chapter II

| Model Compound | Temperature (T ± 0.01) °C | Molar Refractivity (Rm) (cm³/mol) | | | |
		Berthelot (Eq. 2.IX) (Rm ± 0.002)	Gladstone & Dale (Eq. 2.X) (Rm ± 0.0006)	Lorentz-Lorenz (Eq. 2.XI) (Rm ± 0.0003)	Eykman (Eq. 2.XII) (Rm ± 0.0007)
	10.00	132.305	52.8649	31.0713	69.5354
	25.00	131.695	52.8020	31.1159	69.5281
Toluene	45.00	130.870	52.7154	31.1741	69.5164
	65.00	130.086	52.6445	31.2412	69.5265
	85.00	129.286	52.5712	31.3085	69.5365
	10.00	153.001	61.1376	35.9350	80.4181
	25.00	152.369	61.0773	35.9862	80.4190
m-Xylene	45.00	151.503	60.9905	36.0516	80.4137
	65.00	150.680	60.9199	36.1260	80.4306
	85.00	149.860	60.8532	36.2039	80.4554
	10.00	160.623	62.9191	36.4113	82.2505
	25.00	159.868	62.8378	36.4634	82.2309
Styrene	45.00	158.878	62.7352	36.5354	82.2130
	65.00	157.893	62.6350	36.6090	82.1999
	85.00	156.893	62.5319	36.6821	82.1857
	10.00	171.193	68.5717	40.3788	90.2653
	25.00	170.499	68.5059	40.4353	90.2674
Cumene	45.00	169.593	68.4256	40.5146	90.2809
	65.00	168.694	68.3491	40.5964	90.3012
	85.00	167.760	68.2631	40.6745	90.3125
	10.00	177.184	69.7089	40.4803	91.2489
	25.00	177.479	69.9796	40.7083	91.6657
α-methylstyrene	45.00	176.382	69.8572	40.7791	91.6320
	65.00	175.308	69.7433	40.8544	91.6107
	85.00	174.264	69.6408	40.9361	91.6058
	10.00	173.860	69.4208	40.7802	91.2920
	25.00	173.201	69.3643	40.8403	91.3037
Mesitylene	45.00	172.293	69.2805	40.9165	91.3105
	65.00	171.424	69.2114	41.0009	91.3377
	85.00	170.565	69.1491	41.0902	91.3761

Table 6.8. Molar refractivity of alkyl aromatic compounds, calculated with equations 2.IX-2.XII from Chapter II. Continuation

Model Compound	Temperature (T ± 0.01) °C	Molar Refractivity (cm³/mol)			
		Berthelot (Eq. 2.IX) (Rm ± 0.002)	Gladstone & Dale (Eq. 2.X) (Rm ± 0.0006)	Lorentz-Lorenz (Eq. 2.XI) (Rm ± 0.0003)	Eykman (Eq. 2.XII) (Rm ± 0.0007)
p-Cymene	10.00	192.020	76.9363	45.3143	101.2854
	25.00	191.300	76.8727	45.3777	101.2956
	45.00	190.325	76.7826	45.4594	101.3040
	65.00	189.365	76.6993	45.5450	101.3227
	85.00	188.473	76.6413	45.6446	101.3755
Hexylbenzene	10.00	229.289	92.0219	54.2682	121.2092
	25.00	228.459	91.9425	54.3349	121.2110
	45.00	227.327	91.8274	54.4188	121.2030
	65.00	226.261	91.7350	54.5140	121.2245
	85.00	225.173	91.6359	54.6059	121.2395
1-Phenyldecane	10.00	307.016	123.4233	72.8793	162.6572
	25.00	305.987	123.3251	72.9621	162.6603
	45.00	304.583	123.1811	73.0647	162.6488
	65.00	303.285	123.0723	73.1843	162.6818

Similarly to the previous section, it is required to find which correlation better expressed the empirical data of the alkyl aromatic compounds. The best correlation would be the one least temperature invariant, with the lowest standard deviation. Table 6.9 shows the average molar refractivity with its standard deviation for each correlation.

Table 6.9. Average molar refractivity of the selected alkyl aromatic compounds

Model Compound		Molar Refractivity (cm³/mol)				Best Correlation
		Berthelot (Eq. 2.IX) (Rm ± 0.002)	Gladstone & Dale (Eq. 2.X) (Rm ± 0.0006)	Lorentz-Lorenz (Eq. 2.XI) (Rm ± 0.0003)	Eykman (Eq. 2.XII) (Rm ± 0.0007)	
Toluene	Av. Rm	131.239	52.7567	31.1506	69.5266	Eykman
	s	0.968	0.0967	0.0736	0.0078	
m-Xylene	Av. Rm	151.483	60.9957	36.0605	80.4274	Eykman
	s	1.262	0.1150	0.1075	0.0169	
Styrene	Av. Rm	158.831	62.7318	36.5402	82.2160	Eykman
	s	1.494	0.1546	0.1089	0.0255	

Av. Rm: Average molar refractivity.　　　　　　　　　　　　　　　s: standard deviation.

Table 6.9. Average molar refractivity of the selected alkyl
aromatic compounds. Continuation

Model Compound		Molar Refractivity (cm³/mol)				Best Correlation
		Berthelot (Eq. 2.IX) (Rm ± 0.002)	Gladstone & Dale (Eq. 2.X) (Rm ± 0.0006)	Lorentz-Lorenz (Eq. 2.XI) (Rm ± 0.0003)	Eykman (Eq. 2.XII) (Rm ± 0.0007)	
Cumene	Av. Rm	169.548	68.4231	40.5199	90.2855	Eykman
	s	1.373	0.1225	0.1192	0.0208	
α-methylstyrene	Av. Rm	176.123	69.7860	40.7516	91.5526	Eykman
	s	1.337	0.1336	0.1738	0.1714	
Mesitylene	Av. Rm	172.269	69.2852	40.9256	91.3240	Eykman
	s	1.325	0.1102	0.1237	0.0336	
p-Cymene	Av. Rm	190.297	76.7864	45.4682	101.3166	Eykman
	s	1.429	0.1210	0.1313	0.0356	
Hexylbenzene	Av. Rm	227.302	91.8325	54.4284	121.2175	Eykman
	s	1.651	0.1550	0.1354	0.0146	
1-Phenyldecane	Av. Rm	304.565	123.1909	73.0777	162.6703	Eykman
	s	2.029	0.1890	0.1680	0.0221	

Av. Rm: Average molar refractivity.   s: standard deviation.

Table 6.9 shows that the correlation by Eykman is the least temperature-dependent for the selected alkyl aromatic compounds. Followed by the correlation by Lorentz-Lorenz correlation, Gladstone & Dale correlation, and at last, Berthelot's correlation, which has a higher standard deviation.

4.4 Atomic refraction & group contribution

Table 6.10 shows the atomic refraction (AR) of carbon (C), hydrogen (H), and double (C=C) bonds. This table also lists group contribution (GC) of C-H, C-C, and C=C bonds. These values were calculated in Chapter IV and V.

In the present section, Rm is estimated for alkyl aromatic and cyclic compounds using AR and GC.

Table 6.10. Atomic refraction and group contribution for Eykman

Atomic refraction (cm³/mol)			Group contribution (cm³/mol)		
Carbon	Hydrogen	Double bond	C-H Bond	C-C Bond	C=C
6.770	1.782	2.748	3.474	3.38608	9.517

4.4.1 Cyclic

Table 6.11. Rm calculated with the experimental, AR and GC for the selected

cyclic compounds for the correlation by Eykman

Model Compound	Molar Refractivity (cm³/mol)		Average calculated value with exp. data (Rm ± 0.0007)	Delta between average exp. Rm and Rm calculated with AR or GC (cm³/mol)
	Calculated with atomic refraction and group contribution			
Cyclohexane	AR	62.0019	61.21893276	0.7830
	GC	62.00448		0.7855
Cyclohexene	AR	61.186619	59.94635425	1.2403
	GC	61.186619		1.2403
Benzene	AR	59.556057	61.61524446	2.0592
	GC	59.55465		2.0606
Indan	AR	86.993407	86.58146189	0.4119
	GC	86.993407		0.4119
Inden	AR	86.178126	87.54927574	1.3711
	GC	86.17836		1.3709
Decalin	AR	99.7729	98.2529556	1.5199
	GC	99.77888		1.5259
Tetralin	AR	97.327057	96.71132082	0.6157
	GC	97.32905		0.6177
1,2 Dihydronaphthalene	AR	96.511776	98.52356626	2.0118
	GC	96.51244		2.0111
1-Methylnaphthalene	AR	106.030145	111.2168057	5.1867
	GC	106.02991		5.1869

AR: atomic refraction

GC: group contribution

Table 6.11 shows that Rm estimated with AR and GC differs from the Rm calculated with the experimental. The biggest difference between these Rm was 5.2 cm³/mol. This difference could be decreased if the AR and GC coefficients were calculated by regression.

In addition, the difference between $|\text{Rm}_{exp} - \text{Rm}_{AR}|$ and $|\text{Rm}_{exp} - \text{Rm}_{GC}|$ was not bigger than 0.0050 cm³/mol, implying that both, AR and GC, can be used indistinctly.

4.4.2 Alkyl aromatics

Table 6.12. Molar refractivity calculated with the experimental data, AR and GC for the correlation by Eykman for alkyl aromatic model compounds

Model Compound	Molar Refractivity (cm^3/mol)			Delta between average exp. Rm and Rm calculated with AR or GC (cm^3/mol)
	Calculated with atomic refraction and group contribution		Average calculated value with exp. data (Rm ± 0.0007)	
Toluene	AR	69.8897	69.5266	0.3631
	GC	69.8887		0.3621
m-Xylene	AR	80.2234	80.4274	0.2040
	GC	80.2228		0.2045
Styrene	AR	79.4081	82.2160	2.8079
	GC	79.4062		2.8098
Cumene	AR	90.5570	90.2855	0.2715
	GC	90.5569		0.2714
α-Methylstyrene	AR	89.7417	91.5526	1.8109
	GC	89.7403		1.8123
Mesitylene	AR	90.5570	91.3240	0.7670
	GC	90.5569		0.7671
p-Cymene	AR	100.8907	101.3166	0.4260
	GC	100.8910		0.4257
Hexylbenzene	AR	121.5580	121.2175	0.3405
	GC	121.5591		0.3417
1-Phenyldecane	AR	162.8926	162.6703	0.2223
	GC	162.8955		0.2252

AR: atomic refraction

GC: group contribution

Table 6.12 shows that the difference between $\left|Rm_{exp} - Rm_{AR}\right|$ and $\left|Rm_{exp} - Rm_{GC}\right|$ is not bigger than 0.0050 cm^3/mol proving that Rm can be predicted indistinctly with atomic refraction and group contribution.

It was not possible to infer the difference of the refractive index contribution of (C=C)$_{aliphatic}$ compared to (C=C)$_{aromatic}$. Because tables 6.11 and 6.12 do not show a clear tendency with respect to which Rm has a higher value, the calculated with empirical data or the estimated with AR or GC.

5. Conclusions

- The average first derivate of refractive index with respect to density ($dn/d\rho$) for the selected cyclic hydrocarbon compounds was 0.61 ± 0.02. Moreover, it was noticed that the derivate increase with the increase of the saturation of the model compounds when comparing compounds with the same number of rings and the ring containing the same amount of carbons.

- For the alkyl aromatic model compounds the average $dn/d\rho$ was 0.61 ± 0.02. However, it was found that alkyl aromatics with saturated alkyl chains had a higher average $\delta n/\delta \rho$ (0.645 ± 0.008) than those with unsaturated alkyl chains substituent (0.604 ± 0.004).

- The average $dn/d\rho$ of cyclic hydrocarbons (0.61 ± 0.02), and alkyl aromatics with saturated alkyl chains (0.604 ± 0.004) compounds were roughly the same as the slope $dn/d\rho$ (0.6) reported in the literature for hydrocarbons.

- The average $dn/d\rho$ alkyl aromatics with saturated alkyl chains (0.604 ± 0.004) and cyclic hydrocarbons (0.61 ± 0.02) compounds were roughly similar to the average $dn/d\rho$ of the selected alkanes (0.598 ± 0.003), alkenes (0.604 ± 0.002), and alkynes (0.587 ± 0.005).

- The correlation that better expressed the empirical data for alkyl aromatic and cyclic compounds was that by Eykman.

- Atomic refraction and group contribution gave comparable results when used to predict the molar refractivity of alkyl aromatic and cyclic compounds.

6. References

(1)   Strausz, O.; Lown, E. *The Chemistry of Alberta Oil Sands, Bitumen and Heavy Oil*; Alberta Energy Research Institute: Calgary, 2003.

(2)   Yurkanis, P. *Organic Chemistry*; Pearson Education: California, 2006.

(3)   RELXGroup. Reaxys database https://www.reaxys.com/#/login (accessed Sep 20, 2019).

(4)   Kurtz, S. S. Physical Properties and Hydrocarbon Structure. In *The chemistry of petroleum hydrocarbons. Vol 1*; Reinhold Publishing Corporation: New York, 1954; pp 275–331.

CHAPTER VII - FUNDAMENTAL STUDY OF MOLAR REFRACTIVITY WITH ALCOHOL AND CARBOXYLIC ACID MODEL COMPOUNDS

Correlations available in the literature and that relate molar refractivity, refractive index, and density are evaluated using alcohol and carboxylic acid model compounds.

Abstract

Similar to Chapters IV, V, and VI, the objective of the present chapter is to evaluate the fundamental issues about molar refractivity. It was found that for most of the selected compounds the correlation proposed by Eykman $\left(R_M = \left(\frac{n^2-1}{n+0.4}\right) \cdot \frac{M}{\rho}\right)$ was the least temperature-dependent. In the case of propionic acid and butyric acid the correlation by Gladstone & Dale $\left(R_M = (n-1) \cdot \frac{M}{\rho}\right)$ was slightly better.

The orientation polarization ($8.5E^{-23}$ cm^3/mol) of propionic acid was calculated, and it was insignificant compared with the propionic acid molar refractivity (38.5509 ± 0.0007 cm^3/mol). Proving than the orientation polarization is negligible as suggested in the literature.

Keywords: *Carboxylic acids, alcohol, molar refractivity, refractive index, density.*

1. Introduction

Molar refractivity is an intrinsic and temperature invariant property. The literature[1] reports different equations that correlate molar refractivity, refractive index, and density, but it is not clear which is the best equation. The best correlation would be the one for which the calculated molar refractivity is the least temperature-dependent. These correlations have been evaluated in Chapter IV to VI using different hydrocarbons, for which the best correlation was that one by Eykman $\left(R_M = \left(\frac{n^2-1}{n+0.4}\right) \cdot \frac{M}{\rho}\right)$.

The present chapter aims to evaluate the correlations using alcohols and carboxylic acids and to determine, which of the correlations better express the alcohols and carboxylic acids empirical data. The alcohols are organic compounds with one or more hydroxyl groups (-OH) bonded to a carbon atom (C).[2] While the carboxylic acids are organic compounds with a carboxyl group (COOH).[2] These are polar compounds that would be used to verify whether only electronic polarizability plays a role in the calculated molar refractivity, as the literature suggested.

In addition, the first derivative of refractive index with respect to density is calculated for each of the selected model compounds and it is compared with the values obtained for alkanes, alkenes, alkynes, alkyl aromatic and cyclic compound classes studied in Chapter IV to VI. The molar refractivity is also estimated by atomic refraction and group contribution.

2. Experimental

2.1 Materials

The selected model compounds are listed in Table 7.1. The selected alcohols are linear with a hydroxyl group bonded to the first carbon, i.e. *n*-1-alcohols. The selected carboxylic acids are mostly linear, with the exception of isovaleric acid, and 2-methylvaleric acid. The objective was to study the effect of oxygen-containing compounds and carbon number in the molar refractivity.

Table 7.1. Selected carboxylic acid and 1-alcohol compounds

| Compound Class | Reagent | CASRN[a] | Structure | Purity (wt %) | | Supplier |
				Supplier[b]	FID[c]	
Alcohol	Ethanol	64-17-5	CH_3CH_2OH	99	100.0	Commercial Alcohols
	1-Propanol	71-23-8	$CH_3(CH_2)_2OH$	95	100.0	Fisher
	1-Butanol	71-36-3	$CH_3(CH_2)_3OH$	95	100.0	Fisher
	1-Pentanol	71-41-0	$CH_3(CH_2)_4OH$	99	100.0	Acros Organic
	1-Hexanol	111-27-3	$CH_3(CH_2)_5OH$	99	98.7	Alfa Aesar
	1-Heptanol	111-70-6	$CH_3(CH_2)_6OH$	98	99.9	Aldrich
	1-Octanol	111-87-5	$CH_3(CH_2)_7OH$	>99	99.8	Sigma-Aldrich
	1-Nonanol	143-08-8	$CH_3(CH_2)_8OH$	98	99.9	Aldrich
	1-Decanol	112-30-1	$CH_3(CH_2)_9OH$	>98	99.6	Alfa Aesar
Carboxylic Acid	Propionic Acid	79-09-4	CH_3CH_2COOH	99.5	100.0	Sigma-Aldrich
	Butyric Acid	107-92-6	$CH_3(CH_2)_2COOH$	99	99.0	Aldrich
	Isovaleric Acid	503-74-2	$CH_3(CH_2)_3COOH$	99	98.5	Aldrich
	Valeric Acid	109-52-4	$CH_3(CH_2)_3COOH$	99	99.7	Acros Organic
	Hexanoic Acid	142-62-1	$CH_3(CH_2)_4COOH$	99	99.0	Aldrich
	2-Methylvaleric Acid	97-61-0	$CH_3(CH_2)_5COOH$	98	99.1	Aldrich
	Heptanoic Acid	111-14-8	$CH_3(CH_2)_5COOH$	97	98.9	Sigma
	Octanoic Acid	124-07-2	$CH_3(CH_2)_6COOH$	99	98.9	Sigma
	Nonanoic Acid	112-05-0	$CH_3(CH_2)_7COOH$	97	98.4	Acros Organic

[a] CASRN: Chemical Abstracts Services Registry Number

[b] Purity of the material guaranteed by the supplier; the material was not further purified.

[c] Purity calculated based on peak area obtained by GC-FID analysis

Table 7.1 shows that for octanoic acid, isovaleric acid, and 1-hexanol the purity calculated with GC-FID analysis is lower than the one guaranteed by the supplier. However, the purity determined by FID did not take the lower response factor of oxygen-containing groups into account and is a purity based on uncorrected FID response area in the chromatogram.

2.2 Equipment, procedures, methodologies, and calculations

The equipment, procedures, methodologies, and calculations have been explained in detail in Chapter III.

3. Results

Table 7.2 shows the average density of the selected model compounds in the temperature range 10-85 °C. Density measurements were highly repeatable as shown by the calculated standard deviation which is as low as $\pm$ 0.000000 g/cm³ and not higher than $\pm$ 0.000050 g/cm³.

Table 7.2. Average density at different temperatures of selected model compounds

Compound Class	Model Compound	Temperature (T ± 0.001) °C	Average density (ρ ± 0.000003) g/cm³	Standard deviation (g/cm³)
1-Alcohol	Ethanol	10.000	0.798461	0.000003
		25.000	0.785652	0.000002
		45.000	0.768163	0.000002
		65.000	0.749840	0.000002
	1-Propanol	10.000	0.811608	0.000001
		25.000	0.799655	0.000001
		45.000	0.783278	0.000002
		65.000	0.766050	0.000001
		85.000	0.747511	0.000003
	1-Buthanol	10.000	0.817123	0.000001
		25.000	0.805749	0.000000
		45.000	0.790187	0.000001
		65.000	0.773872	0.000001
		85.000	0.757438	0.000001
	1-Pentanol	10.000	0.821792	0.000001
		25.000	0.810877	0.000002
		45.000	0.795948	0.000001
		65.000	0.780342	0.000000
		85.000	0.763779	0.000001
	1-Hexanol	10.000	0.825855	0.000001
		25.000	0.815218	0.000001
		45.000	0.800685	0.000001
		65.000	0.785545	0.000002
		85.000	0.769568	0.000003

Table 7.2. Average density at different temperatures of selected model compounds. Continuation

Compound Class	Model Compound	Temperature (T ± 0.001) °C	Average density (ρ ± 0.000003) g/cm3	Standard deviation (g/cm3)
1-Alcohol	1-Heptanol	10.000	0.829204	0.000001
		25.000	0.818757	0.000004
		45.000	0.804517	0.000001
		65.000	0.789734	0.000001
		85.000	0.774222	0.000001
	1-Octanol	10.000	0.832327	0.000017
		25.000	0.822025	0.000013
		45.000	0.808013	0.000012
		65.000	0.793516	0.000010
		85.000	0.778372	0.000009
	1-Nonanol	10.000	0.834424	0.000001
		25.000	0.824211	0.000000
		45.000	0.810363	0.000001
		65.000	0.796078	0.000000
		85.000	0.781221	0.000001
	1-Decanol	25.000	0.826258	0.000009
		45.000	0.812526	0.000007
		65.000	0.798415	0.000008
		85.000	0.783790	0.000007
Carboxylic Acid	Propionic Acid	10.000	1.004339	0.000031
		25.000	0.988075	0.000035
		45.000	0.966471	0.000036
		65.000	0.944859	0.000037
		85.000	0.923096	0.000036
	Butyric Acid	10.000	0.967535	0.000013
		25.000	0.952602	0.000015
		45.000	0.932751	0.000017
		65.000	0.912888	0.000018
		85.000	0.892903	0.000018

Table 7.2. Average density at different temperatures of selected model compounds. Continuation

Compound Class	Model Compound	Temperature (T ± 0.001) °C	Average density (ρ ± 0.000003) g/cm³	Standard deviation (g/cm³)
Carboxylic Acid	Valeric Acid	10.000	0.948483	0.000001
		25.000	0.934751	0.000002
		45.000	0.916472	0.000002
		65.000	0.898163	0.000002
		85.000	0.879734	0.000002
	Isovaleric Acid	10.000	0.935178	0.000022
		25.000	0.921318	0.000021
		45.000	0.902865	0.000021
		65.000	0.884367	0.000021
		85.000	0.865731	0.000020
	2-Methylvaleric Acid	10.000	0.931423	0.000003
		25.000	0.918298	0.000002
		45.000	0.900737	0.000001
		65.000	0.883057	0.000001
		85.000	0.865196	0.000001
	Hexanoic Acid	10.000	0.935889	0.000018
		25.000	0.922828	0.000016
		45.000	0.905452	0.000017
		65.000	0.888051	0.000017
		85.000	0.870552	0.000017
	Heptanoic Acid	10.000	0.925954	0.000005
		25.000	0.913394	0.000005
		45.000	0.896707	0.000006
		65.000	0.880033	0.000005
		85.000	0.863298	0.000005
	Octanoic Acid	25.000	0.905821	0.000000
		45.000	0.889707	0.000000
		65.000	0.873631	0.000001
		85.000	0.857517	0.000000
	Nonanoic Acid	25.000	0.900674	0.000000
		45.000	0.885001	0.000001
		65.000	0.869373	0.000002
		85.000	0.853726	0.000003

Table 7.3 shows the average refractive index of the selected model compounds in the temperature range 10-85 °C. The standard deviation of the refractive index is also reported in this table, to show the high repeatability of the measurements. The standard deviation was not higher than $\pm$ 0.000050 nD and as low as $\pm$ 0.000000 nD.

Table 7.3. Average refractive index at different temperatures of selected model compounds

Compound Class	Model Compound	Temperature (T ± 0.01) °C	Average Refractive Index (n ± 0.000003) nD	Standard deviation (nD)	Barometric pressure (Patm±0.2) (kPa)
1-Alcohol	Ethanol	10.00	1.365531	0.000001	94.1
		25.00	1.359303	0.000001	
		45.00	1.350951	0.000009	
		65.00	1.342319	0.000022	
	1-Propanol	10.00	1.389099	0.000004	93.8
		25.00	1.383066	0.000001	
		45.00	1.374872	0.000001	
		65.00	1.366262	0.000015	
		85.00	1.357053	0.000005	
	1-Buthanol	10.00	1.403232	0.000004	93.4
		25.00	1.397225	0.000003	
		45.00	1.389106	0.000002	
		65.00	1.380801	0.000008	
		85.00	1.371816	0.000008	
	1-Pentanol	10.00	1.414026	0.000012	93.3
		25.00	1.407890	0.000010	
		45.00	1.399838	0.000001	
		65.00	1.391646	0.000002	
		85.00	1.383007	0.000006	
	1-Hexanol	10.00	1.421994	0.000003	93.5
		25.00	1.416382	0.000006	
		45.00	1.408205	0.000006	
		65.00	1.400126	0.000025	
		85.00	1.391634	0.000008	

Table 7.3. Average refractive index at different temperatures of selected model compounds. Continuation

Compound Class	Model Compound	Temperature (T ± 0.01) °C	Average Refractive Index (n ± 0.000003) nD	Standard deviation (nD)	Barometric pressure (Patm±0.2) (kPa)
1-Alcohol	1-Heptanol	10.00	1.428230	0.000002	
		25.00	1.422425	0.000019	
		45.00	1.414796	0.000002	94.2
		65.00	1.406518	0.000005	
		85.00	1.398163	0.000010	
	1-Octanol	10.00	1.433501	0.000003	
		25.00	1.427648	0.000005	
		45.00	1.419987	0.000008	93.3
		65.00	1.411913	0.000002	
		85.00	1.403637	0.000012	
	1-Nonanol	10.00	1.437800	0.000001	
		25.00	1.431978	0.000001	
		45.00	1.424055	0.000002	93.2
		65.00	1.416392	0.000008	
		85.00	1.408025	0.000001	
	1-Decanol	25.00	1.435481	0.000009	
		45.00	1.427639	0.000003	92.9
		65.00	1.419964	0.000005	
		85.00	1.411718	0.000003	
Carboxylic Acid	Propionic Acid	10.00	1.390790	0.000003	
		25.00	1.384446	0.000019	
		45.00	1.375888	0.000049	94.3
		65.00	1.367425	0.000012	
		85.00	1.358868	0.000012	
	Butyric Acid	10.00	1.402326	0.000005	
		25.00	1.395903	0.000006	
		45.00	1.387401	0.000004	94.5
		65.00	1.378982	0.000003	
		85.00	1.370530	0.000013	

Table 7.3. Average refractive index at different temperatures of selected model compounds. Continuation

Compound Class	Model Compound	Temperature (T ± 0.01) ℃	Average Refractive Index (n ± 0.000003) nD	Standard deviation (nD)	Barometric pressure (Patm±0.2) (kPa)
Carboxylic Acid	Valeric Acid	10.00	1.412671	0.000001	
		25.00	1.406444	0.000002	
		45.00	1.398105	0.000006	93.6
		65.00	1.389977	0.000005	
		85.00	1.381806	0.000006	
	Isovaleric Acid	10.00	1.407459	0.000011	
		25.00	1.401154	0.000005	
		45.00	1.392711	0.000002	93.5
		65.00	1.384483	0.000005	
		85.00	1.376168	0.000007	
	2-Methylvaleric Acid	10.00	1.418225	0.000005	
		25.00	1.411738	0.000001	
		45.00	1.403476	0.000001	93.5
		65.00	1.395234	0.000003	
		85.00	1.387086	0.000005	
	Hexanoic Acid	10.00	1.420941	0.000004	
		25.00	1.414804	0.000004	
		45.00	1.406488	0.000002	93.7
		65.00	1.398395	0.000004	
		85.00	1.390401	0.000003	
	Heptanoic Acid	10.00	1.427049	0.000002	
		25.00	1.421063	0.000005	
		45.00	1.412905	0.000006	93.8
		65.00	1.404984	0.000006	
		85.00	1.396952	0.000002	
	Octanoic Acid	25.00	1.426211	0.000010	
		45.00	1.418411	0.000004	
		65.00	1.410394	0.000048	93.3
		85.00	1.402528	0.000003	

Table 7.3. Average refractive index at different temperatures of
selected model compounds. Continuation

Compound Class	Model Compound	Temperature (T ± 0.01) °C	Average Refractive Index (n ± 0.000003) nD	Standard deviation (nD)	Barometric pressure (Patm±0.2) (kPa)
Carboxylic Acid	Nonanoic Acid	25.00	1.430518	0.000000	93.3
		45.00	1.422539	0.000000	
		65.00	1.414683	0.000006	
		85.00	1.406903	0.000016	

The objective was to measure the refractive index and density at 5 different temperatures (10, 25, 45, 65, and 85 °C). However, it was not possible to do so for some of the model compounds because of their relatively low boiling point, ethanol (78 °C)[3], or their relative high freezing point, 1-decanol (6 °C), octanoic acid (16 °C), and nonanoic acid (9 °C)[3]

4. Discussion

4.1 Precision and accuracy of the data

The precision and accuracy of the data were evaluated in Chapter IV, where the experimental method was validated.

4.2 First derivative of refractive index with respect to density (dn/dρ)

In Chapters IV to VI, the first derivative of refractive index with respect to density (dn/dρ) for all selected linear alkanes, alkenes, alkynes, alkyl aromatic, and cyclic compounds was calculated. The following section evaluates the dn/dρ for the selected carboxylic acid and 1-alcohol compounds.

4.2.1 1-Alcohols

Figure 7.1 presents the refractive index vs density of the selected 1-alcohols. All model compounds follow a linear relationship, which appears to have a similar slope

(dn/dρ), although the slopes are numerically different. Table 7.4 lists the dn/dρ values of each selected 1-alcohol.
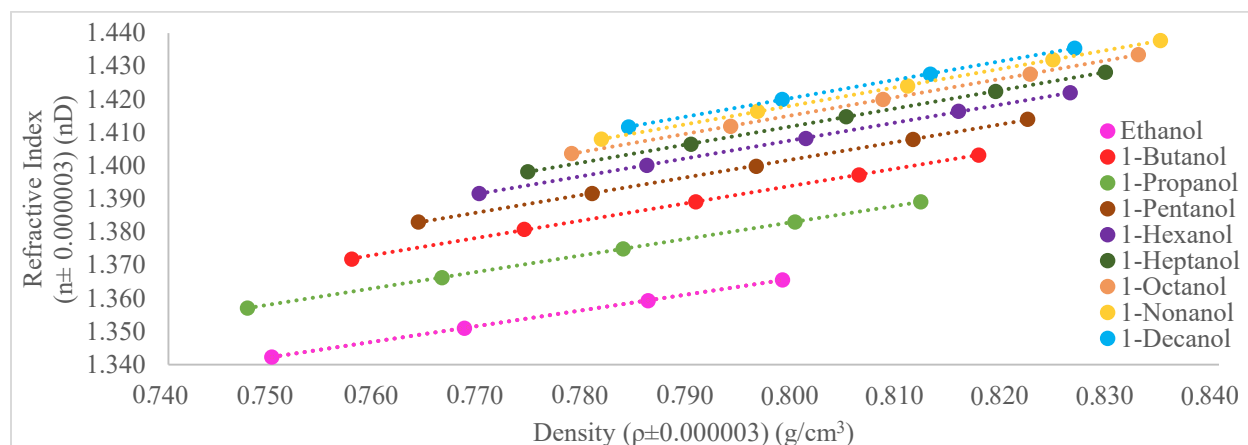
Figure 7.1. Refractive index vs. density of the 1-alcohol model compounds.

Table 7.4 shows that the $dn/d\rho$ values increase as the length of the carbon chain increases. This could be due to the decrease in polarity of the compounds with the increase of the carbon number.

Table 7.4. First derivative of refractive index with respect to density ($dn/d\rho$) for selected 1-alcohol compounds

Model Compound	First derivative ($dn/d\rho \pm 0.0005$)
Ethanol	0.4772
1-Propanol	0.4999
1-Butanol	0.5241
1-Pentanol	0.5336
1-Hexanol	0.5411
1-Heptanol	0.5471
1-Octanol	0.5530
1-Nonanol	0.5582
1-Decanol	0.5880

Table 7.4 shows that as the hydrocarbon character of the alcohols increase (with chain length), the value of the $dn/d\rho$ started to approach 0.6 and the values obtained for

119

the *n*-alkanes (0.598 ± 0.003). In addition, it can be seen that the $dn/d\rho$ increases the most from 1-nonanol and 1-decanol.

This difference between the selected alcohols and hydrocarbons (≈0.6) dn/dρ might be due to the presence of the hydroxyl group, and it could be used to track the change in composition. This will be further discussed in Section 4.2.3 of the present chapter.

4.2.2 Carboxylic Acids

Figure 7.2 presents the refractive index vs. density of the selected carboxylic acids. In all cases, a linear relationship is observed. Furthermore, the refractive index increases with the increase in the carbon number. Whereas, the density decreases with the increase in carbon number. It is worth to notice that the experimental data collected for C_5 and C_6 isomers, i.e. valeric and isovaleric acid, and 2-methylvaleric and hexanoic acids, overlap. It appears that the arrangement of the atoms does not affect the properties being studied as much as the carbon number.
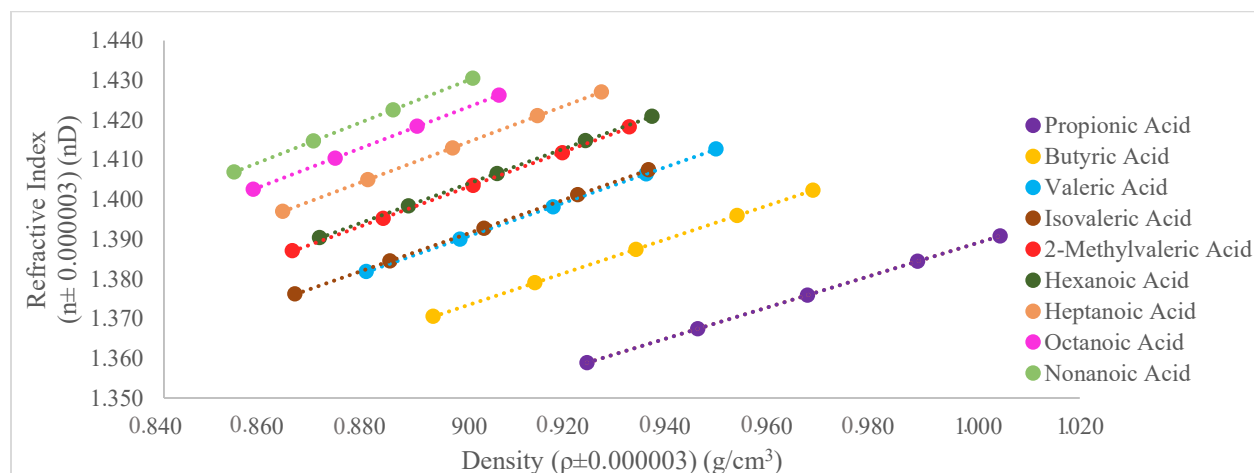
Figure 7.2. Refractive index vs. density of the selected carboxylic acids.

Table 7.5. First derivative of refractive index with respect to density ($dn/d\rho$)

for selected carboxylic acids

Model Compound	First derivative ($dn/d\rho \pm 0.0005$)
Propionic Acid	0.3931
Butyric Acid	0.4260
Valeric Acid	0.4491
Isovaleric Acid	0.4506
2-Methylvaleric Acid	0.4695
Hexanoic Acid	0.4683
Heptanoic Acid	0.4807
Octanoic Acid	0.4911
Nonanoic Acid	0.5030

Table 7.5 lists the values for the dn/dρ of the carboxylic acid model compounds. Same as in the case of the 1-alcohols (see Table 7.4), the value for the dn/dρ increases as the length of the carbon chain increases.

4.2.3 Comparing alkanes, alkenes, alkynes, carboxylic acid, and 1-alcohol compounds

Figure 7.3 shows a plot of refractive index vs density of different compound groups that had been studied. It appears that the compound groups occupied different regions, therefore, refractive index and density could be used to differentiate between them.

In addition, the selected carboxylic acids and 1-alcohols have a different dn/dρ when compared to the other compound classes due to the presence of oxygen. This difference in the slope could be used to detect online changes in composition. For example, it could be used to monitor a particular property of bitumen such as the acid content of bitumen.

Further experiments are required to test this hypothesis, and it is not part of the scope of the present project.
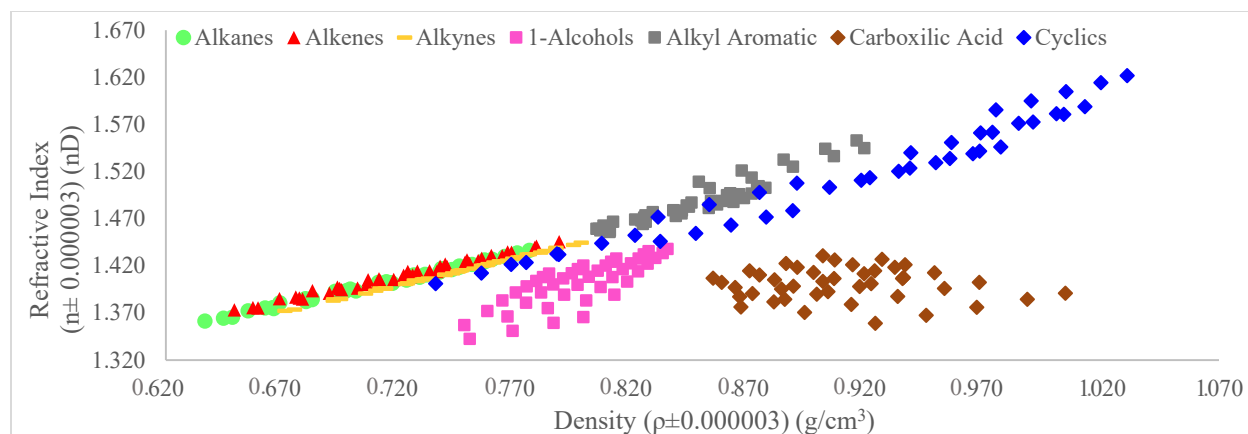
Figure 7.3. Refractive index vs density of different compound groups.

4.3 Molar refractivity

4.3.1 1-Alcohols

Table 7.6 shows the molar refractivity (Rm) of 1-alcohol model compounds in the temperature range 10-85 °C and calculated with equations 2.IX, 2.X, 2.XI, and 2.XII from Chapter II.

Table 7.6. Molar refractivity of selected alcohols calculated with equations 2.IX-2.XII

Model Compound	Temperature (T ± 0.01) °C	Molar Refractivity (Rm) (cm³/mol)			
		Berthelot (Eq. 2.IX) (Rm ± 0.002)	Gladstone & Dale (Eq. 2.X) (Rm ± 0.0006)	Lorentz-Lorenz (Eq. 2.XI) (Rm ± 0.0003)	Eykman (Eq. 2.XII) (Rm ± 0.0007)
Ethanol	10.00	49.890	21.0906	12.9093	28.2580
	25.00	49.709	21.0692	12.9191	28.2548
	45.00	49.483	21.0480	12.9365	28.2606
	65.00	49.264	21.0320	12.9579	28.2748
1-Propanol	10.00	68.826	28.8082	17.5147	38.4694
	25.00	68.598	28.7855	17.5313	38.4718
	45.00	68.298	28.7587	17.5562	38.4807
	65.00	67.983	28.7301	17.5818	38.4897
	85.00	67.653	28.7024	17.6107	38.5037
1-Buthanol	10.00	87.903	36.5770	22.1471	48.7475
	25.00	87.597	36.5408	22.1638	48.7399
	45.00	87.200	36.4989	22.1904	48.7392
	65.00	86.835	36.4729	22.2276	48.7616
	85.00	86.299	36.3850	22.2311	48.7063

Table 7.6. Molar refractivity of selected alcohols calculated with equations 2.IX-2.XII. Continuation

Model Compound	Temperature (T ± 0.01) °C	Molar Refractivity (Rm) (cm³/mol)			
		Berthelot (Eq. 2.IX) (Rm ± 0.002)	Gladstone & Dale (Eq. 2.X) (Rm ± 0.0006)	Lorentz-Lorenz (Eq. 2.XI) (Rm ± 0.0003)	Eykman (Eq. 2.XII) (Rm ± 0.0007)
1-Pentanol	10.00	107.209	44.4107	26.8057	59.0998
	25.00	106.769	44.3415	26.8120	59.0575
	45.00	106.268	44.2815	26.8385	59.0433
	65.00	105.810	44.2416	26.8780	59.0576
	85.00	105.338	44.2040	26.9221	59.0791
1-Hexanol	10.00	126.434	52.2026	31.4352	69.3934
	25.00	126.088	52.1805	31.4737	69.4171
	45.00	125.429	52.0842	31.4909	69.3668
	65.00	124.896	52.0373	31.5366	69.3818
	85.00	124.342	51.9903	31.5857	69.4014
1-Heptanol	10.00	146.570	60.3610	36.2812	80.1706
	25.00	146.078	60.3024	36.3081	80.1559
	45.00	145.519	60.2614	36.3648	80.1848
	65.00	144.787	60.1643	36.3941	80.1468
	85.00	144.150	60.1085	36.4488	80.1651
1-Octanol	10.00	165.059	67.8277	40.7058	90.0239
	25.00	164.474	67.7505	40.7298	89.9924
	45.00	163.810	67.6905	40.7857	90.0063
	65.00	163.051	67.6022	40.8290	89.9881
	85.00	162.324	67.5328	40.8857	89.9983
1-Nonanol	10.00	184.515	75.6893	45.3659	100.4001
	25.00	183.878	75.6082	45.3956	100.3710
	45.00	182.992	75.4899	45.4307	100.3214
	65.00	182.331	75.4559	45.5126	100.3808
	85.00	181.435	75.3458	45.5576	100.3496
1-Decanol	25.00	203.172	83.4219	50.0350	110.6916
	45.00	202.232	83.3040	50.0803	110.6521
	65.00	201.474	83.2548	50.1640	110.7020
	85.00	200.518	83.1431	50.2180	110.6782

Table 7.6 shows that Rm calculated with one correlation cannot be compared to Rm calculated with another correlation. To determine which equation better expresses the

empirical data, the average Rm and its standard deviation are shown in Table 7.7. The best correlation would be the one which calculated Rm that is the least temperature dependent, in other words, the one with the lowest standard deviation.

Table 7.7. Average molar refractivity for the selected 1-alcohol compounds

Model Compound		Molar Refractivity (cm³/mol)				Best Correlation
		Berthelot (Eq. 2.IX) (Rm ± 0.002)	Gladstone & Dale (Eq. 2.X) (Rm ± 0.0006)	Lorentz-Lorenz (Eq. 2.XI) (Rm ± 0.0003)	Eykman (Eq. 2.XII) (Rm ± 0.0007)	
Ethanol	Av. Rm	49.586	21.0600	12.9307	28.2620	Eykman
	s	0.272	0.0255	0.0213	0.0088	
1-Propanol	Av. Rm	68.272	28.7570	17.5589	38.4831	Eykman
	s	0.469	0.0423	0.0385	0.0140	
1-Butanol	Av. Rm	87.167	36.4949	22.1920	48.7389	Eykman
	s	0.631	0.0732	0.0375	0.0204	
1-Pentanol	Av. Rm	106.279	44.2958	26.8513	59.0674	Eykman
	s	0.743	0.0819	0.0488	0.0221	
1-Hexanol	Av. Rm	125.438	52.0990	31.5044	69.3921	Eykman
	s	0.853	0.0911	0.0582	0.0191	
1-Heptanol	Av. Rm	145.421	60.2395	36.3594	80.1646	Eykman
	s	0.972	0.1025	0.0670	0.0145	
1-Octanol	Av. Rm	163.744	67.6808	40.7872	90.0018	Eykman
	s	1.091	0.1169	0.0731	0.0141	
1-Nonanol	Av. Rm	183.030	75.5178	45.4525	100.3646	Eykman
	s	1.221	0.1340	0.0804	0.0303	
1-Decanol	Av. Rm	201.849	83.2809	50.1243	110.6810	Eykman
	s	1.127	0.1156	0.0822	0.0216	

Av. Rm: Average molar refractivity.

s: standard deviation.

Table 7.7 that Rm calculated with the correlation by Eykman (Equation 2.XII) had the lowest standard deviation. Therefore, Rm of the selected 1-alcohols calculated with the correlation by Eykman is the least temperature-dependent

4.3.2 Carboxylic Acids

Table 7.8 shows the Rm of the selected carboxylic acids at different temperatures calculated with equations 2.IX, 2.X, 2.XI, and 2.XII from Chapter II.

Table 7.8. Molar refractivity the selected carboxylic acids, calculated with equations 2.IX-2.XII from Chapter II

Model Compound	Temperature (T ± 0.01) °C	Molar Refractivity (Rm) (cm³/mol)			
		Berthelot (Eq. 2.IX) (Rm ± 0.002)	Gladstone & Dale (Eq. 2.X) (Rm ± 0.0006)	Lorentz-Lorenz (Eq. 2.XI) (Rm ± 0.0003)	Eykman (Eq. 2.XII) (Rm ± 0.0007)
Propionic Acid	10.00	68.914	28.8247	17.5161	38.4823
	25.00	68.728	28.8235	17.5475	38.5150
	45.00	68.454	28.8118	17.5835	38.5461
	65.00	68.199	28.8073	17.6232	38.5867
	85.00	67.935	28.7997	17.6614	38.6242
Butyric Acid	10.00	88.017	36.6384	22.1901	48.8355
	25.00	87.735	36.6186	22.2195	48.8527
	45.00	87.367	36.5948	22.2597	48.8791
	65.00	87.020	36.5785	22.3036	48.9154
	85.00	86.674	36.5632	22.3482	48.9538
Valeric Acid	10.00	107.208	44.4353	26.8312	59.1435
	25.00	106.865	44.4077	26.8634	59.1575
	45.00	106.390	44.3641	26.9021	59.1678
	65.00	105.982	44.3442	26.9534	59.2084
	85.00	105.573	44.3246	27.0049	59.2504
Isovaleric Acid	10.00	107.127	44.4982	26.9101	59.2698
	25.00	106.776	44.4688	26.9417	59.2822
	45.00	106.290	44.4226	26.9797	59.2904
	65.00	105.875	44.4015	27.0309	59.3308
	85.00	105.446	44.3764	27.0802	59.3670
2-Methylvaleric Acid	10.00	126.130	52.1579	31.4431	69.3696
	25.00	125.610	52.0827	31.4575	69.3311
	45.00	125.060	52.0328	31.5032	69.3436
	65.00	124.529	51.9903	31.5529	69.3664
	85.00	124.056	51.9697	31.6147	69.4181

Table 7.8. Molar refractivity the selected carboxylic acids, calculated
with equations 2.IX-2.XII from Chapter II. Continuation

Model Compound	Temperature (T ± 0.01) °C	Molar Refractivity (cm³/mol)			
		Berthelot (Eq. 2.IX) (Rm ± 0.002)	Gladstone & Dale (Eq. 2.X) (Rm ± 0.0006)	Lorentz-Lorenz (Eq. 2.XI) (Rm ± 0.0003)	Eykman (Eq. 2.XII) (Rm ± 0.0007)
Hexanoic Acid	10.00	126.485	52.2461	31.4711	69.4612
	25.00	126.084	52.2131	31.5079	69.4755
	45.00	125.494	52.1481	31.5453	69.4684
	65.00	124.984	52.1114	31.5974	69.4973
	85.00	124.521	52.0922	31.6589	69.5494
Heptanoic Acid	10.00	145.717	60.0388	36.1002	79.7555
	25.00	145.291	60.0113	36.1473	79.7837
	45.00	144.639	59.9437	36.1931	79.7827
	65.00	144.077	59.9078	36.2552	79.8220
	85.00	143.477	59.8580	36.3097	79.8445
Octanoic Acid	25.00	164.629	67.8542	40.8095	90.1477
	45.00	164.014	67.8191	40.8821	90.1966
	65.00	163.289	67.7436	40.9326	90.1952
	85.00	162.636	67.6938	40.9964	90.2268
Nonanoic Acid	25.00	183.828	75.6332	45.4302	100.4239
	45.00	183.013	75.5461	45.4848	100.4167
	65.00	182.246	75.4743	45.5465	100.4288
	85.00	181.518	75.4156	45.6147	100.4581

To determine which correlation better expresses the carboxylic acid data, the average
Rm and its standard deviation were calculated for each model compound. A total of 4
average Rm were calculated per model compound. (See Table 7.9)

Table 7.9. Average molar refractivity of the selected carboxylic acids

Model Compound		Molar Refractivity (cm^3/mol)				Best Correlation
		Berthelot (Eq. 2.IX) (Rm ± 0.002)	Gladstone & Dale (Eq. 2.X) (Rm ± 0.0006)	Lorentz-Lorenz (Eq. 2.XI) (Rm ± 0.0003)	Eykman (Eq. 2.XII) (Rm ± 0.0007)	
Propionic Acid	Av. Rm	68.446	28.8134	17.5863	38.5509	Gladstone & Dale
	s	0.394	0.0107	0.0579	0.0563	
Butyric Acid	Av. Rm	87.362	36.5987	22.2642	48.8873	Gladstone & Dale
	s	0.538	0.0302	0.0635	0.0479	
Valeric Acid	Av. Rm	106.403	44.3752	26.9110	59.1855	Eykman
	s	0.657	0.0456	0.0695	0.0436	
Isovaleric Acid	Av. Rm	106.303	44.4335	29.9886	59.3080	Eykman
	s	0.675	0.0496	0.0682	0.0401	
2-Methylvaleric Acid	Av. Rm	125.077	52.0467	31.5142	69.3658	Eykman
	s	0.827	0.0758	0.0707	0.0334	
Hexanoic Acid	Av. Rm	125.514	52.1622	31.5561	69.4903	Eykman
	s	0.796	0.0658	0.0740	0.0357	
Heptanoic Acid	Av. Rm	144.640	59.9519	36.2011	79.7977	Eykman
	s	0.902	0.0740	0.0835	0.0353	
Octanoic Acid	Av. Rm	163.642	67.7777	40.9052	90.1916	Eykman
	s	0.866	0.0725	0.0791	0.0327	
Nonanoic Acid	Av. Rm	182.651	75.5173	45.5190	100.4319	Eykman
	s	0.994	0.0939	0.0795	0.0182	

Av. Rm: Average molar refractivity.   s: standard deviation.

Table 7.9 shows that the correlation by Eykman is the least temperature-dependent for most of the carboxylic acids, with the exception of propionic and butyric acids. For these two acids, the correlation by Gladstone & Dale has a slightly smaller standard deviation. It raises the question of why these two acids get the least temperature-dependent Rm with Gladstone & Dale equation. Propionic and butyric acid were the two most polar compounds in the study.

In Chapter II, it was shown that orientation (P_O) and distortion polarization (P_D) were neglected from Mosotti-Claussius equation (see Equation 2.VI), and therefore, they are not taken into account when calculating molar refractivity. Only the effects of electronic

polarization are considered in the correlations available in literature to calculate molar refractivity. Propionic and butyric acids are the most polar model compounds used in the present investigation, which could explain why they do not follow the same trend as the rest of the compounds. In other words, it might be possible that the orientation polarization of these compounds have some impact on the overall value of the molar refractivity. The orientation polarization, denoted as P_o in equations 2.VI and 2.VII, of propionic acid was calculated to test this idea. Propionic acid was selected between the two acids in question since it is the most polar, and so it has the highest chance of showing if the P_o has an effect on R_M.

$$P_M = P_O + P_D + P_E = \frac{\varepsilon-1}{\varepsilon+1} \cdot \frac{M}{\rho} \qquad (2.VI)$$

<div align="center">Mosotti–Clausius[8]</div>

Where,

PM: molar polarization (cm^3/mol)

ε: dielectric constant

M: molar mass (g/mol)

$$P_O = \frac{4\pi}{9} \cdot \frac{N_A}{k} \cdot \frac{\mu^2}{T} \qquad (2.VII)$$

<div align="center">Debye[8]</div>

Where,

μ: dipole moment (C.m)

N_A: avogadro number 6.022×10^{23} mol^{-1}

k: Boltzmann constant $1.381 \times$ J·K^{-1}

The calculated orientation polarization is reported in Table 7.10

<div align="center">Table 7.10. Orientation polarization of propionic acid at different temperatures</div>

Temperature (T ± 0.01) °C	Orientation polarization (P_O) (cm^3/mol)
10.00	8.5E-23
25.00	8.5E-23
45.00	8.5E-23
65.00	8.5E-23
85.00	8.5E-23

Table 7.10 shows that the P_O of propionic acid (8.5E-23 cm^3/mol) is significantly smaller than its corresponding Rm (38.5509± 0.0007 cm^3/mol), suggesting that the P_O is negligible as the literature suggests.

It would be interesting to evaluate the molar refractivity correlations with acetic acid to verify if it follows the same trend, and the correlation by Gladstone & Dale gives the lowest standard deviation. Due to time constraints, it was not possible to include this experiment in the present work.

The differences between the standard deviation calculated by Gladstone & Dale and Eykman for propionic and butyric acids are low. Therefore, Eykman is the prefered correlation, since for most of the model compounds the correlation by Eykman is the least temperature-dependent.

4.4 Atomic refraction & group contribution

The atomic refraction (AR) and group contribution (GC) will be calculated for the correlation by Eykman. Table 7.11 shows the AR of carbon (C), hydrogen (H), and double (C=C) bonds. This table also lists GC of C-H, C-C, and C=C bonds. These values were calculated in Chapter IV and V.

In addition, Table 7.11 shows the AR of oxygen and the GC of C-OH, both calculated using ethanol data. And the GC of COOH, calculated with propionic acid data. For the AR it was consider the atom of oxygen connected to a carbon with a single bond (C-O), contributes the same to the Rm as an atom of oxygen connected to a carbon with a double bond (C=O) without the need of correction.

Table 7.11. Atomic refraction and group contribution for the correlation by Eykman

Atomic refraction (cm^3/mol)				Group contribution (cm^3/mol)				
Carbon	Hydrogen	Oxygen	C=C	C-H	C-C	C=C	C-OH	COOH
6.770	1.782	4.031	2.748	3.474	3.386	9.517	7.506	14.408

In the following sections, Rm of the selected carboxylic acids and 1-alcohols is estimated using AR and GC.

4.4.1 1-Alcohol

Table 7.12. Rm calculated with the experimental, AR and GC for the selected
1-alcohols for the correlation by Eykman

Model Compound	Molar Refractivity (cm³/mol)		Average calculated value with exp. data (Rm ± 0.0007)	|Delta between average exp. Rm and Rm calculated with AR or GC (cm³/mol)|
	Calculated with atomic refraction and group contribution			
Ethanol	AR	28.2620	28.2620	0.0000
	GC	28.2620		0.0000
1-Propanol	AR	38.5957	38.4831	0.1126
	GC	38.5961		0.1131
1-Buthanol	AR	48.9293	48.7389	0.1904
	GC	48.9302		0.1913
1-Pentanol	AR	59.2630	59.0674	0.1955
	GC	59.2643		0.1968
1-Hexanol	AR	69.5966	69.3921	0.2045
	GC	69.5984		0.2063
1-Heptanol	AR	79.9303	80.1646	0.2344
	GC	79.9324		0.2322
1-Octanol	AR	90.2639	90.0018	0.2621
	GC	90.2665		0.2647
1-Nonanol	AR	100.5976	100.3646	0.2330
	GC	100.6006		0.2360
1-Decanol	AR	110.9312	110.6810	0.2503
	GC	110.9347		0.2537

Table 7.12 shows that Rm estimated with AR and GC are nearly the same as the Rm calculated with the experimental. In addition, the difference between $\left|Rm_{exp} - Rm_{AR}\right|$ and $\left|Rm_{exp} - Rm_{GC}\right|$ was not bigger than $0.0050 \text{ cm}^3/\text{mol}$, therefore, the Rm estimated with AR is comparable with the one estimated with GC.

4.4.2 Carboxylic Acids

Table 7.13. Rm calculated with the experimental data, AR and GC for the correlation by Eykman for the selected carboxylic acids

Model Compound	Molar Refractivity (cm³/mol)		Average calculated value with exp. data (Rm ± 0.0007)	Delta between average exp. Rm and Rm calculated with AR or GC (cm³/mol)
	Calculated with atomic refraction and group contribution			
Propionic Acid	AR	39.0632	38.5509	0.5123
	GC	38.5509		0.0000
Butyric Acid	AR	49.3969	48.8873	0.5096
	GC	48.8849		0.0024
Valeric Acid	AR	59.7305	59.1855	0.5450
	GC	59.2190		0.0335
Isovaleric Acid	AR	59.7305	59.3080	0.4225
	GC	59.2190		0.0890
2-Methylvaleric Acid	AR	70.0642	69.3658	0.6984
	GC	69.5531		0.1873
Hexanoic Acid	AR	70.0642	69.4903	0.5738
	GC	69.5531		0.0628
Heptanoic Acid	AR	80.3978	79.7977	0.6001
	GC	79.8872		0.0895
Octanoic Acid	AR	90.7315	90.1916	0.5399
	GC	90.2213		0.0297
Nonanoic Acid	AR	101.0651	100.4319	0.6332
	GC	100.5553		0.1235

In Table 7.13, it can be seen that the difference between $\left|Rm_{exp} - Rm_{AR}\right|$ and $\left|Rm_{exp} - Rm_{GC}\right|$ is bigger than 0.0050 cm³/mol, therefore, Rm_{AR} is not comparable to the Rm_{GC}. For all the selected carboxylic acids, the molar refractivity calculated with GC is more accurate than the one calculated with AR. This could be due to the assumption made for the AR. Where an oxygen atom from a C-O and C=O bond, contribute the same. Analyzing the data from Table 7.13, it appears that an oxygen atom from a C-O bonds contributes more than an oxygen in a C=O bond.

5. Conclusions

▪ The first derivate of refractive index with respect to density ($dn/d\rho$) appears to decrease with the increase of polarity of the model compounds.

▪ The difference between $dn/d\rho$ of alkanes (0.598 ± 0.003), alkenes (0.604 ± 0.002), and alkynes (0.587 ± 0.005) and $dn/d\rho$ of carboxylic acids (0.46 ± 0.02) and 1-alcohols (0.54 ± 0.03) could be used to detect online changes in composition, for example, acid content in bitumen.

▪ The correlation that better expressed the empirical data for 1-alcohol model compounds was that by Eykman.

▪ The correlation by Eykman was the least temperature-dependent for most of the selected carboxylic acids, with the exception of propionic and butyric acids, for which the correlation by Gladstone & Dale was a slightly least temperature-dependent.

▪ The orientation polarization of propionic acid was calculated. The Po (8.5E-23 cm^3/mol) was insignificant compare with the propionic acid molar refractivity (38.5509± 0.0007 cm^3/mol). Proving than the Po is in negligible as suggested by the theory.

▪ Atomic refraction and group contribution gave comparable results when used to predict the molar refractivity of 1-alcohols.

▪ Group contribution was more accurate than atomic refraction when estimating the molar refractivity of most of the selected carboxylic acid, with the exception of isovaleric acid.

6. References

(1)   Kurtz, S. S. Physical Properties and Hydrocarbon Structure. In *The chemistry of petroleum hydrocarbons. Vol 1*; Reinhold Publishing Corporation: New York, 1954; pp 275–331.

(2)   McMurry, J. *Organic Chemistry*, 5th ed.; Brooks/Cole: California, 200AD.

(3)   RELXGroup. Reaxys database https://www.reaxys.com/#/login (accessed Sep 20, 2019).

CHAPTER VIII - FUNDAMENTAL STUDY OF MOLAR REFRACTIVITY WITH SULFUR CONTAINING COMPOUNDS AS MODEL COMPOUNDS

Different molar refractivity correlations are evaluated using sulfur-containing compounds as model compounds. The objective is to study the effect of sulfur compounds in the refractive index and molar refractivity

Abstract

Different equations are reported in the literature to calculate molar refractivity, but it is not clear which equation is the best one. These equations correlate molar refractivity, refractive index, and density. The present chapter seeks to evaluate these correlations and determine which equation better expressed the empirical data of the selected sulfur compounds.

Similarly to Chapters IV-VII, accurate and high precision refractive index and density data of the selected sulfur compounds were collected and used to evaluate the different correlations. The correlation by Eykman $\left(R_M = \left(\frac{n^2-1}{n+0.4} \right) \cdot \frac{M}{\rho} \right)$ was the least temperature-dependent for all the sulfur compounds.

The selected linear-non aromatic sulfur compounds overlap with the data of alkanes, alkenes, and alkynes model compounds in a refractive index vs density plot. In addition, it was observed that tetrahydrothiophene grouped with thiophenes and not with the non-cyclic thioethers.

Keywords: *sulfur, molar refractivity, refractive index, density, Eykman.*
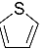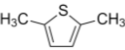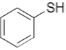
1. Introduction
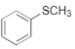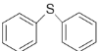
The methodology explained in Chapter IV was followed to evaluate the different molar refractivity correlations reported in the literature. Sulfur-containing compounds were selected as model compounds. As Chapter VI, the model compounds cannot be grouped in one compound class. The objective was to study the effect of sulfur heteroatoms in the refractive index and molar refractivity. The present investigation will be limited to hydrocarbons containing one sulfur atom (S).

2. Experimental

2.1 Materials

Table 8.1 shows the selected sulfur compounds and the purity of the reagents. For all the selected model compounds the purity calculated based on the peak area obtained by GC-FID analysis was higher than the purity guarantee for the supplier for all the selected sulfur compounds.

Table 8.1. Selected model compounds

Reagent	CASRN[a]	Structure	Purity (wt %) Supplier[b]	FID[c]	Supplier
Dimethyl Sulfide	75-18-3	$H_3C - S - CH_3$	>99	99.8	Sigma-Aldrich
Tetrahydrothiophene	110-01-0		>99	99.9	TCI
Thiophene	110-02-1		>99	99.8	Sigma-Aldrich
2,5-Dimethylthiophene	638-0-8		98.5	99.7	Acros Organic
Benzenethiol	110-06-5		97	99.8	Sigma-Aldrich
Thioanisole	100-68-5		>99	100.0	Sigma-Aldrich
Di-n-butyl sulfide	544-40-1	$H_3C(CH_2)_3 - S - (CH_2)_3CH_3$	97	100.0	Alfa Aesar
Diphenyl sulfide	136-66-2		98	99.4	Aldrich
1-Hexadecanethiol	2917-26-2	$CH_3(CH_2)_{15}SH$	>95	99.4	Aldrich

[a] CASRN: Chemical Abstracts Services Registry Number
[b] Purity of the material guaranteed by the supplier; the material was not further purified.
[c] Purity calculated based on peak area obtained by GC-FID analysis

2.2 Equipment, procedures, methodologies, and calculations

The equipment, procedures, methodologies, and calculations have been explained in detail in Chapter III.

The density meter and refractometer were placed inside the fume hood to reduce exposure to the vapors while performing the measurements. Inhaling benzenethiol may cause respiratory irritation or even be fatal.[1]

3. Results

Table 8.2 shows the average density at different temperatures of each one of the selected model compounds. The density values are reported with their standard deviation which is not higher than $\pm$ 0.000025 g/cm^3 and as low as $\pm$ 0.000001 g/cm^3, proving the high repeatability of the measurements.

Table 8.2. Average density at different temperatures of selected model compounds

Model Compound	Temperature (T $\pm$ 0.001) °C	Average density ($\rho \pm$ 0.000003) g/cm^3	Standard deviation (g/cm^3)
Dimethyl Sulfide	10.000	0.842505	0.000014
	25.000	0.860324	0.000014
Tetrahydrothiophene	10.000	1.008452	0.000001
	25.000	0.994130	0.000006
	45.000	0.974865	0.000007
	65.000	0.955319	0.000005
	85.000	0.935427	0.000004
Thiophene	10.000	1.076212	0.000015
	25.000	1.058468	0.000003
	45.000	1.034477	0.000003
	65.000	1.009978	0.000003

Table 8.2. Average density at different temperatures of selected model compounds. Continuation

Model Compound	Temperature (T ± 0.001) °C	Average density (ρ ± 0.000003) g/cm³	Standard deviation (g/cm³)
2,5-Dimethylthiophene	10.000	0.995492	0.000003
	25.000	0.980205	0.000002
	45.000	0.959761	0.000004
	65.000	0.939143	0.000005
	85.000	0.918254	0.000015
Benzenethiol	10.000	1.087125	0.000008
	25.000	1.072713	0.000010
	45.000	1.053496	0.000010
	65.000	1.034210	0.000012
	85.000	1.014792	0.000013
Thioanisole	10.000	1.066744	0.000014
	25.000	1.052792	0.000015
	45.000	1.034191	0.000015
	65.000	1.015533	0.000016
	85.000	0.996766	0.000016
Di-*n*-butyl sulfide	10.000	0.846635	0.000004
	25.000	0.834349	0.000003
	45.000	0.817884	0.000002
	65.000	0.801273	0.000002
	85.000	0.784452	0.000003
Diphenyl Sulfide	10.000	1.121196	0.000001
	25.000	1.108730	0.000003
	45.000	1.092220	0.000001
	65.000	1.075792	0.000002
	85.000	1.059402	0.000001
1-Hexadecanethiol	25.000	0.843443	0.000018
	45.000	0.829549	0.000008
	65.000	0.815735	0.000003
	85.000	0.801958	0.000004

Each average refractive index (see Table 8.3) and average density (see Table 8.2) are means of nine measurements.

Table 8.3 shows the average refractive index at different temperatures of the selected model compounds with its standard deviation. The standard deviation shows the high repeatability of the measurements. The deviation was not higher than ± 0.000070 nD and as low as ± 0.000000 nD.

Table 8.3. Average refractive index at different temperatures of selected model compounds

Model Compound	Temperature (T ± 0.01) °C	Average Refractive Index (n ± 0.000003) nD	Standard deviation (nD)	Barometric pressure (Patm±0.2) (kPa)
Dimethyl Sulfide	10.00	1.441843	0.000002	93.7
	25.00	1.432089	0.000015	
Tetrahydrothiophene	10.00	1.510203	0.000007	
	25.00	1.502339	0.000005	
	45.00	1.491814	0.000005	93.4
	65.00	1.481233	0.000010	
	85.00	1.470569	0.000025	
Thiophene	10.00	1.535191	0.000008	
	25.00	1.525657	0.000002	
	45.00	1.512780	0.000000	93.8
	65.00	1.499851	0.000005	
2,5-Dimethylthiophene	10.00	1.518899	0.000002	
	25.00	1.510308	0.000003	
	45.00	1.498831	0.000006	93.1
	65.00	1.487347	0.000010	
	85.00	1.475847	0.000007	
Benzenethiol	10.00	1.595949	0.000015	
	25.00	1.587165	0.000021	
	45.00	1.575552	0.000003	94.4
	65.00	1.564089	0.000056	
	85.00	1.552543	0.000030	
Thioanisole	10.00	1.592662	0.000005	
	25.00	1.584240	0.000050	
	45.00	1.572996	0.000004	93.5
	65.00	1.561885	0.000018	
	85.00	1.550725	0.000069	

Table 8.3. Average refractive index at different temperatures of
selected model compounds. Continuation

Model Compound	Temperature (T ± 0.01) °C	Average Refractive Index (n ± 0.000003) nD	Standard deviation (nD)	Barometric pressure (Patm±0.2) (kPa)
Di-*n*-butyl sulfide	10.00	1.457625	0.000004	
	25.00	1.450705	0.000004	
	45.00	1.441337	0.000005	94.0
	65.00	1.431843	0.000006	
	85.00	1.422431	0.000003	
Diphenyl Sulfide	10.00	1.638475	0.000018	
	25.00	1.630933	0.000003	
	45.00	1.620874	0.000006	93.2
	65.00	1.611051	0.000006	
	85.00	1.601265	0.000007	
1-Hexadecanethiol	25.00	1.460842	0.000009	
	45.00	1.452677	0.000005	93.6
	65.00	1.444681	0.000007	
	85.00	1.436819	0.000005	

As mentioned in Chapter III, the aim was to measure the refractive index and density at 5 different temperatures (10, 25, 45, 65, and 85 °C), but this was not possible for all the reagents due to their relative low boiling, dimethyl sulfide (35 °C), and thiophene (82 °C), or their relative high freezing point, 1-hexadecanethiol (20 °C). For the last one, it was required to heat it up to unfreeze the reagent, since it was frozen at room temperature.

4. Discussion

4.1 Precision and accuracy of the data

The accuracy of the data was checked in Chapter IV. It was found that the collected data is precise and has good agreement with the literature.[2]

4.2 First derivative of refractive index with respect to density.

Figure 8.1 shows a plot of refractive index vs density of the selected sulfur compounds. In this plot, the data of the compounds appear to be grouped depending on their structure. Linear, non-aromatic chains had the lowest refractive index and density, followed by heterocyclics, and, at last, sulfur-substituted aromatic compounds. And even though the tetrahydrothiophene is a heterocyclic thioether, but it is not aromatic, it resembles thiophenes more than non-cyclic thioethers.
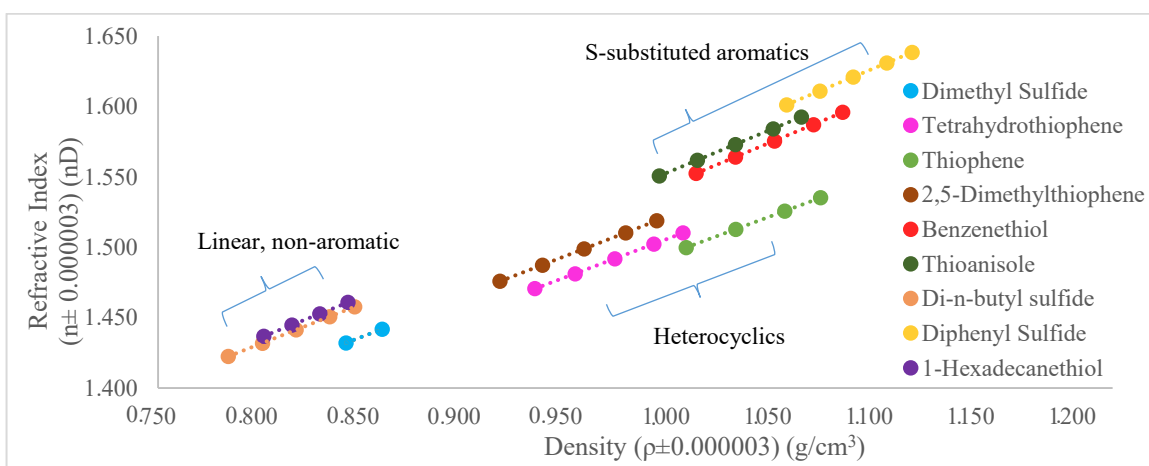
Figure 8.1. Refractive index vs. density of the selected sulfur compounds.

Figure 8.1 also shows that the refractive index vs density of all the sulfur model compounds followed a linear trend. Table 8.4 shows the slope of the linear trend of each model compound. The slope of the linear sulfur compounds increased with the increase of the length of the carbon chain, while the sulfur aromatic compounds have a slope of nearly 0.6. For the thiophenes, the slope appears to increase with the absence of double bonds, when comparing tetrahydrothiophene (0.5429 ± 0.0005) with thiophene (0.5338 ± 0.0005).

Table 8.4. Slope ($dn/d\rho$) of the linear trend of refractive index vs density

for the selected sulfur compounds

Model Compound	First derivative ($dn/d\rho \pm 0.0005$)
Dimethyl Sulfide	0.5474
Tetrahydrothiophene	0.5429
Thiophene	0.5338
2,5-Dimethylthiophene	0.5577
Benzenethiol	0.5998
Thioanisole	0.5993
Di-*n*-butyl sulfide	0.5669
Diphenyl Sulfide	0.6024
1-Hexadecanethiol	0.5791
Average	0.57
Standard deviation	0.03

4.2.1 Comparing alkanes, alkenes, alkynes, alkyl aromatic, cyclic, carboxylic acid, and 1-alcohol compounds

As mentioned in Chapter VII, the difference in the $dn/d\rho$ slope could potentially be used to detect changes following on reaction in complex mixtures.

In Figure 8.2 refractive index vs density of different compounds have been plotted. It can be seen that the studied compound classes appear to be organized in regions. The linear sulfur compounds overlap with the alkanes, alkenes, and alkynes. While the sulfur aromatic compounds are located close to the alkyl aromatic compounds.
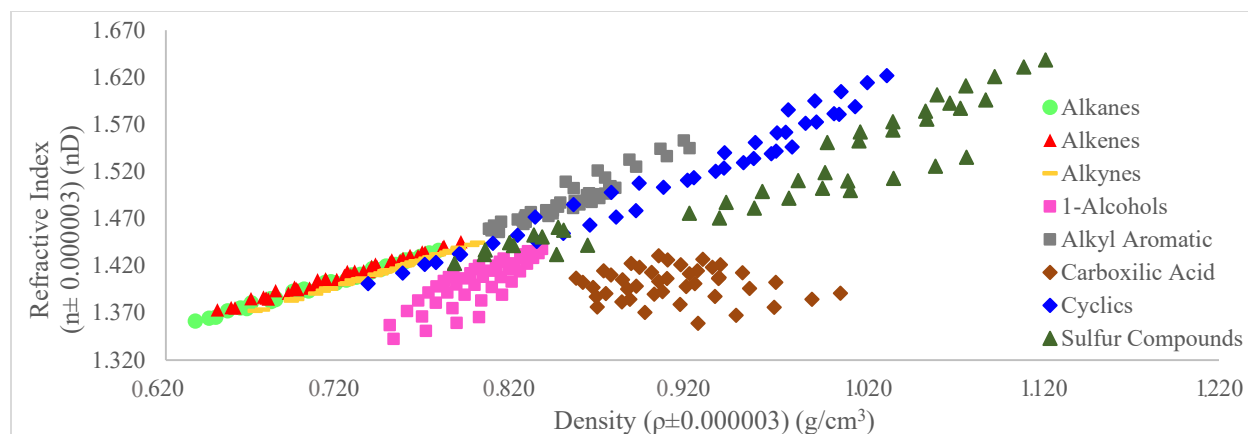
Figure 8.2. Refractive index vs density of different compound classes.

4.3 Molar refractivity

Table 8.5 shows the molar refractivity (Rm) of sulfur model compounds at different temperatures calculated with equations 2.IX-2.XII from Chapter II.

Table 8.5. Molar refractivity of selected sulfur compounds calculated with equations 2.IX-2.XII

Model Compound	Temperature (T ± 0.01) °C	Molar Refractivity (Rm) (cm³/mol)			
		Berthelot (Eq. 2.IX) (Rm ± 0.002)	Gladstone & Dale (Eq. 2.X) (Rm ± 0.0006)	Lorentz-Lorenz (Eq. 2.XI) (Rm ± 0.0003)	Eykman (Eq. 2.XII) (Rm ± 0.0007)
Dimethyl sulfide	10.00	77.916	31.9086	19.1021	42.3031
	25.00	77.496	31.8642	19.1308	42.2995
Tetrahydro-thiophene	10.00	111.885	44.5722	26.1371	58.5724
	25.00	111.398	44.5174	26.1680	58.5582
	45.00	110.751	44.4460	26.2101	58.5423
	65.00	110.116	44.3795	26.2553	58.5339
	85.00	109.493	44.3190	26.3042	58.5346
Thiophene	10.00	106.078	41.8421	24.3476	54.8151
	25.00	105.536	41.7856	24.3866	54.8053
	45.00	104.801	41.7074	24.4378	54.7901
	65.00	104.099	41.6419	24.4964	54.7930

Table 8.5. Molar refractivity of selected sulfur compounds calculated
with equations 2.IX-2.XII. Continuation

| Model Compound | Temperature (T ± 0.01) °C | Molar Refractivity (Rm) (cm^3/mol) | | | |
		Berthelot (Eq. 2.IX) (Rm ± 0.002)	Gladstone & Dale (Eq. 2.X) (Rm ± 0.0006)	Lorentz-Lorenz (Eq. 2.XI) (Rm ± 0.0003)	Eykman (Eq. 2.XII) (Rm ± 0.0007)
2,5-Dimethyl-thiophene	10.00	147.303	58.4790	34.2003	76.7641
	25.00	146.621	58.4076	34.2490	76.7526
	45.00	145.707	58.3102	34.3124	76.7353
	65.00	144.810	58.2185	34.3786	76.7266
	85.00	143.940	58.1378	34.4509	76.7335
Benzenethiol	10.00	156.808	60.4049	34.4856	78.5631
	25.00	156.043	60.3141	34.5296	78.5253
	45.00	155.047	60.1996	34.5905	78.4830
	65.00	154.104	60.1009	34.6584	78.4609
	85.00	153.145	59.9972	34.7238	78.4338
Thioanisole	10.00	178.902	69.0031	39.4354	89.7802
	25.00	178.116	68.9239	39.4952	89.7654
	45.00	177.056	68.8133	39.5717	89.7398
	65.00	176.049	68.7187	39.6554	89.7349
	85.00	175.036	68.6220	39.7380	89.7286
Di-n-butyl sulfide	10.00	194.332	79.0729	47.1145	104.6129
	25.00	193.664	79.0240	47.1829	104.6436
	45.00	192.717	78.9393	47.2642	104.6616
	65.00	191.733	78.8425	47.3393	104.6664
	85.00	190.834	78.7777	47.4320	104.7138
Diphenyl sulfide	10.00	279.874	106.0743	59.7435	137.2960
	25.00	278.879	105.9998	59.8459	137.3154
	45.00	277.515	105.8865	59.9743	137.3243
	65.00	276.256	105.8027	60.1147	137.3691
	85.00	275.003	105.7190	60.2542	137.4147
1-Hexadecanethiol	25.00	347.582	141.2451	84.0776	186.7874
	45.00	345.991	141.0665	84.1771	186.7517
	65.00	344.507	140.9211	84.2913	186.7571
	85.00	343.124	140.8080	84.4207	186.8032

Table 8.5 shows that the Rm calculate with one correlation is different from the Rm calculated with another correlation. To determine which Rm is least temperature-

dependent, the average Rm and its standard deviation were calculated and are shown in Table 8.6. The best correlation would be the one in which the calculated Rm has the lowest standard deviation.

Table 8.6. Average molar refractivity for the selected sulfur compounds

Model Compound		Molar Refractivity (cm³/mol)				Best Correlation
		Berthelot (Eq. 2.IX) (Rm ± 0.002)	Gladstone & Dale (Eq. 2.X) (Rm ± 0.0006)	Lorentz-Lorenz (Eq. 2.XI) (Rm ± 0.0003)	Eykman (Eq. 2.XII) (Rm ± 0.0007)	
Dimethyl sulfide	Av. Rm	77.706	31.8864	19.1164	42.3013	Eykman
	s	0.296	0.0314	0.0203	0.0026	
Tetrahydro-thiophene	Av. Rm	110.729	44.4468	26.2149	58.5483	Eykman
	s	0.960	0.1019	0.0669	0.0167	
Thiophene	Av. Rm	105.128	41.7443	24.4171	54.8009	Eykman
	s	0.863	0.0878	0.0645	0.0115	
2,5-Dimethyl-thiophene	Av. Rm	145.676	58.3106	34.3182	76.7424	Eykman
	s	1.351	0.1379	0.1000	0.0155	
Benzenethiol	Av. Rm	155.029	60.2033	34.5976	78.4932	Eykman
	s	1.466	0.1627	0.0960	0.0514	
Thioanisole	Av. Rm	177.032	68.8162	39.5791	89.7498	Eykman
	s	1.551	0.1531	0.1212	0.0220	
Di-n-butyl sulfide	Av. Rm	192.656	78.9313	47.2666	104.6597	Eykman
	s	1.414	0.1227	0.1253	0.0368	
Diphenyl sulfide	Av. Rm	277.505	105.8965	59.9865	137.3439	Eykman
	s	1.957	0.1438	0.2044	0.0478	
1-Hexadecane-thiol	Av. Rm	345.301	141.0102	84.2417	186.7748	Eykman
	s	1.919	0.1890	0.1479	0.0246	

Av. Rm: Average molar refractivity.

s: standard deviation.

Table 8.6 shows that Rm with the lowest standard deviation is the one calculated with the correlation by Eykman (Equation 2.XII). Therefore, the correlation by Eykman is the equation that better expresses the empirical data of the selected sulfur compounds.

4.4 Atomic refraction & group contribution

In this section, the molar refractivity calculated with the correlation by Eykman will be estimated by atomic refraction (AR) and group contribution (GC). Table 8.7 shows the AR contribution of carbon (C), hydrogen (H), and double (C=C) bonds. And the GC of C-H, C-C, and C=C bonds. These values were calculated in Chapter IV to VII.

Using dimethyl sulfide data the AR of sulfur (S), and the GC of C-S bond were calculated. In addition, using benzenethiol Rm the GC of S-H was calculated. (See Table 8.7)

Table 8.7. Atomic refraction and group contribution for the correlation by Eykman

Atomic refraction (cm^3/mol)				Group contribution (cm^3/mol)				
Carbon	Hydrogen	Sulfur	C=C	C-H	C-C	C=C	C-S	S-H
6.770	1.782	18.070	2.748	3.474	3.386	9.517	10.729	11.68

Table 8.8 shows the estimated Rm of the selected sulfur compounds.

Table 8.8. Rm calculated with the experimental, AR and GC with the

correlation by Eykman for the selected model compounds

Model Compound		Molar Refractivity (cm^3/mol)		Delta between average exp. Rm and Rm calculated with AR or GC (cm^3/mol)
		Calculated with atomic refraction and group contribution	Average calculated value with exp. data (Rm ± 0.0007)	
Dimethyl Sulfide	AR	42.3013	42.3013	0.0000
	GC	42.3013		0.0000
Tetrahydrothiophene	AR	59.4050	58.5483	0.8567
	GC	59.4076		0.8593
Thiophene	AR	57.7744	54.8009	2.9736
	GC	57.7743		2.9735
2,5-Dimethylthiophene	AR	78.4417	76.7424	1.6993
	GC	78.4425		1.7001
Benzenethiol	AR	77.6265	78.4932	0.8668
	GC	78.4932		0.0000
Thioanisole	AR	87.9601	89.7498	1.7897
	GC	87.9600		1.7898
Di-*n*-butyl sulfide	AR	104.3032	104.6597	0.3565
	GC	104.3058		0.3539

Table 8.8. Rm calculated with the experimental, AR and GC with the correlation
by Eykman for the selected model compounds. Continuation

Model Compound	Molar Refractivity (cm³/mol)		Average calculated value with exp. data (Rm ± 0.0007)	|Delta between average exp.| Rm and Rm calculated with AR or GC (cm^3/mol) |
	Calculated with atomic refraction and group contribution			
Diphenyl sulfide	AR	133.6189	137.3439	3.7250
	GC	133.6186		3.7253
1-Hexadecanethiol	AR	186.9724	186.7748	0.1976
	GC	187.8458		1.0709

Table 8.8 shows that Rm estimated with AR and GC are approximately the same as the Rm calculated with the experimental data. The highest difference between the Rm calculated with the Rm estimated is less than 4 cm^3/mol. Moreover, the Rm estimated with AR is comparable with the one estimated with GC for most of the selected model compounds. Benzenethiol and 1-hexadecanethiol for which Rm calculated with GC were more precise than the ones calculated with AR.

5. Conclusions

▪ The first derivative of refractive index with respect to density $(dn/d\rho)$ for linear non-aromatic sulfur compounds increased with the increase of the carbon chain length.

▪ In a plot of refractive index vs density, the selected linear-non aromatic sulfur compounds overlap with the data of alkanes, alkenes, and alkynes model compounds. In addition, it was observed that tetrahydrothiophene grouped with thiophenes and not with the non-cyclic thioethers.

▪ The molar refractivity calculated with the correlation by Eykman was the least temperature-dependent for all the selected sulfur compounds.

▪ Atomic refraction and group contribution gave comparable results for most of the selected sulfur compounds, with the exception of benzenethiol and 1-hexadecanethiol. For the last two, the molar refractivity calculated with group contribution was more accurate.

146

6. References

(1) Sigma-Aldrich.Co. Benzenethiol Safety Data Sheet www.sigmaaldrich.com (accessed Dec 1, 2019).

(2) RELXGroup. Reaxys database https://www.reaxys.com/#/login (accessed Sep 20, 2019).

CHAPTER IX - FUNDAMENTAL STUDY OF OXYGEN SOLUBILITY IN HYDROCARBONS – TITRATION METHOD (1st METHOD)

Evaluation of an adaptation of the titration method by McKeown et al. (1956)[1], for the determination of dissolved oxygen in hydrocarbons. The materials, procedure, results, and analysis of the experimental data are presented.

Abstract

The objective of the present chapter was to use a modified titration method to experimentally determine oxygen solubility in hydrocarbons by using *n*-heptane as a model hydrocarbon. The principle of this titration method was to convert ferrous to ferric ion and manganese (II) to manganese (III) ions proportional to the amount of oxygen dissolved in the *n*-heptane. The amount of ferric and manganese (III) ions produced were quantified by titration with standardized sodium thiosulfate. The experimental method did not successfully determine the oxygen solubility in *n*-heptane. This method could not replicate the literature results.

Keywords: *Oxygen solubility, hydrocarbons, n-heptane, ferric ion, titration.*

1. Introduction

As mentioned in Chapter I, oxygen (O_2) solubility in hydrocarbons is important for different oxidation processes such as liquid-phase autoxidation to produce organic chemicals and oxidative degradation of organic effluents by aerobic microorganisms.[2–5] Winkler titration method is a commonly used method to determine dissolved oxygen in aqueous samples.[6] But it is challenging to determine dissolved oxygen in hydrocarbons as titrants react with hydrocarbons.

McKeown et al. (1956)[1] proposed a technique (modified Winkler[6] procedure) for the determination of dissolved oxygen of hydrocarbons. This method consists of mixing a hydrocarbon with an alkaline suspension of ferrous and manganous hydroxides. The ferrous and manganous hydroxide reacts with the dissolved oxygen in the hydrocarbon to form ferric hydroxide. Then neutralization of the system with hydrochloric acid and followed by the separation of the aqueous and organic phases. Then the addition of potassium iodide (KI) to the aqueous phase, and followed by the titration with standardized sodium thiosulfate. The amount of oxygen in the hydrocarbon, proportional to the ferric ion formed can be calculated.

The objective of the present chapter was to use a modified McKeown et al. (1956)[1] titration method to experimentally determine oxygen solubility in hydrocarbons. The McKeown titration method was modified by reducing the volume of the chemicals and the size of the required apparatus. *n*-heptane was used as model hydrocarbon to evaluate if the concentration of oxygen dissolved in the hydrocarbon can be experimentally determined accurately and precisely.

2. Experimental

2.1 Materials

The reagents used in the present Chapter are listed in table 9.1.

Table 9.1. Reagents used in determination of oxygen solubility in hydrocarbons

Reagent	CASRN[a]	Structure	Purity (wt %)[b]	Concentration (N)	Supplier
Ferrous ammonium sulfate	7783-85-9	$(NH_4)_2Fe(SO_4)_2$	-	0.25	Ricca
Hydrochloric acid	7647-01-0	HCl	-	5.0	Ricca
Manganous Sulfate	15244-36-7	$MnSO_4$	>99.9	-	Sigma-Aldrich
n-Heptane	142-82-5	$CH_3(CH_2)_5CH_3$	99.8	-	Fisher
Potassium iodide crystals	7681-11-0	KI	>99	-	Fisher
Sodium hydroxide	1310-73-2	NaOH	-	2.5	Sigma-Aldrich
Sodium thiosulfate standardized	7772-98-7	$Na_2O_3S_2$	-	0.1	Alfa Aesar
Starch indicator	9005-84-9	-	-	-	Ricca

[a] CASRN: Chemical Abstracts Services Registry Number

[b] Purity of the material guaranteed by the supplier; the material was not further purified.

2.2 Procedure

The aim of this procedure was to form ferric ion (Fe^{3+}) in proportion to the amount of oxygen dissolved in n-heptane. The procedure followed was an adaptation of McKeown et al. (1956)[1]. The original set-up used by McKeown et al. (1956) (see in Figure 9.1), consisted in using an ampoule connected to an inert gas line, and a vacuum line. Also, they used a glass funnel to add the solutions to the ampoule. The present research decreased the amount of reagents used by 5 times, decreasing the size of the set-up. In addition, the original set-up was replaced by a three neck flask, connected to two lines, inert gas and vacuum, with the third mouth closed with a septum (see Figure 9.2). The reagents were added to the flask by injecting them through the septum using a glass syringe.
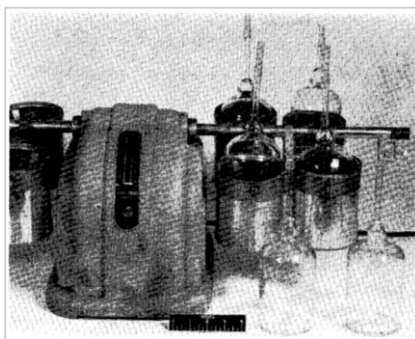

Figure 9.1. Equipment used for the determination of dissolved oxygen by McKeown et al. (1956).[1]

It consisted of mixing a manganous-ferrous solution, NaOH and *n*-heptane. After 30 min of stirring, HCl was added to neutralize the NaOH. Afterward, the aqueous and organic phases were separated. Then potassium iodide crystals were added and the solution was left to rest. After, 45 min, the solution was titrated using starch indicator and sodium thiosulfate.

2.3 Methodology

n-Heptane was bubbled with air for three hours to saturate the sample with oxygen. While bubbling, a manganous-ferrous solution was prepared, containing equals parts of 0.2 N manganous sulfate, 0.2 N ferrous ammonium sulfate, and 0.2 N hydrochloric acid. (10.0 ± 0.5) mL of the manganous-ferrous solution, and a stirrer in a 3-neck round bottom flask. After, a mouth of the flask was closed with a septum and the other two with glass valves. One valve was connected to a vacuum line and the other to an inert gas line (see figure 9.2). Then, the solution was purged by making three cycles of vacuum and inert gas.
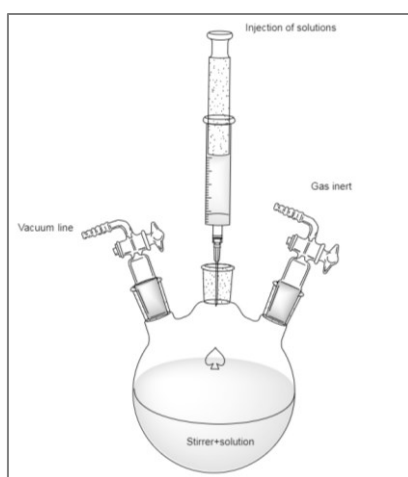

Figure 9.2. Experimental set-up adapted from McKeown et al.[1]

Using a glass syringe the following solutions were injected through the septum: (4.0 ± 0.5) mL of NaOH, and (50.0 ± 0.5) mL of *n*-heptane. After the solution was stirred for 30 min. Then, (5.0 ± 0.5) mL of HCl 5 N was added.

The aqueous and organic phases were separated. One gram of potassium iodide (KI) was added to the aqueous phase. The solution was left to rest for 45 min. Afterward, it was titrated with 0.1 N sodium thiosulfate and starch indicator.

A blank run was done for each experiment. The blank was done following the previous methodology but bubbling the *n*-heptane with nitrogen to displace the oxygen from the sample. The first and second aliquots were done with (50.0 ± 0.5) mL of *n*-heptane while the third round used (250.0 ± 0.5) mL of hydrocarbon, increasing the amount of all the reagents by 5.

All the experiments were conducted at room temperature (20 ± 1) °C.

2.4 Calculations

To calculate the oxygen solubility of hydrocarbons the following equation was used,

$$C_O = \frac{V_{thiosulfate\ (sample-blank)} \cdot N_{thiosulfate} \cdot 5603}{V_{sample}} \qquad (9.\text{I})[1]$$
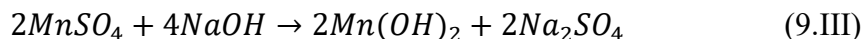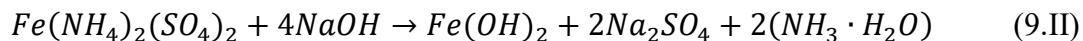
Where,

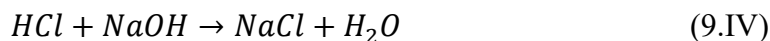C_O: concentration of oxygen in the hydrocarbon (mL/L)

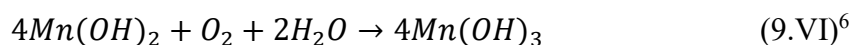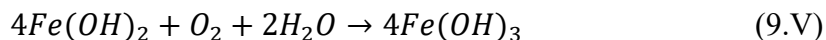V: volume (mL)

N: normality (N)

2.5 Chemical reactions

The following reactions would occur simultaneously between the manganous-ferrous solution and NaOH:
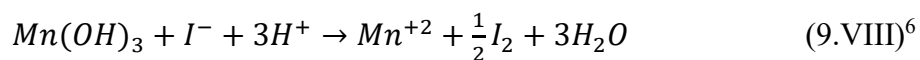
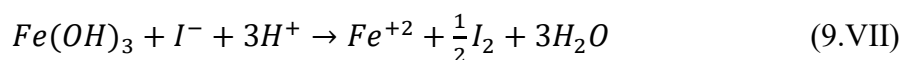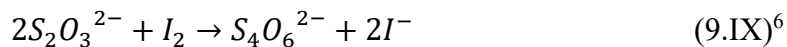$$Fe(NH_4)_2(SO_4)_2 + 4NaOH \rightarrow Fe(OH)_2 + 2Na_2SO_4 + 2(NH_3 \cdot H_2O) \qquad (9.\text{II})$$

$$2MnSO_4 + 4NaOH \rightarrow 2Mn(OH)_2 + 2Na_2SO_4 \qquad (9.\text{III})$$

$$HCl + NaOH \rightarrow NaCl + H_2O \qquad\qquad (9.\text{IV})$$

After the next reactions, between the reagents and the oxygen dissolved in the hydrocarbon, took place:

$$4Fe(OH)_2 + O_2 + 2H_2O \rightarrow 4Fe(OH)_3 \qquad\qquad (9.\text{V})$$

$$4Mn(OH)_2 + O_2 + 2H_2O \rightarrow 4Mn(OH)_3 \qquad\qquad (9.\text{VI})^6$$

When the KI was added to the aqueous phase the following reactions took place:

$$Fe(OH)_3 + I^- + 3H^+ \rightarrow Fe^{+2} + \frac{1}{2}I_2 + 3H_2O \qquad\qquad (9.\text{VII})$$

$$Mn(OH)_3 + I^- + 3H^+ \rightarrow Mn^{+2} + \frac{1}{2}I_2 + 3H_2O \qquad\qquad (9.\text{VIII})^6$$

Finally, the titration reaction was,

$$2S_2O_3{}^{2-} + I_2 \rightarrow S_4O_6{}^{2-} + 2I^- \qquad\qquad (9.\text{IX})^6$$

Every 4 moles of $S_2O_3{}^{2-}$ corresponded to 1 mole of O$_2$.

3. Results

Table 9.2 shows the volume of sodium thiosulfate (standardized) used during the titration. For aliquots 1 and 3 the volume of sodium thiosulfate used for the air saturated sample is lower than the blank (nitrogen saturated sample). While aliquot 2 showed the contrary behavior.

Table 9.2. Volume of sodium thiosulfate (standardized) added
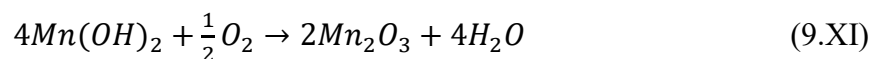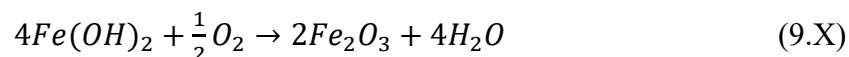to the aqueous phase during the titration process

Aliquot number	Volume of the sample $(V_s \pm 0.5)$ (mL)	Volume of sodium thiosulfate standardized $(V_t \pm 0.1)$ (mL)	
		Air saturated	Nitrogen saturated
1	50.0	0.4	0.5
2	50.0	1.3	1.0
3	250.0	14.6	18.6

4. Discussion

4.1 Discussion of the results

Contrary to what was expected, table 9.2 shows that for the first and third aliquots the volume of sodium thiosulfate used was higher when titrating the sample saturated with N_2 than the one saturated with air. These results implied that the reaction path showed in Section 2.5 of the present Chapter did not proceeded as expected.

Some undesired reactions that could be occurring are 9.X and 9.XI. If these reactions take place, $Fe(OH)_2$ and $Mn(OH)_2$ are consumed, becoming competitive reactions with reactions 9.V and 9.VI.

$$4Fe(OH)_2 + \frac{1}{2}O_2 \rightarrow 2Fe_2O_3 + 4H_2O \qquad (9.X)$$

$$4Mn(OH)_2 + \frac{1}{2}O_2 \rightarrow 2Mn_2O_3 + 4H_2O \qquad (9.XI)$$

Other possible reactions that could be taking place is the decomposition of manganous and ferrous hydroxides (see reaction 9.XII and 9.XIII).

$$2Fe(OH)_3 \rightarrow Fe_2O_3 + 3H_2O \qquad (9.XII)$$

154

$$2Mn(OH)_3 \rightarrow Mn_2O_3 + 3H_2O \qquad\qquad (9.\text{XIII})$$
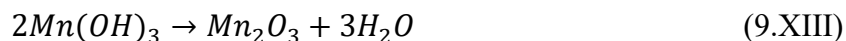
Any of these 4 reactions would decrease the amount of $Fe(OH)_3$ and $Mn(OH)_3$ available for reactions 9.VII and 9.VIII. Therefore, the amount of ferric ion (Fe^{3+}) would not be proportional to the amount of oxygen dissolved in *n*-heptane.

4.2 Effect of the volume of the sample

Table 9.2 also shows that the volume of the third sample was 5 times bigger than the others. The increase in the volume was done to verify if the quantity of the reagents affected the method, which it should not. However, as tables 9.2 and 9.3 show the results were not better regardless of the volume.

Table 9.3. Concentration of oxygen in *n*-heptane

Aliquot number	Concentration of oxygen ($C_O \pm 0.01$) (mL/L)[a]	Average concentration of oxygen ($C_O \pm 0.01$) (mL/L)[a]	Standard deviation of concentration (mL/L)	Concentration of oxygen reported in the literature[1] (mL/L)[b]
1	-1.12	1.12	3.2	
2	3.36			61.8[b]
3	-8.96	-	-	

[a]: at (20.5 ± 0.1) °C

[b]: at 24 °C

The negative concentration of oxygen in *n*-heptane shown in table 9.3 is because the blank of those samples appeared to have more oxygen than the samples bubbled with air (see table 9.2). In addition, it can be seen that not even the concentration of oxygen in *n*-heptane for the second aliquot is close to the literature[1] data.

4.3 Assumption made while adapting the methodology

A possible reason why this adaptation of the methodology of McKeown et al. [1] was not able to reproduce the results obtained by the literature[1] might be that the manganous-ferrous

solution was prepared with equal parts of 0.2 N ferrous ammonium sulfate, 0.2 N manganous sulfate, and 0.2 N hydrochloric acid, while the literature does not specify the proportion that these reagents should be mixed.

5. Conclusions

- A modified titration method of McKeown et al. (1956)[1] was applied to experimentally determine oxygen solubility in hydrocarbon (*n*-heptane).

- The oxygen concentrations in *n*-heptane was not successfully determined with the modified titration method of McKeown et al. (1956)[1]

6. References

(1) Mckeown, A. B.; Hibbard, R. R. Determination of Dissolved Oxygen in Hydrocarbons. *Anal. Chem.* **1956**, *28* (9), 1490–1492. https://doi.org/10.1021/ac60117a044.

(2) Chen, K. C.; Wu, J. Y.; Liou, D. J.; Hwang, S. C. J. Decolorization of the Textile Dyes by Newly Isolated Bacterial Strains. *J. Biotechnol.* **2003**, *101* (1), 57–68. https://doi.org/10.1016/S0168-1656(02)00303-6.

(3) Nigam, P.; Banat, I. M.; Singh, D.; Marchant, R. Microbial Process for the Decolorization of Textile Effluent Containing Azo, Diazo and Reactive Dyes. *Process Biochem.* **1996**, *31* (5), 435–442. https://doi.org/10.1016/0032-9592(95)00085-2.

(4) Siddiquee, M. N.; De Klerk, A.; Nazemifard, N. Application of Microfluidics to Control Product Selectivity during Non-Catalytic Oxidation of Naphthenic-Aromatic Hydrocarbons. *React. Chem. Eng.* **2016**, *1* (4), 418–435. https://doi.org/10.1039/c6re00010j.

(5) Siddiquee, M. N.; De Klerk, A. In Situ Measurement of Liquid Phase Oxygen during Oxidation. *Ind. Eng. Chem. Res.* **2016**, *55* (23), 6607–6618. https://doi.org/10.1021/acs.iecr.6b00949.

(6) Jeffery, G. H.; Bassett, J.; Mendham, J.; Denney, R. C. *Vogel's. Textbook of Quantitative Chemical Analysis*, 5th ed.; Longman Scientific & Technical: New York, 1989.

CHAPTER X - FUNDAMENTAL STUDY OF OXYGEN SOLUBILITY IN HYDROCARBONS – EQUILIBRIUM LIQUID-VAPOUR (2nd METHOD)

In this chapter, a second method to determine oxygen solubility in hydrocarbons was developed and it is used to calculate the Henry's constant is studied. The methodology, calculations, results, and analysis of the experimental data are presented.

Abstract

Most of the methods available in the literature to determine oxygen solubility and Henry's constant are for aqueous systems. The aim of the present study is to develop and test a methodology to measure oxygen solubility and calculate Henry's constant that is suitable for hydrocarbons, using *n*-dodecane as a model compound. The method being evaluated consisted of monitoring the change in oxygen pressure in the gas-liquid system and using it to calculate the desired values. The experimentally determined dissolved oxygen concentration in *n*-dodecane at (20.5 ± 0.1) °C and (19.59 ± 0.01) psi$_a$ $((135.07 \pm 0.07)$ kPa absolute) was (13 ± 2) (mol/m^3), and corresponding Henry's constant was (0.09 ± 0.01) (mol/m^3·kPa). The relatively low standard deviation and good agreement of the results with the literature validated the experimental method.

Keywords: *Oxygen solubility, hydrocarbons, n-dodecane, Henry's constant.*

1. Introduction

As mentioned in Chapter I, oxygen (O_2) solubility in hydrocarbons is important for different oxidation processes such as liquid-phase oxidation to produce petrochemicals and oxidative degradation of organic effluents by aerobic microorganisms.[1–4] Most of the methods used to calculate the solubility of O_2 in a liquid require Henry's constant of that specific system.[5] Methods to experimentally determine both, oxygen solubility and Henry's constant, involved an aqueous liquid phase.

Finding an experimental approach that allows the determination of oxygen solubility in hydrocarbons and its Henry's constant was the main objective of this chapter. The approach used consisted in measured the concentration of oxygen dissolved in hydrocarbons once the system had reached the liquid-vapor equilibrium and then calculate the Henry's constant.

The hydrocarbon used to developed and verify the method was *n*-dodecane. The *n*-dodecane was put in contact with the oxygen and the pressure of the system was monitored. The change in the pressure was later on analyzed to finally calculate the concentration of O_2 dissolved in the *n*-dodecane, and its corresponding Henry's constant

2. Experimental

2.1 Materials

Table 10.1 presents the specifications of the reagents used in the present study. Reagents were used without further purification.

Table 10.1. Reagents used in the present chapter.

| Reagent | CASRN[a] | Structure | Purity | | | Supplier |
| | | | Supplier[b] | FID[c] | | |
			(wt %)	(vol %)	(wt %)	
n-Dodecane	287-92-8	$CH_3(CH_2)_{10}CH_3$	99	-	99.9	Sigma-Aldrich
Oxygen	7782-44-7	O_2	-	99.993	-	PRAXAIR

[a] CASRN: Chemical Abstracts Services Registry Number

[b] Purity of the material guaranteed by the supplier; the material was not further purified.

[c] Purity calculated based on peak area obtained by GC-FID analysis

Table 10.1 shows the high purity of the oxygen used, this ensured that the experiments were conducted in an oxygen atmosphere.

2.2 Equipment

The equipment used is listed in table 10.2.

Table 10.2. Instruments used in the oxygen solubility determination

Equipment	Description
Oxygen and carbon dioxide gas analyzer	Brand: Alpha Omega Instruments
	Model: Series 9600
Vacuum pump	Brand: Heidolph Instuments
	Model: ROTAVAC vario Pumping unit
Pressure Transducer (PT)	Brand: Swagelok
	Model: PTI-S-NG10-12AO
	Readability: ($\pm$ 0.001) psi
	($\pm$ 0.006) kPa

The vacuum pump was used to remove the air from the system, and the oxygen analyzer to monitor the level of oxygen in the experiment atmosphere by measuring the oxygen percentage of the exit gas stream. The pressure transducer was used to monitor the experimental pressure.

2.3 Procedure

The experimental procedure consisted of putting the hydrocarbon (*n*-dodecane) in contact with the oxygen (O_2) inside the reactor at approximately and pressurize it with O_2. The O_2 would dissolve in the *n*-dodecane causing the pressure in the reactor to drop. The change in pressure can be used to quantify the moles of O_2 that dissolved in the hydrocarbon, allowing the calculation of O_2 solubility and Henry's constant. Figure 10.1 shows an image of the set-up used.

Figure 10.1. Experimental set-up.

It was considered that the hydrocarbon was saturated with O_2 when the system reached liquid-vapor equilibrium. It was assumed that when the reactor pressure variated less or equal than 0.075 psi$_g$ (0.5 kPa) in 30 min the system had reached equilibrium.

To accurately measure the reactor pressure, PT-101 and PI-103 were used (see figure 10.2). The reactor was pressurized at approximately 8 psi$_g$ (55 kPa gauge) because the PT could only work at pressures equal or lower to (10.000 ± 0.001) psi$_g$ $((68.948 \pm 0.007)$ kPa gauge). It is important to mention that the valves used to regulate the entrance of the oxygen to the reactor are hand valves, therefore pressurizing at exactly (8.000 ± 0.001) psi$_g$ $((55.158 \pm 0.007)$ kPa gauge) was not possible, but the exact pressure was recorded.
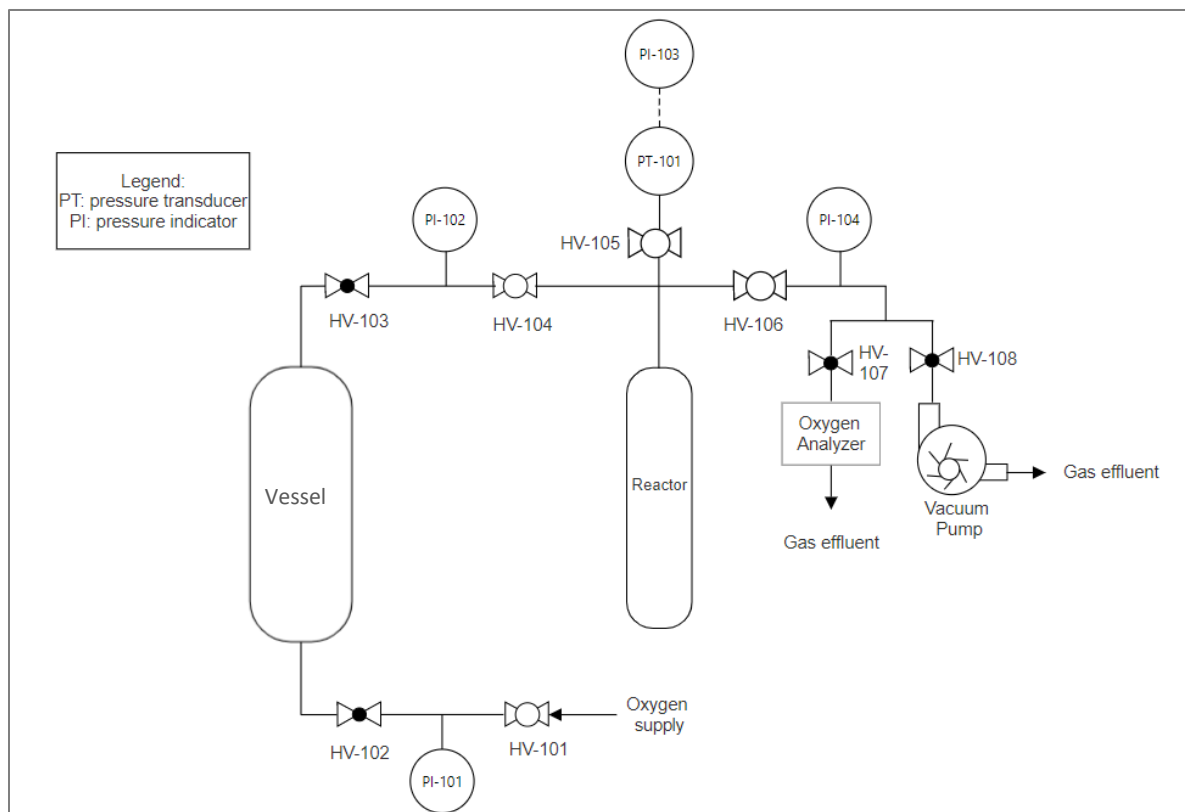
Figure 10.2. P&ID of the experimental set-up used to indirectly measure oxygen solubility.

2.4 Methodology

To understand the present methodology refer to figure 10.2, where the P&ID of the experimental set-up is shown. All the experiments were conducted at room conditions, these conditions were recorded for each experiment.

The reactor was removed from the set-up and purged with the model compound three times and dried with air. The reactor used for our work was a flow reactor with one side plugged, but in principle, any vessel capable of containing the pressure without leaking can be used.

After, the reactor was filled with (50.00± 0.05) mL of *n*-dodecane using a glass syringe. Once filled, the reactor was reconnected to the set-up, and the atmosphere of the system was purged. To accomplish this all the valves were opened with the exception of HV-101 and HV-107. Then, the vacuum pump was turned on for approximately 13 min, during which the system

was at approximately (-7.0± 0.5) psi$_g$ ((-48.3 ± 3.5) kPa gauge), this was done to remove the air from the system. Afterward, HV-108 was closed, and then the pump was switched off. Continuing with the purge process, oxygen was supplied to the system by opening HV-101; HV-107 was also opened to allow the gases to exit the system. The flow of oxygen continued at approximately 4 L/min until the oxygen analyzer indicated that the oxygen percentage was 100 %, or after 5 h, and then the oxygen percentage was registered.

To end the purge process, HV-104, HV-105, HV-106, and HV-107 were closed. Then the pressure pump was pressurized at approximately 10 psi$_g$ (69 kPa gauge) when the desired pressure was reached HV-101 was closed. After the pressure of the reactor was recorded. Subsequently, the reactor was pressurized. For this, HV-105 and HV-104 were opened, and the reactor was pressurized to approximately 8 psi$_g$ (55 kPa gauge), then HV-104 was closed and after registering the pressure in the reactor, HV-105 was also closed.

Afterward, the pressure in the reactor was recorded every 30 min by opening HV-105 and closing it after the measurement. The experiment was considered over when the pressure in the reactor changed (0.075 ± 0.001) psi$_g$ ((0.517 ± 0.007) kPa) or less in 30 min.

This methodology was repeated twice, using two more aliquots of *n*-dodecane.

2.4.1 Leak check

To check for leaks, the whole system, with the reactor empty and dry, was pressurized at (8.065 ± 0.001) psi$_g$ ((55.606 ± 0.007) kPa), keeping HV-101, HV-105, HV-106, HV-107, and HV-108 and left for 48 h. After the time was past HV-105 was opened and the final pressured was (7.855 ± 0.001) psi$_g$ ((54.158 ± 0.007) kPa).

The system lost a total of (0.210± 0.001) psi$_g$ ((1.448± 0.007) kPa) in 48 h, showing that the leak is negligible since the experiments took a maximum of 4 h.

HV-105 was kept closed during the experiment due to a leak found in the connection between the tubing and PT-101, even though the leak was fixed, due to time constraints it was not possible to repeat the leak test, therefore it was preferred to keep HV-105 closed.

2.5 Calculations

To calculate the oxygen solubility of hydrocarbons and Henry's constant of the same system, the following equations were used;

2.5.1 Oxygen solubility equations

To calculate the oxygen solubility, the absolute pressure of the system is required. To calculate this pressure the following equation was used:

$$P_{abs} = P_g \cdot \frac{O\%}{100} + (P_{atm})$$ (10.I)[6]

Where,

$P_{O,abs}$: oxygen absolute pressure (psi_a)

$P_{O,g}$: oxygen relative pressure (psi_g)

P_{atm}: atmospheric (psi)

O%: percentage of oxygen

Knowing the absolute pressure of the system, the moles of oxygen in the gas phase was calculated using equation 10.II,

$$n_{O2,gas} = \frac{P_{o,abs} \cdot V}{R \cdot T}$$ (10.II)[6]

Where,

V: volume (L)

n_{O2}: moles of oxygen (mol)

R ideal gas constant (1.206 L·psi/mol·K)

T: temperature (K)

After the final moles of oxygen in the liquid phase were calculated as the moles of oxygen loss from the gas phase plus the initial moles of oxygen in the liquid (the ratio of $\frac{P_{i,react}}{P_{f,system}}$ was used to account for these moles) using the following equation,

$$n_{f,O2,liq} = \left(1 - \frac{P_{O,i,react}}{P_{O,f,system}}\right) \cdot \left(n_{i,O2,gas} - n_{f,O2,gas}\right)$$ (10.III)[6]

Where,

f: final

i: initial

react: reactor

Knowing the final moles of oxygen in the liquid, the initial moles were calculated with equation 10.IV.

$$n_{i,O2,liq} = \frac{n_{f,O2,liq} \cdot P_{O,i,react}}{P_{O,f,system}}$$ (10.IV)[6]

Then, the total moles of oxygen in the liquid:

$$n_{T,O2,liq} = n_{i,O2,liq} + n_{f,O2,liq}$$ (10.V)

Where,

T: total

Finally, the solubility of oxygen in hydrocarbons was calculated with the following equation,

$$C_{O,liq} = \frac{n_{T,O2,liq}}{0.001 \cdot V_{liq}}$$ (10.VI)

Where,

C: concentration (mol/m^3)

2.5.2 Henry's constant

Henry's constant for oxygen dissolved in hydrocarbons was determined by using equation 10.VII.

$$H = C_{O,liq} / \left(6.89476 \cdot P_{O,f,system}\right)$$ (10.VII)[6]

Where,

H: Henry's constant (mol/m^3·kPa)

3. Results

In this section, the collected data is reported. Table 10.3 shows the room conditions at the time of the experiments. Room temperature and pressure are important values since the experiment was conducted at room temperature, and it is pressure-dependent due to the oxygen.

Table 10.3. Room conditions

	Aliquot number		
	1	**2**	**3**
Temperature (T ± 0.1) (°C)	20.9	20.2	20.5
Pressure (P_{abs} ± 2) (mbar)	931	923	926
Humidity (H ± 2) (%)	21	18	19

The pressure reported in table 10.3 was used to calculate the absolute pressure inside the reactor with equation 10.I. And the temperature was used to calculate the moles of oxygen in the gas using equation 10.II.

Table 10.4 shows the measured pressured at different intervals of times for each aliquot. It is important to notice that all the pressures were recorded with HV-101, HV-104, HV-106, HV-107, and HV-108 closed. In addition, HV-105 was opened immediately before taking the measurements and closed immediately after.

Table 10.4. Experimental data collected for each of the aliquots

Aliquot number	Oxygen (%O±0.1) (%)	Time (min)	PI-101[a] (P_1± 0.5) (psig) ((P_1±3) (kPag))	PI-102 (P_2± 0.5) (psig) ((P_2±3) (kPag))	PI-103 (P_3± 0.001) (psig) ((P_3±0.007) (kPag))	Mol of O_2 in gas phase in the reactor (M±0.0005) mol
1	100.0	0	8.2 (57)	9.2 (63)	0.264 (1.820)	0.0283
		1	6.5 (45)	7.5 (52)	6.535 (45.057)	0.0412
		30	6.5 (45)	7.5 (52)	6.444 (44.430)	0.0410
		60	6.4 (44)	7.4 (51)	6.316 (43.547)	0.0408
		90	6.4 (44)	7.4 (51)	6.145 (42.368)	0.0404
		180	6.4 (44)	7.4 (51)	6.120 (42.196)	0.0404
		210	6.4 (44)	7.4 (51)	6.092 (42.003)	0.0403

[a]: PI-101 had an error of + 1 psi.

Table 10.4. Experimental data collected for each of the aliquots. Continuation

Aliquot number	Oxygen (%O±0.1) (%)	Time (min)	PI-101[a] (P₁± 0.5) (psig) ((P₁±3) (kPag))	PI-102 (P₂± 0.5) (psig) ((P₂±3) (kPag))	PI-103 (P₃± 0.001) (psig) ((P₃±0.007) (kPag))	Mol of O₂ in gas phase in the reactor (M±0.0005) mol
		0	10.6 (73)	9.6 (66)	0.063 (0.434)	0.0277
		1	8.5 (59)	7.5 (52)	7.644 (52.704)	0.0430
		30	8.6 (59)	7.6 (52)	7.545 (52.021)	0.0428
2	97.4	60	8.6 (59)	7.6 (52)	7.402 (52.035)	0.0425
		90	8.6 (59)	7.6 (52)	7.201 (49.649)	0.0421
		180	8.6 (59)	7.6 (52)	7.157 (49.346)	0.0420
		210	8.6 (59)	7.6 (52)	7.122 (49.104)	0.0419
		0	11.2 (77)	10.2 (70)	0.100 (0.689)	0.0278
		1	8.9 (61)	7.9 (54)	8.001 (55.165)	0.0432
		30	8.9 (61)	7.9 (54)	7.911 (54.544)	0.0432
		60	8.9 (61)	7.9 (54)	7.746 (53.407)	0.0430
3	94.3	90	8.9 (61)	7.9 (54)	7.619 (52.531)	0.0427
		180	8.9 (61)	7.9 (54)	7.565 (52.159)	0.0424
		210	8.9 (61)	7.9 (54)	7.403 (51.042)	0.0420
		240	8.9 (61)	7.9 (54)	7.376 (50.856)	0.0420

[a]: PI-101 had an error of + 1 psi.

Table 10.4 shows that the pressure changed only in the reactor section (measured by PI-103), where oxygen was expected to dissolve in the n-dodecane. PI-101 and PI-102 showed the pressure on the vessel, these pressures were not used in any calculation. This table also shows the moles of oxygen in the gas phase in the reactor.

4. Discussion

4.1 Assumptions

As table 10.4 shows, when the pressure in the reactor varies less or equal to (0.075 ± 0.001) psi$_g$ $((0.517 \pm 0.007)$ kPa) in 30 min, the experiment was stopped. In the last 30 min of the experiments, the delta moles of O_2 in the phase inside the reactor was equal to (0.0001 ± 0.0005) mol. This can be interpreted as the system reached equilibrium liquid-vapor, proving that the experiment reaches equilibrium when the delta pressure is (0.075 ± 0.001) psi$_g$ $((0.517 \pm 0.007)$ kPa) or less in 30 min.

It was also assumed that the temperature of the hydrocarbon was equal to the room temperature. It was not possible to verify if this assumption was corrected with the current methodology. However, adding a thermocouple in the reactor to measure the liquid temperature can be done in the future. It was not possible to do this modification in the present research due to time constraints.

4.2 Precision

The precision of an experimental value can be estimated by calculating the uncertainty of the value. The uncertainty can be calculated trough error propagation, which considers the error of the instruments used for the direct measurement.[7,8] Accounting only for systematics errors, and under the assumption that all of those errors were presented during the experiment at their maximum value, in other words, it gives the maximum uncertainty that could be generated due to systematic errors.[7,8] The present research calculated error propagation using partial derivate (see equation 10.VIII). The resulting error is shown in the column headings.

$$\Delta f = \frac{\delta f}{\delta x} \Delta x + \frac{\delta f}{\delta y} \Delta y + \cdots + \frac{\delta f}{\delta z} \Delta z \qquad \text{(10.VIII)}$$

Where,
f: dependant variable
x, y, z: independent variables
Δ: error associate to a variable

168

The uncertainty can also be calculated with the standard deviation. Standard deviation, contrary to the error propagation, accounts for the variability of the value being measured or calculated.[7,8] Therefore it considers systematic and random errors that could have occurred during the experimental phase.[7,8] The standard deviation of the final results have been calculated in a column next to their corresponding value.

$$s = \sqrt{\frac{\sum_{i=1}^{N}(x_i - \bar{x})^2}{N-1}}$$ (10.IX)[9]

Where,

s: sample standard deviation

N: number of observations

x_i: value of i

$\bar{x}$: mean

Another difference between calculating the uncertainty through error propagation or standard deviation is that error propagation can be used even before starting the experiments, once the instruments have been selected.[8] In contrast, the standard deviation requires at least two data points to be calculated.[8]

The concentration of oxygen in *n*-dodecane was calculated using equations from 10.I to 10.VI, and Henry's constant was calculated using equation 10.VII. The results with their respective uncertainties are shown in table 10.5.

Table 10.5. Experimentally determined solubility and Henry's constant of

O_2 dissolved in *n*-dodecane

Aliquot number	Concentration $(C \pm 15)$ (mol/m^3)	Average Concentration $(C \pm 15)$ (mol/m^3)	Standard deviation of the concentration (mol/m^3)	Henry's constant. $(H \pm 0.1)$ $(mol/m^3 \cdot kPa)$	Average Henry's constant $(H \pm 0.1)$ $(mol/m^3 \cdot kPa)$	Standard deviation of the average Henry's constant $(mol/m^3 \cdot kPa)$
1	10			0.0740		
2	14	13	2	0.0999	0.09	0.01
3	14			0.0997		

Table 10.5 shows that the average concentration can be expressed as (13 ± 15) (mol/m^3), which uncertainty, calculated through error propagation, is bigger than the value, implying that the result is not precise due to the relatively high uncertainty. However, table 10.5 also shows that the concentration could be expressed as (13 ± 2) (mol/m^3), where the uncertainty was calculated with the standard deviation.

The same analysis applies for the Henry's constant, which can be expressed as (0.1 ± 0.1) (mol/m^3·kPa), error propagation, or (0.09 ± 0.01) (mol/m^3·kPa), with standard deviation. Being the uncertainty calculated with the standard deviation the preferred one.

Because it is possible, in this study the uncertainty has been calculated and reported by the two methods, error propagation, and standard deviation. However, since standard deviation accounts for the variability of the value, it is considered more significant than the error propagation method.[8]

4.3 Accuracy

Once the precision of the data was studied, the accuracy of the data must be analyzed. To accomplish this, the results must be compared to literature[10] data. Table 10.6 shows oxygen concentration and Henry's constant calculated from the mol fraction of oxygen dissolved in n-dodecane reported in the literature[10]. It is important to mention that the mol fraction shown in table 10.6 comes from theoretical calculations and not from empirical data. In addition, the mol fraction was extrapolated from a two points linear equation (See figure 10.3).

Table 10.6. Solubility and Henry's constant of O$_2$ dissolved in n-dodecane at 20 °C calculated with literature[10] data

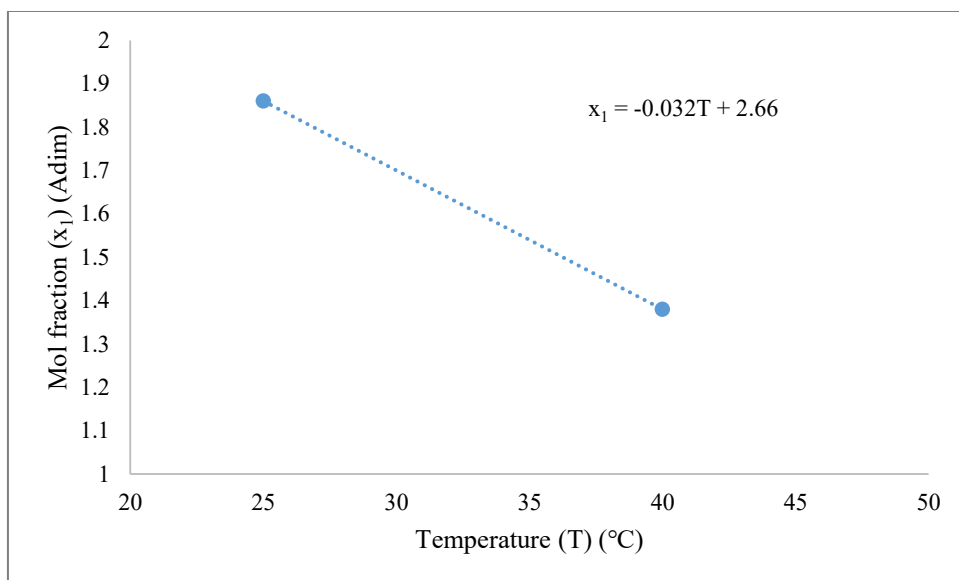| Mol fraction[10] (Adim)	Concentration (mol/m^3)	Henry's constant (mol/m^3·kPa)
0.002	8.8	0.087

Figure 10.3. Mol fraction of oxygen in *n*-dodecane vs. temperature.[10]

The difference between the concentration calculated from the experimental data, (13 ± 2) (mol/m^3), and the calculated from literature[10] is $\Delta C = 4.2 \ mol/m^3$. While the difference between Henry's constant calculated from the experimental data $(0.09 \pm 0.01) \ (mol/m^3 \cdot kPa)$ and the literature[10] is $\Delta H = 0.003 \ mol/m^3 \cdot kPa$. Both of the deltas were close to the uncertainty of the experimental data, showing good agreement with the literature[10].

Since the experimental calculated data prove to be precise and accurate, it validates the experimental method used.

5. Conclusions

A new method to experimentally measure the dissolved oxygen in liquid hydrocarbon (*n*-dodecane) was developed. The key findings are:

▪ The standard deviation showed that the experimentally calculated oxygen solubility in *n*-dodecane and Henry's constant are precise.

▪ The experimentally calculated oxygen solubility in *n*-dodecane and Henry's constant are in good agreement with the literature[10].

171

▪ The experimental method proved to be precise and accurate to determine oxygen solubility in *n*-dodecane and Henry's constant.

6. References

(1) Chen, K. C.; Wu, J. Y.; Liou, D. J.; Hwang, S. C. J. Decolorization of the Textile Dyes by Newly Isolated Bacterial Strains. *J. Biotechnol.* **2003**, *101* (1), 57–68. https://doi.org/10.1016/S0168-1656(02)00303-6.

(2) Nigam, P.; Banat, I. M.; Singh, D.; Marchant, R. Microbial Process for the Decolorization of Textile Effluent Containing Azo, Diazo and Reactive Dyes. *Process Biochem.* **1996**, *31* (5), 435–442. https://doi.org/10.1016/0032-9592(95)00085-2.

(3) Siddiquee, M. N.; De Klerk, A.; Nazemifard, N. Application of Microfluidics to Control Product Selectivity during Non-Catalytic Oxidation of Naphthenic-Aromatic Hydrocarbons. *React. Chem. Eng.* **2016**, *1* (4), 418–435. https://doi.org/10.1039/c6re00010j.

(4) Siddiquee, M. N.; De Klerk, A. In Situ Measurement of Liquid Phase Oxygen during Oxidation. *Ind. Eng. Chem. Res.* **2016**, *55* (23), 6607–6618. https://doi.org/10.1021/acs.iecr.6b00949.

(5) Ramesh, H.; Mayr, T.; Hobisch, M.; Borisov, S.; Klimant, I.; Woodley, J. M. Measurement of Oxygen Transfer from Air into Organic Solvents. *J Chem Technol Biotechnol* **2016**, *91*, 832–836. https://doi.org/10.1002/jctb.4862.

(6) Cengel, Y. A.; Boles, M. A. *Termodinámica*, 7th ed.; Mc Graw Hill: Mexico D.F, 2012.

(7) Currell, G. *Scientific Data Analysis*; Oxford University Press: Oxford, 2015.

(8) Francis, P. *Standard Uncertainty, Standard Error and Standard Deviation*; Australia, 2018.

(9) Triola, M. F. *Elementary Statistics, Technology Update*, 11th Ed.; Pearson, Ed.; 2012.

(10) Battino, R. Solubility Data Series: Oxygen an Ozone. *Pergamon Press* **1981**, *7*, 233.

CHAPTER XI – CONCLUSION TO A FUNDAMENTAL STUDY OF MOLAR REFRACTIVITY AND OXYGEN SOLUBILITY

This chapter concludes the research topics. The major conclusions
and proposed future research are presented.

1. Introduction

Sometimes, to go forward we need to look at the beginning. This statement describes the work done in the present research, where some unsolved fundamental issues about refractive index and oxygen solubility in hydrocarbons were revisited and evaluated.

The molar refractivity study evaluated different equations that correlate molar refractivity, refractive index, molar mass, and density. These correlations are available in the literature,[1] however, it is not clear which equation better express the empirical data. To find the best correlation high precision and accurate refractive index and density data were collected for different model compounds. The data were used to test the correlations and to recommend the most appropriate correlation for relating refractive index, molar mass, and density to the molar refractivity, something that was not available in the literature.

On the other hand, the oxygen solubility study developed and tested a method to measure the concentration of oxygen dissolved in hydrocarbons. The dissolved oxygen concentration was used to calculate the Henry's constant. Two experimental methods were evaluated. The first was a modification of the titration method by McKeown et al. (1956),[2] and the second method was based on measuring the pressure change resulting from oxygen dissolved in the hydrocarbon.

The main conclusions of this study are presented in the following section. For ease of reference, the conclusions were separated based on topic.

2. Conclusions

2.1 Refractive index and molar refractivity

- The method to collect refractive index and density was validated by comparing the collected data to literature[3–5] data. The collected data proved to be accurate and precise. The study contributed new measurements of the temperature dependent refractive index and density of a range of pure compounds.

- The average first derivative (slope) of the refractive index with respect to density of alkanes (0.598 ± 0.003), alkenes, (0.604 ± 0.002), and alkynes (0.587 ± 0.005) were roughly the same as the 'rule of thumb' value reported in literature[1] (0.6) for hydrocarbons. For other compound classes, there were larger differences.

- The molar refractivity calculated with the correlation by Eykman was the least temperature-dependent relationship between the molar refractivity and refractive index, molar mass, and density. Only two exceptions were noted, namely, propionic acid and butyric acid. For these acids, the correlation by Gladstone & Dale was slightly better than the Eykman correlation.

- The orientation polarization $(8.5 \times 10^{-23}$ $cm^3/mol)$ of propionic acid was negligible when compared to its molar refractivity $(38.5509 \pm 0.0007$ $cm^3/mol)$. The origin of the somewhat poorer performance of the Eykman correlation for propionic acid and butyric acid was left unresolved.

- The molar refractivity estimated with atomic refraction (AR) and group contribution (GC) were comparable. Both methods resulted in reasonable predictions of the molar refractivity based on structure.

2.2 Oxygen solubility in hydrocarbons

2.2.1 First method

- A modification of the titration method by McKeown et al. (1956)[2] was applied to experimentally determine the dissolved oxygen in n-heptane. However, the oxygen concentration was not successfully determined. This approach was abandoned.

2.2.2 Second method

- An experimental method to determine the dissolved oxygen in hydrocarbons based on the change in pressure resulting from oxygen dissolution was developed. The calculated oxygen solubility in n-dodecane and Henry's constant obtained by this method were in good agreement with the literature. It indicated that the experimental method was accurate. In addition, the low standard deviation of the experimentally calculated oxygen solubility in n-dodecane and Henry's constant, indicated that the method had good repeatability.

3. Future work recommendations

3.1 Refractive index and molar refractivity

The study employed only pure components as model compounds. Working with mixtures will deepen the knowledge of the topic. Binary mixtures would be the next step to enable the correlation of refractive index to the chemical composition in the future, as well as derivation of appropriate mixing rules for refractive index.

In addition, it could be verified if the difference between the first derivative of refractive index with respect to density of carboxylic acids and hydrocarbons could be used to detect online changes on bitumen acid content.

3.2 Oxygen solubility in hydrocarbons

The main limitation in this section of the study is that it was done at room temperature even though oxygen solubility and Henry's constant are temperature-dependent. In further work, a thermocouple and temperature control could be added to the system to enable the measurement of the oxygen solubility at different temperatures.

Secondly, only one model compound was used, further experiments could be conducted using different hydrocarbons.

4. References

(1)   Kurtz, S. S. Physical Properties and Hydrocarbon Structure. In *The chemistry of petroleum hydrocarbons. Vol 1*; Reinhold Publishing Corporation: New York, 1954; pp 275–331.

(2)   Mckeown, A. B.; Hibbard, R. R. Determination of Dissolved Oxygen in Hydrocarbons. *Anal. Chem.* **1956**, *28* (9), 1490–1492. https://doi.org/10.1021/ac60117a044.

(3)   RELXGroup. Reaxys database https://www.reaxys.com/#/login (accessed Sep 20, 2019).

(4)   Devi, R.; Gahlyan, S.; Rani, M.; Maken, S. Thermodynamic and Acoustic Properties of Binary Mixtures of Diisopropyl Ether, Benzene and Alkanes at 298.15, 308.15 and 318.15 K: Prigogine-Flory-Patterson Theory and Graph Theory. *J. Mol. Liq.* **2019**, *275*, 364–377. https://doi.org/10.1016/j.molliq.2018.11.045.

(5)   Kashyap, P.; Rani, M.; Gahlyan, S.; Tiwari, D. P.; Maken, S. Volumetric, Acoustic and Optical Properties of Binary Mixtures of 2-Propanol with n-Alkanes (C6-C10) from 293.15 K to 303.15 K. *J. Mol. Liq.* **2018**, *268*, 303–314. https://doi.org/10.1016/j.molliq.2018.07.043.

BIBLIOGRAPHY

This is a consolidated bibliography listing all of the cited references in the thesis.

- Alberty, R. A.; Daniels, F. *Physical Chemistry*, 3ed ed.; Wiley: New York, 1966.
- Angle, C. W.; Long, Y.; Hamza, H.; Lue, L. Precipitation of Asphaltenes from Solvent-Diluted Heavy Oil and Thermodynamic Properties of Solvent-Diluted Heavy Oil Solutions. *Fuel* **2006**, *85* (4), 492–506. https://doi.org/10.1016/j.fuel.2005.08.009.
- AntonPaar. *Service Manual Abbemat 3200 Abbemat 3100 Abbemat 3000*; 2017.
- AntonPaar. *Service Manual: DMA^{TM} 4100/4500/5000 M SCU, DSA^{TM} 5000 / SDA^{TM} M SCU*; 2018.
- Arnon, S. *Visible Light Communication*; Cambridge University Press, 2015. https://doi.org/10.1017/CBO9781107447981.001.
- Atkins, P. W. *Physical Chemistry*, 3rd ed.; Oxford University Press: Oxford, 1986.
- Battino, R. Solubility Data Series: Oxygen an Ozone. *Pergamon Press* **1981**, *7*, 233.
- Bayat, M.; Sattarin, M.; Teymouri, M. Prediction of Asphaltene Self-Precipitation in Dead Crude Oil. *Energy and Fuels* **2008**, *22* (1), 583–586. https://doi.org/10.1021/ef700536z.
- Buckley, J. S.; Hirasaki, G. J.; Liu, Y.; Von Drasek, S.; Wang, J. X.; Gill, B. S. Asphaltene Precipitation and Solvent Properties of Crude Oils. *Pet. Sci. Technol.* **1998**, *16* (3–4), 251–285. https://doi.org/10.1080/10916469808949783.
- Bueche, F. J.; Hecht, E. *General Physics*, 10th ed.; Mc Graw Hill, 1997.
- Carroll, J. J. Henry's Law Revisited. *Chem. Eng. Prog.* **1999**, *1*, 49–56.
- Carroll, J. J. What Is Henry's Law? *Chem. Eng. Prog.* **1991**, *9*, 48–52.
- Castillo, J.; Gutierrez, H.; Ranaudo, M.; Villarroel, O. Measurement of the Refractive Index of Crude Oil and Asphaltene Solutions: Onset Flocculation Determination. *Energy and Fuels* **2010**, *24* (1), 492–495. https://doi.org/10.1021/ef900861d.
- Cengel, Y. A.; Boles, M. A. *Termodinámica*, 7th ed.; Mc Graw Hill: Mexico D.F, 2012.
- Chen, K. C.; Wu, J. Y.; Liou, D. J.; Hwang, S. C. J. Decolorization of the Textile Dyes by Newly Isolated Bacterial Strains. *J. Biotechnol.* **2003**, *101* (1), 57–68. https://doi.org/10.1016/S0168-1656(02)00303-6.

- Collins English Dictionary. Definition of "fundamental research" https://www.collinsdictionary.com/dictionary/english/fundamental-research (accessed Nov 12, 2019).

- Costa Gomes, M. F.; Grolier, J.-P. Determination of Henry's Law Constants for Aqueous Solutions of Tetradeuteriomethane between 285 and 325 K and Calculation of the H/D Isotope Effect. *Phys. Chem. Chem. Phys.* **2001**, *3*, 1047–1052. https://doi.org/10.1039/b008755f.

- Currell, G. *Scientific Data Analysis*; Oxford University Press: Oxford, 2015.

- Devi, R.; Gahlyan, S.; Rani, M.; Maken, S. Thermodynamic and Acoustic Properties of Binary Mixtures of Diisopropyl Ether, Benzene and Alkanes at 298.15, 308.15 and 318.15 K: Prigogine-Flory-Patterson Theory and Graph Theory. *J. Mol. Liq.* **2019**, *275*, 364–377. https://doi.org/10.1016/j.molliq.2018.11.045.

- Dias, A. M. A.; Bonifácio, R. P.; Marrucho, I. M.; Pádua, A. A. H.; Costa Gomes, M. F. Solubility of Oxygen in N-Hexane and in n-Perfluorohexane. Experimental Determination and Prediction by Molecular Simulation. *Phys. Chem. Chem. Phys.* **2003**, *5* (3), 543–549. https://doi.org/10.1039/b207512c.

- Eghbali, M. H.; Nazar, A. R. S.; Tavakoli, T. A Simple Method for Oil Content Determination of Petroleum Waxes by Refractive Index Measurement. *Pet. Sci. Technol.* **2014**, *32* (7), 856–861. https://doi.org/10.1080/10916466.2011.601504.

- European Commission. Community Framework for State Aid for Research and Development and Innovation. *Off. J. Eur. Union* **2007**, *92* (5), 1286–1298.

- Fischer, K.; Noll, O.; Gmehling, J. Experimental Determination of the Oxygen Solubility in Benzene. *J. Chem. Eng. Data* **2001**, *46* (6), 1504–1505. https://doi.org/10.1021/je010163i.

- Francis, P. *Standard Uncertainty, Standard Error and Standard Deviation*; Australia, 2018.

- Gladstone, J. H.; Dale, T. P. Researches on the Refraction, Dispersion and Sensitiveness of Liquids. *Philos. Trans. R. Soc. A* **1863**, *153*, 317–343.

- Glasstone, S.; Lewis, D. *Elements of Physical Chemistry*, 2nd ed.; Macmillan: London, 1960.

- Goossens, A. G. Prediction of the Hydrogen Content of Petroleum Fractions. *Ind. Eng. Chem. Res.* **1997**, *36* (6), 2500–2504. https://doi.org/10.1021/ie960772x.

- Gouw, T. H.; Vlugter, J. C. Physical Properties of Fatty Acid Methyl Esters. III Dispersion. *J. Am. Oil Chem. Soc.* **1964**, *41* (7), 514–515. https://doi.org/10.1007/BF02670037.

• Hiatt, M. H. Determination of Henry's Law Constants Using Internal Standards with Benchmark Values. *J. Chem. Eng. Data* **2013**, *58* (4), 902–908. https://doi.org/10.1021/je3010535.

• Hosseinifar, P.; Jamshidi, S. Development of a New Generalized Correlation to Characterize Physical Properties of Pure Components and Petroleum Fractions. *Fluid Phase Equilib.* **2014**, *363*, 189–198. https://doi.org/10.1016/j.fluid.2013.11.043.

• Jeffery, G. H.; Bassett, J.; Mendham, J.; Denney, R. C. *Vogel's. Textbook of Quantitative Chemical Analysis*, 5th ed.; Longman Scientific & Technical: New York, 1989.

• Kashyap, P.; Rani, M.; Gahlyan, S.; Tiwari, D. P.; Maken, S. Volumetric, Acoustic and Optical Properties of Binary Mixtures of 2-Propanol with n-Alkanes (C6-C10) from 293.15 K to 303.15 K. *J. Mol. Liq.* **2018**, *268*, 303–314. https://doi.org/10.1016/j.molliq.2018.07.043.

• Kurtz, S. S. Physical Properties and Hydrocarbon Structure. In *The chemistry of petroleum hydrocarbons. Vol 1*; Reinhold Publishing Corporation: New York, 1954; pp 275–331.

• Kutsuna, S. Experimental Determination of Henry's Law Constants of Difluoromethane (HFC-32) and the Salting-out Effects in Aqueous Salt Solutions Relevant to Seawater. *Atmos. Chem. Phys.* **2017**, *17* (12), 7495–7507. https://doi.org/10.5194/acp-17-7495-2017.

• Levy, J. B.; Hornack, F. M.; Levy, M. A. Simple Determination of Henry's Law Constant for Carbon Dioxide. *J. Chem. Educ.* **1987**, *64* (3), 260–261. https://doi.org/10.1021/ed064p260.

• Li, J.; Heath, J. An Introduction to Capacitance Spectroscopy in Semiconductors. In *Capacitance spectroscopy of semiconductors*; Tainan, 2018; pp 1–22.

• Magee, P. E. Nitrogen as Health Hazard. *R. Swedish Acad. Sci.* **2019**, *6* (2), 123–125.

• Mckeown, A. B.; Hibbard, R. R. Determination of Dissolved Oxygen in Hydrocarbons. *Anal. Chem.* **1956**, *28* (9), 1490–1492. https://doi.org/10.1021/ac60117a044.

• McMurry, J. *Organic Chemistry*, 5th ed.; Brooks/Cole: California, 200AD.

• Modarress, H.; Vakili-Nezhaad, G. R. A New Characterization Factor for Hydrocarbons and Petroleum Fluids Fractions. *Oil Gas Sci. Technol.* **2002**, *57* (2), 149–154. https://doi.org/10.2516/ogst:2002011.

• Mohebbi, V.; Naderifar, A.; Behbahani, R. M.; Moshfeghian, M. Determination of Henry's Law Constant of Light Hydrocarbons Gases at Low Temperature. *J. Chem. Thermodyn.* **2012**, *51*, 8–11. https://doi.org/10.1016/j.jct.2012.02.014.

• Montoya Sánchez, N.; de Klerk, A. Autoxidation of Aromatics. *Appl. Petrochemical Res.* **2018**, *8* (2), 55–78. https://doi.org/10.1007/s13203-018-0199-4.

• Nahar, S. N. Phase - Separation Characteristics of Bitumen and Their Relation to Damage - Healing, Wöhrmann Print Service, Zutphen, 2016.

• Nigam, P.; Banat, I. M.; Singh, D.; Marchant, R. Microbial Process for the Decolorization of Textile Effluent Containing Azo, Diazo and Reactive Dyes. *Process Biochem.* **1996**, *31* (5), 435–442. https://doi.org/10.1016/0032-9592(95)00085-2.

• Nirmalakhandan, N.; Brennan, R. A.; Speece, R. E. Predicting Hernry's Law Constant and the Effect of Temperature on Henry's Law Constant. **1997**, *31* (6), 1471–1481.

• Perry, R.; Green, D. *Perry's Chemical Engineer's Handbook*; Mc Graw Hill, 1999.

• Poling, B.; Prausnitz, J.; O'Connell, J. *The Properties of Gases and Liquids*, 5th ed.; Mc Graw Hill, 2001.

• Ramesh, H.; Mayr, T.; Hobisch, M.; Borisov, S.; Klimant, I.; Woodley, J. M. Measurement of Oxygen Transfer from Air into Organic Solvents. *J Chem Technol Biotechnol* **2016**, *91*, 832–836. https://doi.org/10.1002/jctb.4862.

• RELXGroup. Reaxys database https://www.reaxys.com/#/login (accessed Sep 20, 2019).

• Siddiquee, M. N.; De Klerk, A. In Situ Measurement of Liquid Phase Oxygen during Oxidation. *Ind. Eng. Chem. Res.* **2016**, *55* (23), 6607–6618. https://doi.org/10.1021/acs.iecr.6b00949.

• Siddiquee, M. N.; De Klerk, A.; Nazemifard, N. Application of Microfluidics to Control Product Selectivity during Non-Catalytic Oxidation of Naphthenic-Aromatic Hydrocarbons. *React. Chem. Eng.* **2016**, *1* (4), 418–435. https://doi.org/10.1039/c6re00010j.

• Sigma-Aldrich.Co. Benzenethiol Safety Data Sheet www.sigmaaldrich.com (accessed Dec 1, 2019).

• Simmonds, C. *Alcohol. Its Production, Properties, Chemistry and Industrial Applications*; London, 1919.

• Smith, J. M.; Van Ness, H. C.; Abbott, M. M. *Introduction to Chemical Engineering Thermodynamics*, 7th ed.; Mc Graw Hill, 2005.

• Strausz, O.; Lown, E. *The Chemistry of Alberta Oil Sands, Bitumen and Heavy Oil*; Alberta Energy Research Institute: Calgary, 2003.

- Taylor, S. D.; Czarnecki, J.; Masliyah, J. Refractive Index Measurements of Diluted Bitumen Solutions. *Fuel* **2001**, *80* (14), 2013–2018. https://doi.org/10.1016/S0016-2361(01)00087-4.

- The Editors of Encyclopaedia Britannica. Atomic Theory https://www.britannica.com/science/atomic-theory (accessed Nov 12, 2019).

- Ting, P. D.; Gonzales, D. L.; Hirasaki, G. J.; Chapman, W. G. Application of the PC-SAFT Equation of State to Asphaltene Phase Behavior. In *Asphaltenes, heavy oils and petroleomics*; Springer: Texas, 2007; Vol. 53, pp 1689–1699. https://doi.org/10.1017/CBO9781107415324.004.

- Tracy, B. Quotable Quote https://www.goodreads.com/quotes (accessed Nov 23, 2019).

- Triola, M. F. *Elementary Statistics, Technology Update*, 11th Ed.; Pearson, Ed.; 2012.

- Vendruscolo, F.; Rossi, M. J.; Schmidell, W.; Ninow, J. L. Determination of Oxygen Solubility in Liquid Media. *ISRN Chem. Eng.* **2012**, *2012*, 1–5. https://doi.org/10.5402/2012/601458.

- Wang, F.; Evangelista, R. F.; Threatt, T. J.; Tavakkoli, M.; Vargas, F. M. Determination of Volumetric Properties Using Refractive Index Measurements for Nonpolar Hydrocarbons and Crude Oils. *Ind. Eng. Chem. Res.* **2017**, *56* (11), 3107–3115. https://doi.org/10.1021/acs.iecr.6b04773.

- Wattana, P.; Wojciechowski, D. J.; Bolaños, G.; Fogler, H. S. Study of Asphaltene Precipitation Using Refractive Index Measurement. *Pet. Sci. Technol.* **2003**, *21* (3–4), 591–613. https://doi.org/10.1081/LFT-120018541.

- Yaffe, D.; Cohen, Y.; Espinosa, G.; Arenas, A.; Giralt, F. A Fuzzy ARTMAP-Based Quantitative Structure-Property Relationship (QSPR) for the Henry's Law Constant of Organic Compounds. *J. Chem. Inf. Comput. Sci.* **2003**, *43* (1), 85–112. https://doi.org/10.1021/ci025561j.

- Yañez Jaramillo, L. M.; De Klerk, A. Partial Upgrading of Bitumen by Thermal Conversion at 150-300 °C. *Energy and Fuels* **2018**, *32* (3), 3299–3311. https://doi.org/10.1021/acs.energyfuels.7b04145.

- Yarranton, H. W.; Okafor, J. C.; Ortiz, D. P.; Van Den Berg, F. G. A. Density and Refractive Index of Petroleum, Cuts, and Mixtures. *Energy and Fuels* **2015**, *29* (9), 5723–5736. https://doi.org/10.1021/acs.energyfuels.5b01376.

- Yurkanis, P. *Organic Chemistry*; Pearson Education: California, 2006.

- Zachariah, A.; De Klerk, A. Thermal Conversion Regimes for Oilsands Bitumen. *Energy and*

Fuels **2016**, *30* (1), 239–248. https://doi.org/10.1021/acs.energyfuels.5b02383.